Geol. Mag. **151** (*4*), *2014, pp. 692–731.* © *Cambridge University Press 2013*
doi:10.1017/S0016756813000563

Eocene development of the northerly active continental margin of the Southern Neotethys in the Kyrenia Range, north Cyprus

ALASTAIR H.F. ROBERTSON*†, GILLIAN A. McCAY*, KEMAL TASLI‡ & AŞEGÜL YILDIZ§

*School of GeoSciences, University of Edinburgh, Grant Institute, West Mains Road, Edinburgh EH9 3JW, UK
‡Department of Geological Engineering, Mersin University, Mersin 33343, Turkey
§Department of Geological Engineering, Aksaray University, Aksaray 68100, Turkey

(*Received* 14 January 2013; *accepted* 21 June 2013; *first published online* 25 September 2013)

Abstract – We focus on an active continental margin related to northwards subduction during the Eocene in which sedimentary melange ('olistostromes') forms a key component. Maastrichtian – Early Eocene deep-marine carbonates and volcanic rocks pass gradationally upwards into a thick succession (<800 m) of gravity deposits, exposed in several thrust sheets. The lowest levels are mainly siliciclastic turbidites and debris-flow deposits. Interbedded marls contain Middle Eocene planktonic/benthic foraminifera and calcareous nannofossils. Sandstones include abundant ophiolite-derived grains. The higher levels are chaotic debris-flow deposits that include exotic blocks of Late Palaeozoic – Mesozoic neritic limestone and dismembered ophiolite-related rocks. A thinner sequence (<200 m) in one area contains abundant redeposited Paleogene pelagic limestone and basalt. Chemical analysis of basaltic clasts shows that some are subduction influenced. Basaltic clasts from unconformably overlying alluvial conglomerates (Late Eocene – Oligocene) indicate derivation from a supra-subduction zone ophiolite, including boninites. Taking account of regional comparisons, the sedimentary melange is interpreted to have formed within a flexurally controlled foredeep, floored by continental crust. Gravity flows including large limestone blocks, multiple debris flows and turbidites were emplaced, followed by southwards thrust imbrication. The emplacement was possibly triggered by the final closure of an oceanic basin to the north (Alanya Ocean). Further convergence between the African and Eurasian plates was accommodated by northwards subduction beneath the Kyrenia active continental margin. Subduction zone rollback may have triggered collapse of the active continental margin. Non-marine to shallow-marine alluvial fans prograded southwards during Late Eocene – Oligocene time, marking the base of a renewed depositional cycle that lasted until latest Miocene time.

Keywords: sedimentary melange, olistostrome, easternmost Mediterranean, Eocene, active continental margin.

1. Introduction

The easternmost Mediterranean is an excellent region to study the sedimentary, magmatic, metamorphic and tectonic processes related to ocean basin closure and continental collision. The Kyrenia Range in the north of Cyprus (Fig. 1) provides useful insights into such processes. The range is here loosely divided into Western, Central and Eastern ranges, plus the Karpas Peninsula (Fig. 2). The Kyrenia Range forms part of the former active continental margin of the Southern Neotethyan Ocean that was finally uplifted as a result of Plio-Quaternary collision-related tectonic processes, providing excellent exposure of deep-sea sedimentary and tectonic features. The Kyrenia Range includes an Eocene sedimentary melange that was traditionally interpreted as an olistostrome (Ducloz, 1972; Baroz, 1979).

The geological history of the Kyrenia Range (Robertson & Woodcock, 1986; Figs 1, 2) began with rifting of the Southern Neotethys during Middle–Late Permian and Triassic time and continued with passive margin subsidence during Jurassic and Early Cretaceous time, when the Southern Neotethys Ocean opened as the most southerly of several Mesozoic oceanic basins in the Eastern Mediterranean region. Northwards subduction began during the Late Cretaceous and continued to affect the Kyrenia Range until continental collision began in this area during Miocene time (Robertson & Woodcock, 1980; Şengör & Yılmaz, 1981; Robertson & Dixon, 1984; Robertson, 1998).

We will use the traditional stratigraphy (as shown on the Geological Map of Cyprus, 1979), coupled with the equivalent Turkish nomenclature, as given by Hakyemez *et al.* (2002). In contrast, the stratigraphy of the Miocene epoch has now been partially redefined based on recent work (Hakyemez *et al.* 2002; McCay *et al.* 2013). The place names mentioned (Fig. 3) are given in both Turkish and Greek (where available), to allow the features described to be located in the field. The timescale of Gradstein, Ogg & Smith (2004) is used here.

We present new field-based evidence of the biostratigraphy, sedimentology and structure of the Eocene sedimentary melange. We also give chemical evidence

†Author for correspondence: Alastair.Robertson@ed.ac.uk

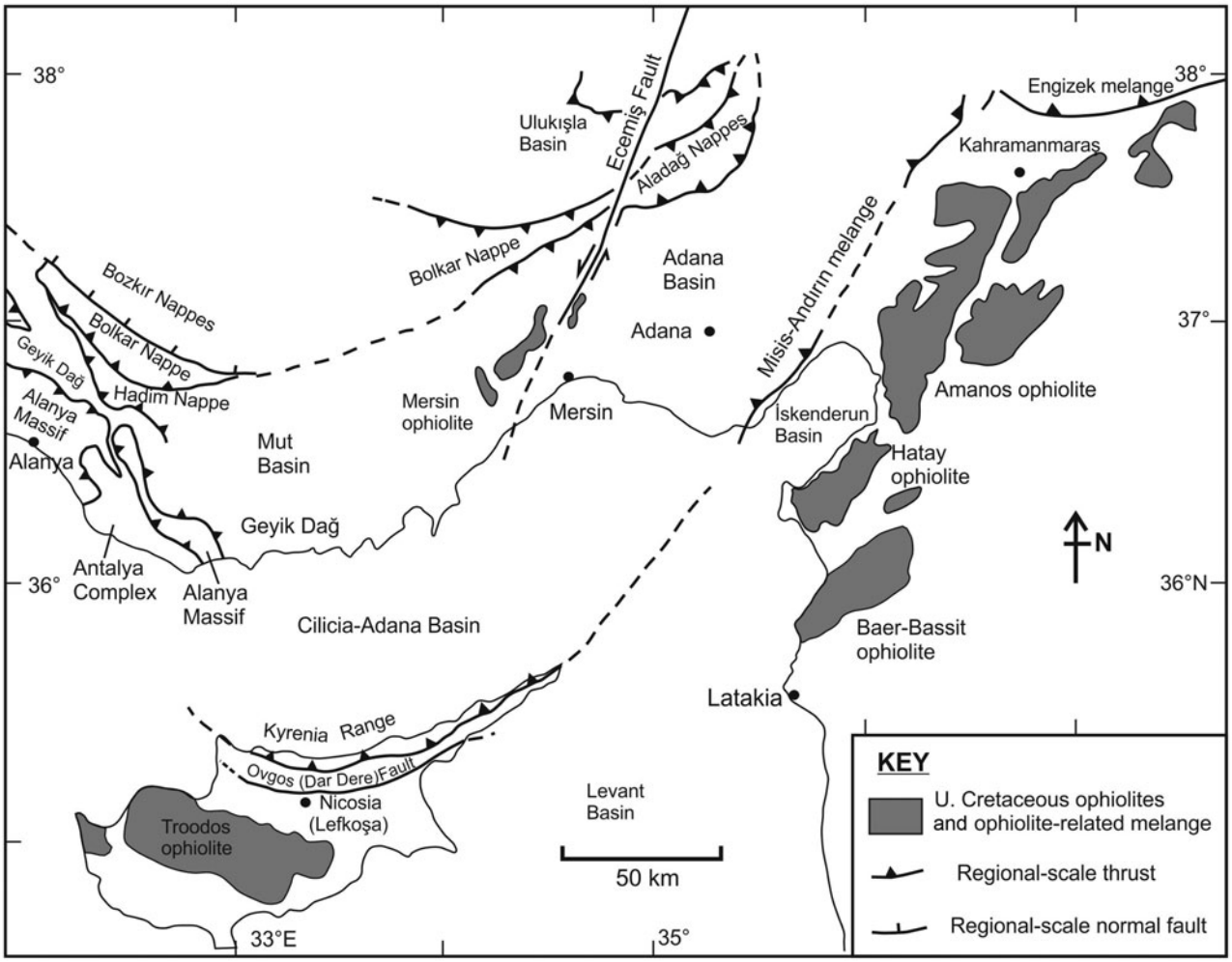

Figure 1. Outline tectonic map showing the location of the Kyrenia Range in the easternmost Mediterranean region. Upper Cretaceous ophiolites are potential sources of debris in the Eocene sedimentary rocks discussed. Also indicated are the main tectonic lineaments (thrust and strike-slip faults) that were active during the Eocene, the time period on which this study is focused.

for the origin of basaltic clasts within the sedimentary melange and from mafic igneous clasts within a conglomerate near the base of the unconformably overlying Late Eocene – Oligocene succession. We then interpret the evidence as a whole in terms of the geological development of the Kyrenia Range in the context of the wider region, especially southern Turkey. Previous work, including biostratigraphical data, is summarized in the online Supplementary Material available at http://journals.cambridge.org/geo.

1.a. Nomenclature

The most important, but by no means the only, unit discussed here is a melange. Melange can be defined as a mappable unit made up of blocks, either of single or multiple lithologies, with or without a sedimentary matrix (e.g. American Geological Institute, 1961). Melanges may have sedimentary or tectonic origins or both (e.g. Raymond, 1984). Melanges play an important role in the interpretation of many orogenic belts (e.g. Cloos & Shreve, 1988; Taira, Tokuyama & Soh, 1989).

The traditional terms olistostrome and wildflysch, as widely used in orogenic belts (e.g. Alps, Apennines and Appalachians) (e.g. Şengör 2003) are today best classified as types of sedimentary melange and are equivalent to large-scale mass-flow units. Sedimentary melanges (i.e. including olistostromes) are important because they record chaotic (i.e. extreme) gravity-driven processes. Sedimentary melanges reflect gravitational instability on a very large scale, whereas tectonic melanges result from large-scale shearing, brecciation and fragmentation.

Sedimentary melanges occur widely in both extensional settings (i.e. rifts and passive margins) and contractional (i.e. active margin and collisional) settings (e.g. Mulder & Cochonat, 1996; Huhnerbach & Masson, 2004; Evans *et al.* 2005). A range of processes, including tectonics, sediment loading, oversteepening, diapirism, sea-level change, storm activity and gas hydrate release, can trigger mass movements on different scales.

Sedimentary melange is characteristic of a wide variety of active and collision-related settings related to ocean basin subduction and closure. In particular,

https://doi.org/10.1017/S0016756813000563 Published online by Cambridge University Press

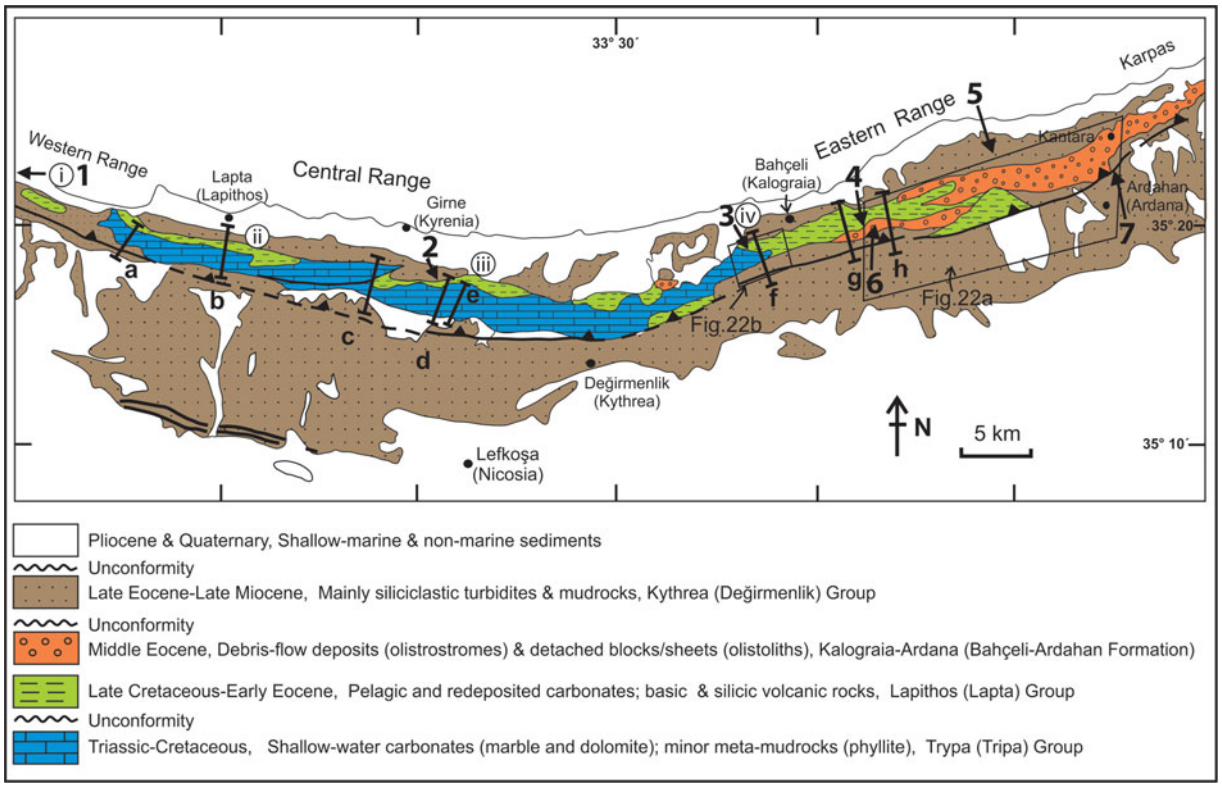

Figure 2. (Colour online) Outline geological map of the Kyrenia Range, which is subdivided into the Western, Central and Eastern ranges and the Karpas Peninsula; i–iv: local cross-sections shown in Figure 6; 1–7: measured sedimentary logs shown in Figure 9; a–h: location of structural traverses shown in Figure 23.

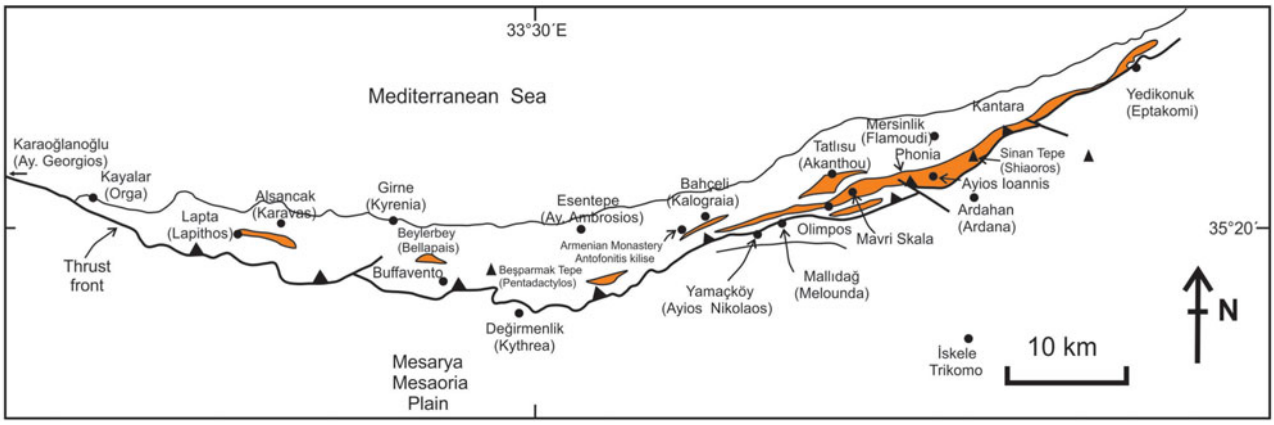

Figure 3. (Colour online) Outline of the Kyrenia Range geology showing the places mentioned in the text (Turkish and Greek equivalents in most cases). Outcrop of the Kalaograia–Ardana (Bahçeli–Ardahan) Formation is shaded.

sedimentary melange commonly relates to subduction, accretion and mass wasting in submarine trenches and forearc settings (e.g. western USA: Cowan & Page 1975; Himalayas: Liu & Einsele, 1999; Taiwan: Chang, Angelier & Huang, 2000). However, comparable melanges can also form in foredeep settings where the front of an overriding thrust sheet collapses to form large-scale mass-flow units (i.e. the traditional Wildflysch of the Swiss Alps; e.g. Şengör, 2003). In some cases the formation of melange in an oceanic accretionary setting is followed by the formation of additional sedimentary melange in a foredeep setting related to collision and overthrusting of a continental margin, as documented in Greece, Oman and Turkey (e.g. Robertson, Parlak & Ustaömer, 2009). Sedimentary melange can also relate to mud diapirism and mud volcanism (e.g. Williams, Pigram & Dow, 1984), and is documented in the Eastern Mediterranean Sea (e.g. Robertson *et al.* 1996). In addition, sedimentary melanges and mass-flow units play an important role in the geology of Cyprus as a whole as represented by the Miocene Pakhna Formation (Lord *et al.* 2009) and

https://doi.org/10.1017/S0016756813000563 Published online by Cambridge University Press

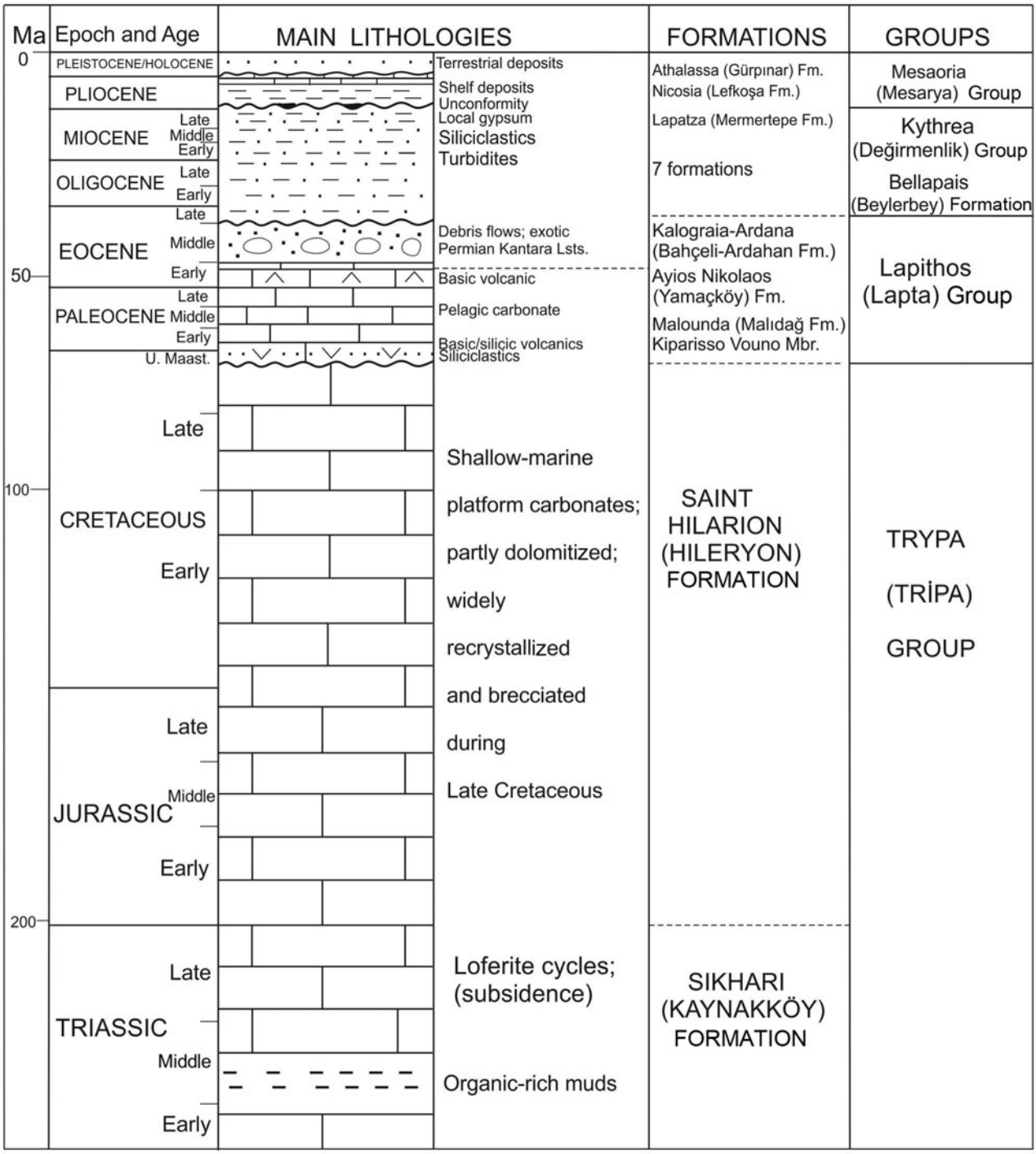

Figure 4. Summary stratigraphy of the Kyrenia Range, from Robertson, Taslı and İnan (2012*b*).

the Moni Melange (Robertson 1977*a*) both in southern Cyprus, and the Kathikas Melange in SW Cyprus (Swarbrick & Naylor 1980). Here, we consider the example of an Eocene sedimentary melange (equivalent to olistostromes) that was formed in a contractional, active margin setting.

2. Lithostratigraphy

The existence of Eocene 'olistostromes' has long been known in the Kyrenia Range (see Ducloz, 1972; Cleintaur, Knox & Ealey, 1977; Baroz, 1979). They were interpreted as having formed either in a subduction trench or in a flexurally controlled foredeep (Robertson & Woodcock, 1986). The emplacement of the olistostromes in the Kyrenia Range was then followed by south-verging thrusting (Ducloz, 1972; Baroz, 1979). Afterwards the thrust belt was unconformably overlain by conglomerates of Late Eocene – Oligocene age, marking the base of a contrasting cycle of marine clastic-dominated deposition (Ducloz, 1972; Baroz, 1979; Robertson & Woodcock, 1986; McCay & Robertson, 2012). Conglomerates at the base of this overlying succession contain igneous clasts that shed

https://doi.org/10.1017/S0016756813000563 Published online by Cambridge University Press

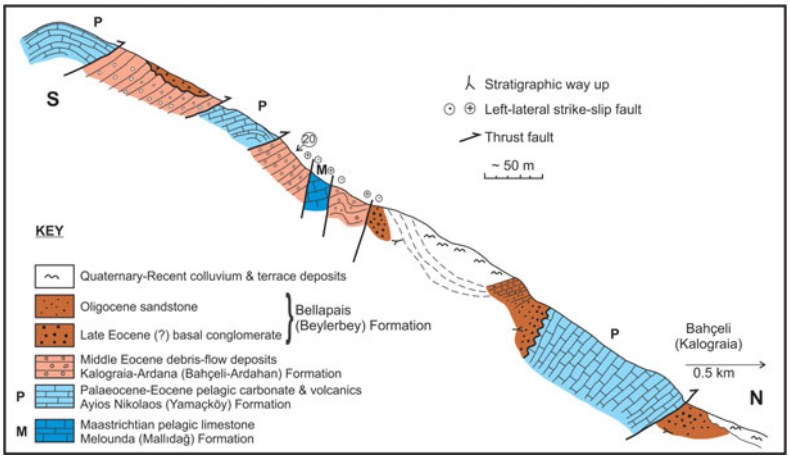

Figure 5. (Colour online) Sketch cross-section of the type area of the Kalaograia–Ardana (Bahçeli–Ardahan) Formation, south of Bahçeli (Kalaograia) village (Figs 2, 3). Note the folding and backthrusting at this location. This section is also affected by high-angle strike-slip displacement (Late Miocene?). No. 20 (ringed) shows the location of a sample collected for nannofossil dating (for species list, see online Supplementary Material available at http://journals.cambridge.org/geo).

light on the source of ophiolitic rocks in the region and thus on the regional tectonic model.

The sedimentary melange (olistostromes) was mapped as the Kalaograia–Ardana Flysch on the three maps that accompany the Cyprus Geological Memoir No. 9 (Ducloz, 1972) and as the Ardana–Kalogrea Formation on the Geological Map of Cyprus (1979). Isolated masses of Late Palaeozoic limestone were interpreted as olistoliths (i.e. detached blocks) within this unit. Baroz (1979) introduced the term Kalaograia–Ardana Formation to distinguish this unit from underlying well-stratified pelagic limestones and volcanic rocks of Maastrichtian – Early Eocene age, and also from overlying terrigenous clastic sedimentary rocks of Late Eocene – Late Miocene age (Fig. 4). In conjunction with the first mapping of the entire Kyrenia Range, Hakyemez *et al.* (2002) retained the same definition of the formation but utilized Turkish names for the type area. Accordingly, we use the term Kalaograia–Ardana (Bahçeli–Ardahan) Formation.

The type area, Bahçeli (Kalaograia) village, is located on the northern flank of the Kyrenia Range while Ardahan (Ardana) is to the south (Fig. 3). The succession in the type area near Bahçeli (Kalaograia) is incomplete and strongly deformed (Fig. 5), while Ardahan (Ardana) is located on Miocene sedimentary rocks. Baroz (1979) described several additional sections, in particular a thick succession that is well exposed in the Eastern Range near Agios Ioannis (Fig. 3). This and several other successions discussed here are shown in Figure 6. Baroz (1979) defined several formations and members within the Kalaograia–Ardana (Bahçeli–Ardahan) Formation, as summarized in the online Supplementary Material available at http://journals.cambridge.org/geo. However, we use an informal stratigraphy here because formal stratigraphical subdivision is not appropriate for describing a melange (see Fig. 7).

3. Biostratigraphy

New data are presented here for planktonic foraminifera and calcareous nannofossils. Existing biostratigraphical information is presented in the online Supplementary Material available at http://journals.cambridge.org/geo. In outline, the succession of the underlying Lapithos (Lapta) Group (Melounda (Mallıdağ) and Ayios Nikolaos (Yamaçköy) formations) is dated as Maastrichtian – Early Eocene (see Henson, Browne & McGinty, 1949; Baroz, 1979; Hakyemez *et al.* 2002; Hakyemez & Özkan-Altıner, 2007; Robertson, Parlak & Ustaömer, 2012*a*). The succession passes transitionally upwards into the Kalaograia–Ardana (Bahçeli–Ardahan) Formation. Baroz (1979) reported that the matrix of the Kalaograia–Ardana Formation (as named by him) varies from Middle Eocene to Late Eocene based on foraminifera. Large foraminifera characteristic of the Middle Eocene were reported from the Central Range ('Milous Breccia'). Facies in the Central and Eastern ranges ('Armenian Monastery Breccia') were inferred to be no younger than Middle Eocene based on planktonic foraminifera (see Fig. 8).

The oldest age reported from the unconformably overlying succession of the Kythrea (Değirmenlik) Group is Late Eocene based on the planktonic foraminifer *Globorotalia cerroazulensis*, reported in two thin intercalations of marl close to basal conglomerates from near Kayalar (Orga) (Fig. 3). Marls higher in the succession are better dated as Oligocene (Baroz, 1979; McCay *et al.* 2013).

A Permo-Carboniferous age for the exotic blocks (Kantara Limestone) in the melange was suggested by Reichel (1945*a*, *b*). P. Knup and others (in Baroz, 1979) later reported a Middle–Late Permian age for some of the exotics. Baroz (1979) inferred a variety of Middle–Late Permian – Late Cretaceous ages. In addition, other

https://doi.org/10.1017/S0016756813000563 Published online by Cambridge University Press

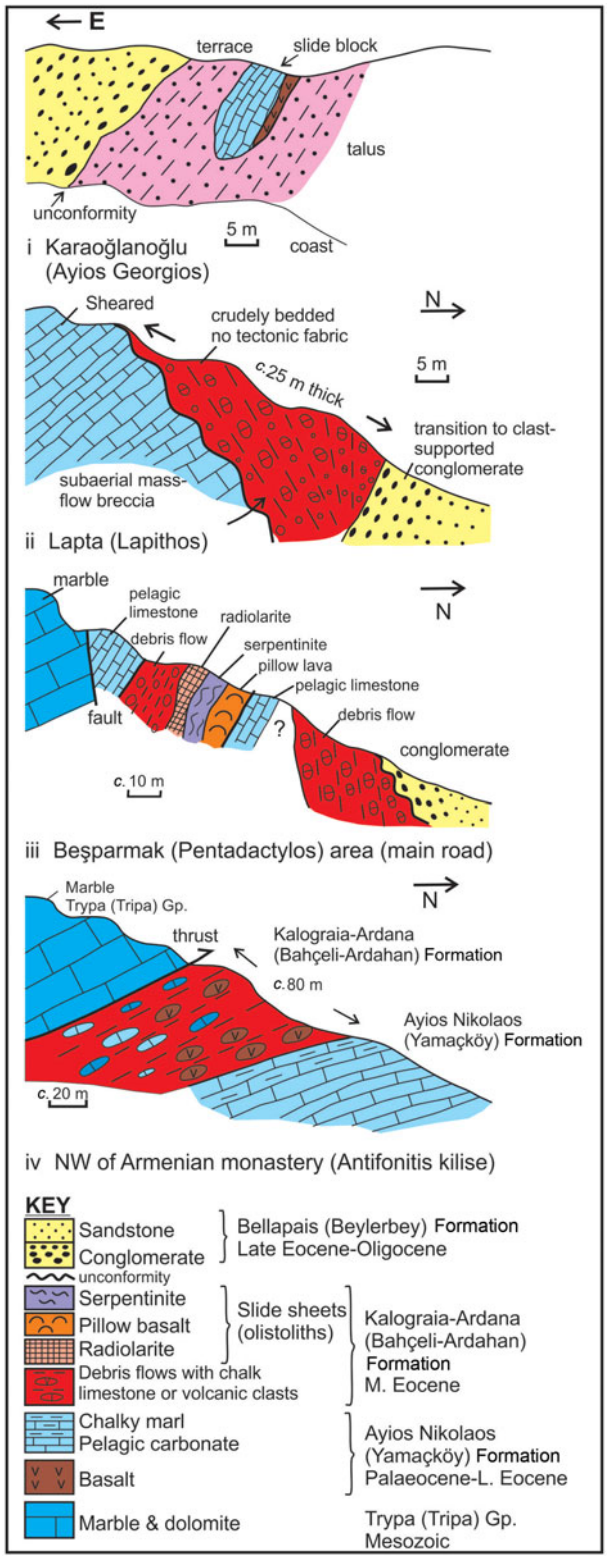

Figure 6. (Colour online) Field relations of key outcrops. (i) Block of pelagic limestone plus lava (Lapithos/Lapta Group) within debris-flow deposits of the Kalaograia–Ardana (Bahçeli–Ardahan) Formation, unconformably overlain by Upper Eocene – Oligocene conglomerates. Near Karaoğlanoğlu (Ayios Georgios), Western Range (see Fig. 2). (ii) Mass-flow unit largely made up of Lower Eocene nummulitic limestone; located between underlying Paleogene pelagic carbonates and depositionally overlying Upper Eocene – Oligocene conglomerates; east of Lapta (Lapithos), Central Range (see Fig. 2, locality 2). (iii) Debris-flow deposits of the Kalaograia–Ardana (Bahçeli–Ardahan) Formation associated with exotic blocks of serpentinized harzburgite, pillow basalt and radiolarite; unconformably overlain by Upper Eocene – Oligocene conglomerates (Bellapais/Beylerbey Formation); Kyrenia road, west of Beşparmak (Pentadactylos) (see Fig. 9, locality 3). (iv) Paleogene pelagic carbonates, transitional upwards into debris-flow deposits dominated by redeposited Paleogene pelagic carbonates, limestones and basaltic lavas; NW of the Armenian monastery (Antifonitis kilise) (see Fig. 9, locality 4).

exotic blocks include Upper Triassic pelagic limestone with the pelagic bivalve, *Halobia* sp., Jurassic pelagic limestone with *Saccocoma* sp. and *Globochaete* sp., Middle Jurassic limestone with the benthic foraminifer *Protopeneroplis* sp., Cretaceous pelletal and micritic limestone with orbitolinids, miliolids, *Cuneolina* sp. and *Pithonella* sp. and also Late Cretaceous limestone with rudist bivalve debris (*Hippurites sp*). Early–Middle Eocene planktonic foraminifera were reported from the matrix of the limestone blocks (G. Bizon in Baroz, 1979).

3.a. Planktonic foraminiferal data

A Middle Eocene (Lutetian) age was determined during this study based on planktonic foraminifera that were extracted from marls in the lower and middle parts of the succession of the Kalaograia–Ardana (Bahçeli–Ardahan) Formation in the Eastern Range. The complete listing of the foraminifera identified is given in the online Supplementary Material available at http://journals.cambridge.org/geo.

Muddy samples, each weighing *c.* 1 kg were crushed and soaked in dilute (10 %) hydrogen peroxide for 12–24 hours to help disaggregate the foraminiferal tests from their matrix. Some degree of etching took place but this did not affect the biostratigraphic identification. The residues were washed through a 100 μm screen and dried in an oven at <50 °C. About 900 specimens were picked and cleaned using ultrasonic agitation during 10–15 second intervals. The planktonic foraminifera were studied using an optical microscope with ×40 and ×100 magnifications. The preservation of the planktonic foraminifera was assessed visually as being moderate to poor due to dissolution. The planktonic foraminifera were imaged using a field emission scanning electron microscope at the Mersin University of Advanced Technology, Education and Application Centre. The age assignments are based on the well-established zonal distributions of planktonic foraminiferal species (e.g. Pearson *et al.* 2006).

Several samples were studied from the lower to middle parts of the formation (see online Supplementary Material available at http://journals.cambridge.org/geo), specifically from a well-exposed forest road section between Mallıdağ (Melounda) and the crest of the range (*c.* 1 km NE of Mallıdağ (Melounda); Figs 8, 9, log 4). Several samples suggest a Middle Eocene (Lutetian age) or even a middle Lutetian age. The maximum likely age range inferred here is Early Eocene (late

https://doi.org/10.1017/S0016756813000563 Published online by Cambridge University Press

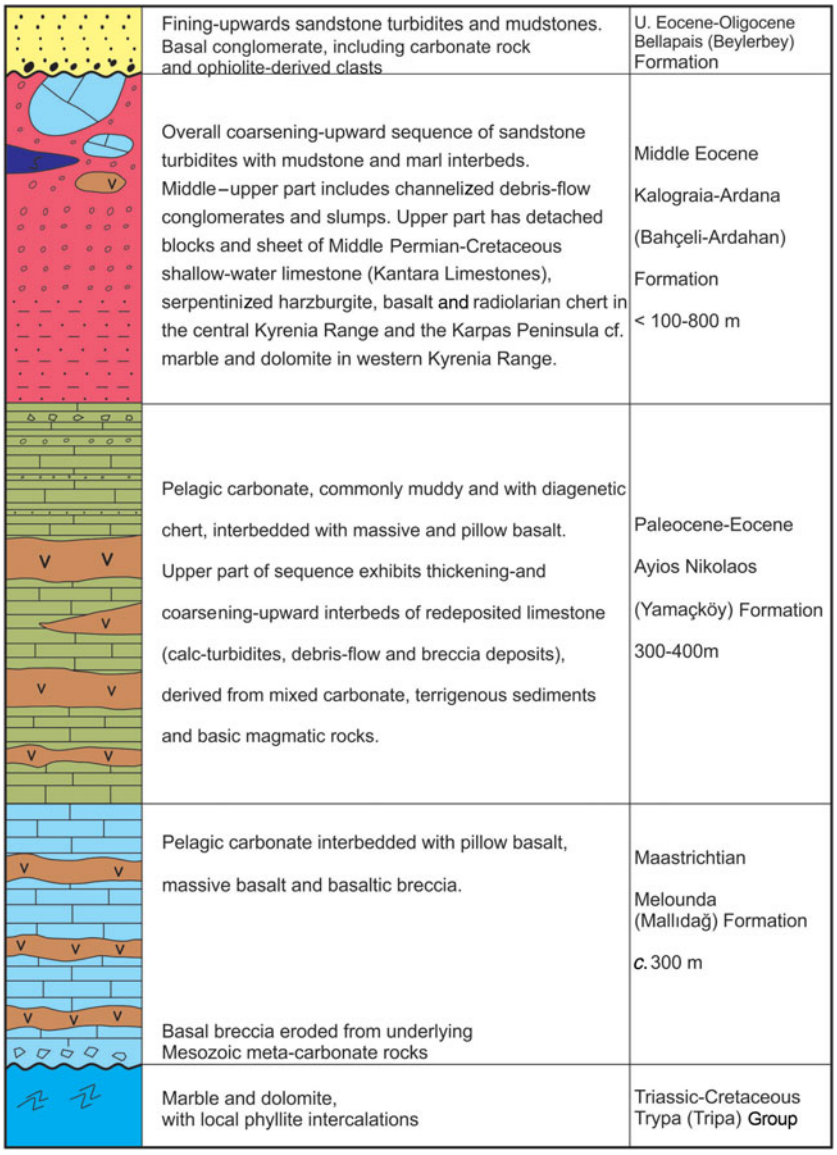

Figure 7. (Colour online) Simplified sedimentary log of the Maastrichtian – Middle Eocene mega-sequence in the Kyrenia Range (between two unconformities) that begins with transgressive sub-aqueous carbonate breccias and ends with the Middle Eocene Kalaograia–Ardana (Bahçeli–Ardahan) Formation; unconformably overlain by the basal conglomerates of the Upper Eocene – Oligocene Bellapais (Beylerbey) Formation. No complete intact succession is exposed in any one section; see Figure 9 for logs of local partial successions (data from Baroz, 1979 and this study).

Ypresian) to late Middle Eocene (Bartonian). Additional samples were studied from the middle part of the succession further NE, along the Geçitkale–Mersinlik (Lefkoniko–Flamoudi) new road section (Fig. 9, log 6). The dated samples are from the middle part of the succession (the lower part is not exposed). The maximum age inferred range is late Ypresian – earliest Bartonian (E8–E11), while several samples suggest a Lutetian (E8–E11) or even middle Lutetian age (top E9).

In summary, the assemblage *Globigerinatheka* sp., *Hantkenina* sp., *Globorotalia bullbrooki* (= *Acarinina bullbrooki*), *Globorotalia spinulosa* (= new valid name *Morozovelloides crassatus* in Pearson *et al.* 2006), *Globorotalia aragonensis* (*Morozovella aragonensis*) and *Truncorotaloides topilensis* (= *Acarinina topilensis*) supports a Middle Eocene age for much of the Kalaograia–Ardana (Bahçeli–Ardahan) Formation.

3.b. Nannofossil data

Samples of marl were collected from the same sections that were studied for planktonic foraminifera, plus one additional section. Smear slides were examined using an Ortholux polarizing microscope with an oil-immersion objective at a magnification of ×1600 and the nannofossils were identified and dated according to the widely accepted biostratigraphy of Martini (1971), Perch-Nielsen (1985) and Varol (1999). Representative taxa are shown in Figure 10, while a complete list of the taxa is given in the online Supplementary Material available at http://journals.cambridge.org/geo.

Samples of pale-coloured chalky marl were studied from the section (between Mallıdağ (Melounda) and the crest of the range; see Fig. 9, log 6). Samples from near the base of the succession contain

https://doi.org/10.1017/S0016756813000563 Published online by Cambridge University Press

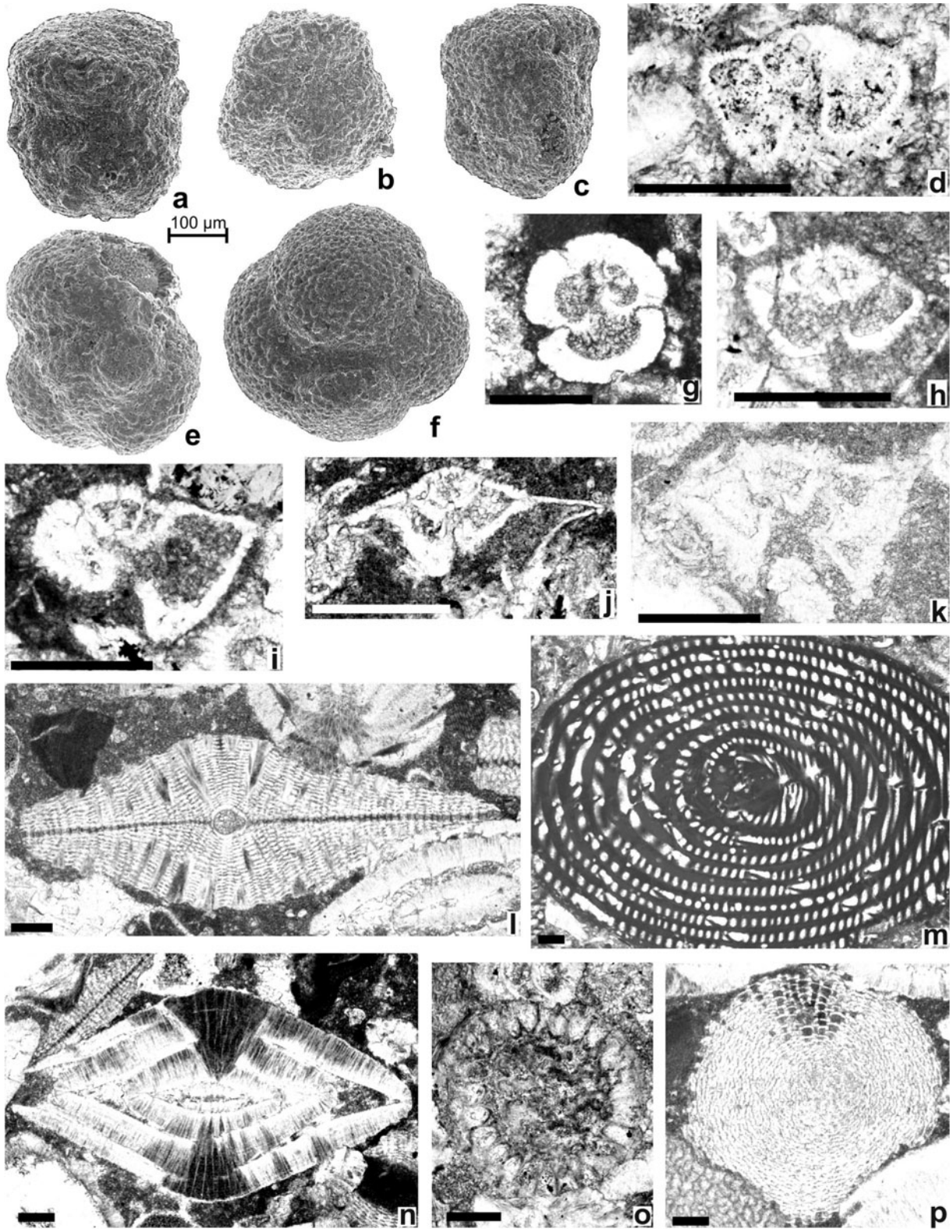

Figure 8. Scanning electron micrographs (SEMs) and photomicrographs of planktonic foraminifera from hemipelagic marls interbedded with terrigenous gravity flows from the lower part of the Middle Eocene Kalaograia–Ardana (Bahçeli–Ardahan) Formation, 1 km NE of Mallıdağ (Melounda). (a–d) *Acarinina bullbrooki*, (a–c) SEM images, sample K10/67: (a) umbilical; (b) spiral; and (c) edge sides; (d) sample K10/17; (e) *Turborotalia frontosa*, SEM image, spiral side, sample K10/72; (f) *Globigerinatheka* sp., SEM image, umbilical side, sample K10/60; (g) *Globigerinatheka* sp., sample K10/6; (h) *Igorina broedermanni*, sample K10/16; (i) *Acarinina praetopilensis*, sample K10/7; (j) *Morozovelloides crassatus*, sample K10/16; (k) *Morozovelloides coronatus*, sample K10/16; (l) *Orbitoclypeus ramaraoi ramaraoi*, sample K10/52; (m) *Alveolina* cf. *A. ellipsoidalis*, sample K10/19; (o) *Chapmanina* sp., sample K10/33; (p) *Sphaerogypsina globulus*, sample K10/52. Scale bars: 0.2 mm. See Supplementary Publication Table S1 for the complete list of the assemblages identified in each sample and Supplementary Publication Table S2 (available at http://journals.cambridge.org/geo) for the author index of species mentioned in figure above and the text.

https://doi.org/10.1017/S0016756813000563 Published online by Cambridge University Press

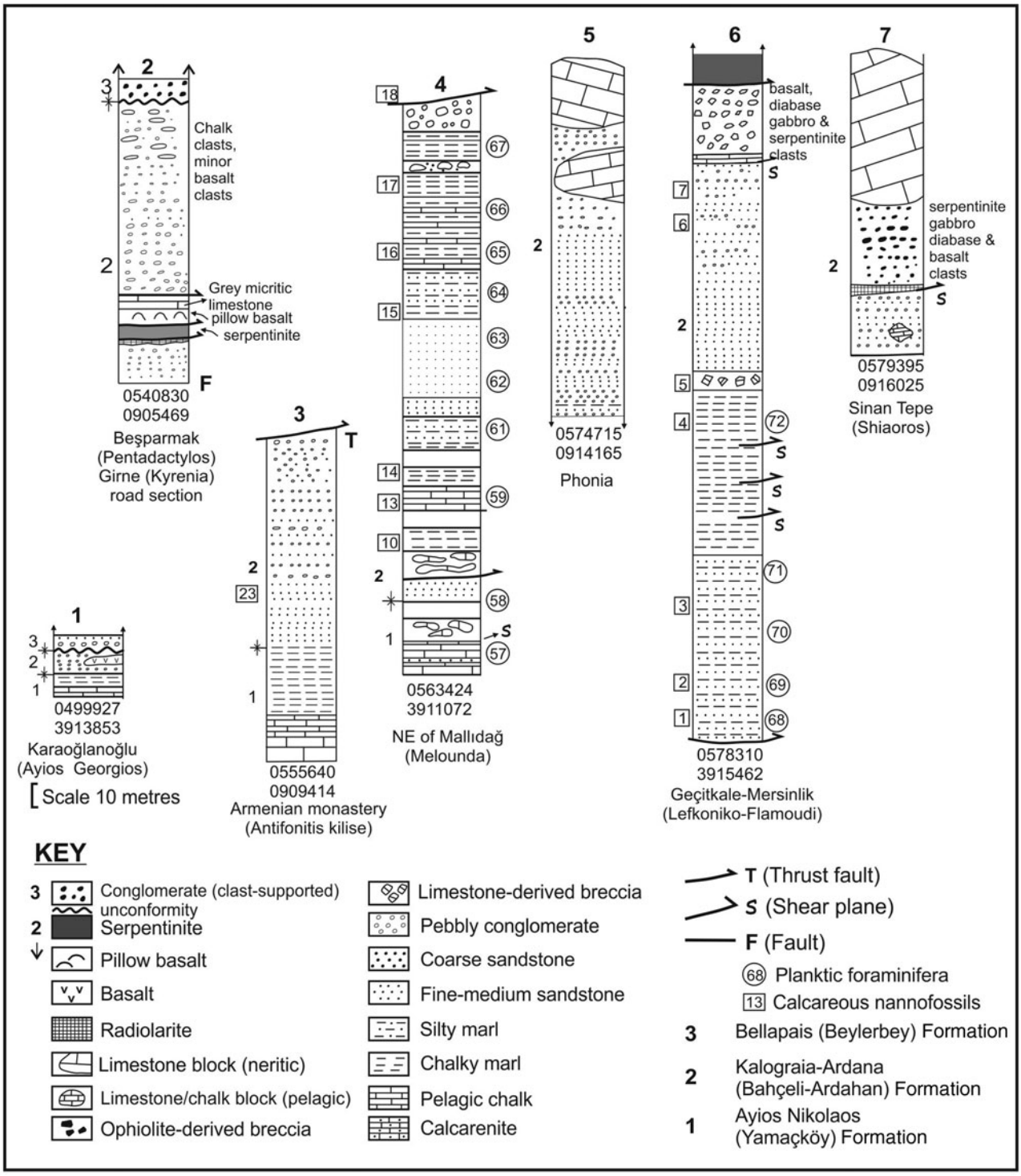

Figure 9. Measured sedimentary logs 1–7 of local partial successions in the Eocene Kalaograia–Ardana (Bahçeli–Ardahan) Formation and adjacent units. The succession as a whole is dissected by Eocene thrusting as discussed in the text. See Figure 2 for the locations of the logs.

nannofossil assemblages that are diagnostic of the Middle–Late Eocene (Bartonian–Priabonian). Samples from higher in the section are mainly suggestive of a Middle Eocene – Early Oligocene age. One sample contains an assemblage of Middle–Late Eocene – Early Oligocene? age (i.e. Bartonian–Priabonian–Latdorfian?). Palaeocene, Early Eocene and some Middle Eocene nannofossils are reworked. The topographically highest sample is from pelagic carbonate with scattered nodules of replacement chert. This can be lithologically correlated with the Ayios Nikolaos (Yamaçköy) Formation. A Palaeocene – Early Eocene (Danian–Ypresian) assemblage is present in this sample. The Kalaograia–Ardana (Bahçeli–Ardahan)

https://doi.org/10.1017/S0016756813000563 Published online by Cambridge University Press

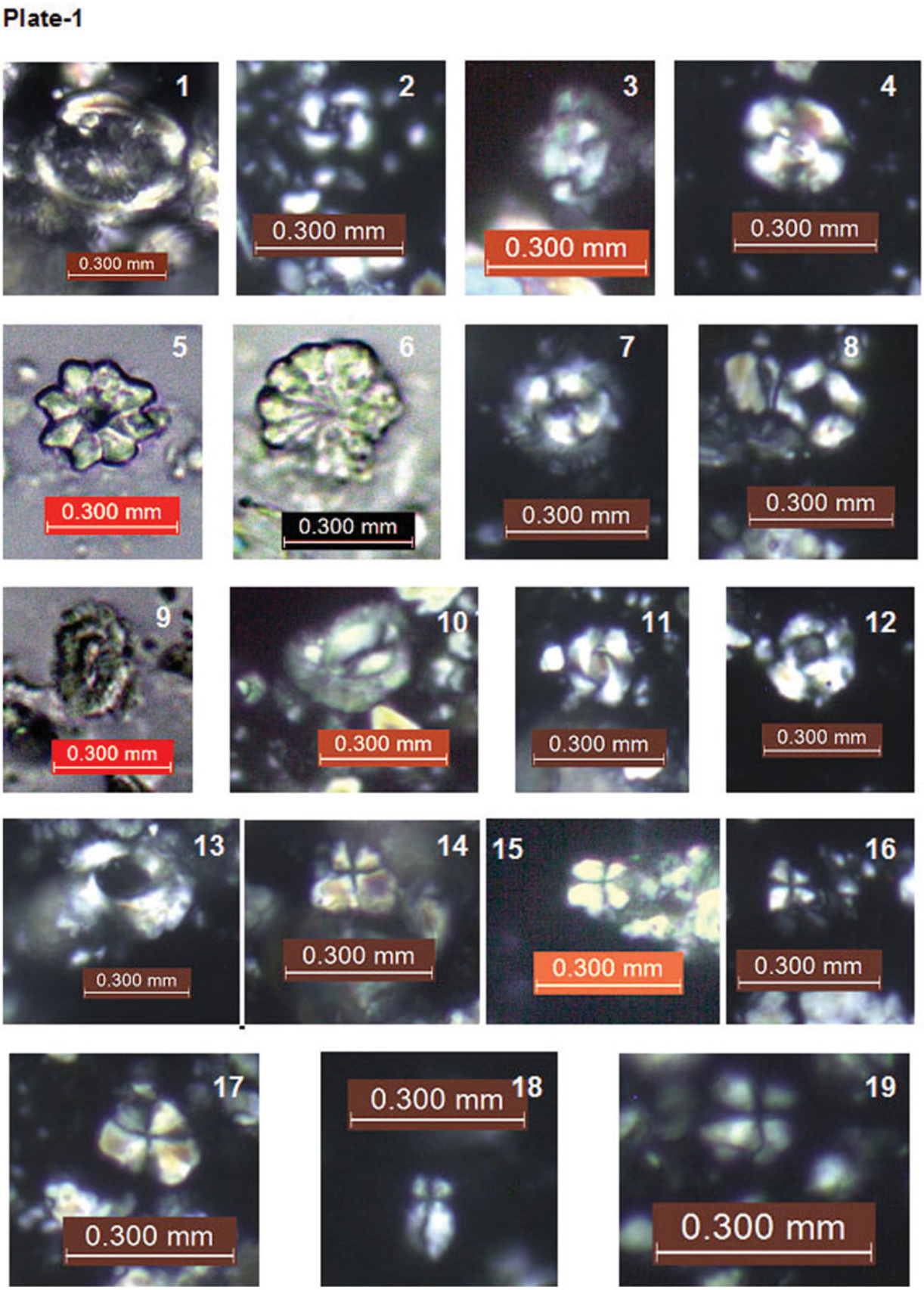

Figure 10. (Colour online) Optical micrographs of calcareous nannofossils. (1) *Chiasmolithus oamaruensis* (Deflandre), sample no. K-12-2; forest road 1 km NE of Mallıdağ (Melounda); (2) *Cribrocentrum reticulatum* (Gartner & Smith), sample no. K-12-6; Geçitkale-Mersinlik (Lefkoniko–Flamoudi) new road section; (3) *Coccolithus pelagicus* (Wallich), sample no. K-12-2; higher in same new road section as (3); (4) 4- *Dictyococcites bisectus* (Hay, Mohler & Wade), sample no. K-12-3; same section; higher in succession; (5) *Discoaster saipanensis* Bramlette & Riedel, sample no. K-12-6; same section; higher in succession; (6) *Discoaster multiradiatus* (Bramlette & Riedel), sample no. K-12-7; same section; higher in succession; (7) *Ericsonia formosa* (Kamptner), sample no. K-12-2; base of formation in the Geçitkale-Mersinlik (Lefkoniko–Flamoudi) new road section; (8)

https://doi.org/10.1017/S0016756813000563 Published online by Cambridge University Press

Formation is, therefore, terminated upwards by a thrust fault in this section, in agreement with the mapping by Baroz (1979).

An additional sequence that is transitional between the Ayios Nikolaos (Yamaçköy) Formation and the Kalaograia–Ardana (Bahçeli–Ardahan) Formation was sampled along the forest road running along the crest of the range directly north of Yamaçköy (Ayios Nikolaos) (see also Baroz, 1979). The nannofossil assemblages there suggest an overall Middle Eocene – Oligocene? (Bartonian–Oligocene?) age. One sample is more specifically of a Middle Eocene (Lutetian) age, while Palaeocene – Early Eocene nannofossils are interpreted as being reworked.

Further samples (K-12-2 to -7) were collected along the Geçitkale–Mersinlik (Lefkoniko–Flamoudi) new road section (Figs 9 (log 6), 11). The nannofossils are suggestive of a Middle Eocene – Oligocene? (Bartonian–Oligocene?) age. One sample (K-12-6) contains a Late Eocene – Oligocene? (Priabonian?–Oligocene) assemblage, while nannofossils of Palaeocene – Early Eocene and Middle Eocene are reworked. One sample from a highly deformed section in the type area south of Bahçeli (Kalaograia) (Figs 3, 5) was found to have a non-specific Middle Eocene – Early Oligocene (Lutetian–Latdorfian) assemblage. Lastly, one sample was dated from chalky debris-flow deposits in the middle part of the succession along the access road to Antifonitis monastery (Antifonitis kilise) (Fig. 3). A Middle Eocene – Oligocene? (Bartonian–Oligocene?) assemblage is present, while Palaeocene – Early Eocene and Middle Eocene nannofossils are reworked.

Taken together, the planktonic foraminiferal and nannofossil age data indicate that the Kalaograia–Ardana (Bahçeli–Ardahan) Formation is of Middle Eocene age (ranging up to and including the Bartonian). The overlying cover is dated as being of Late Eocene – Oligocene age.

4. Sedimentary successions

In the Middle Eocene, the Kalaograia–Ardana (Bahçeli–Ardahan) Formation varies according to its location in the Eastern, Central and Western Kyrenia Range (Fig. 2), as documented in the following sections.

4.a. Successions in the Eastern Range

A sedimentary transition is exposed in several outcrops from the underlying Palaeocene – Lower Eocene Ayios Nikolaos (Yamaçköy Formation) to the Kalaograia–Ardana (Bahçeli–Ardahan) Formation. An easily accessible succession is located along the forest road to the northeast of Mallıdağ (Melounda) (Fig. 9, log 4). The underlying sediments of the Lower Eocene Ayios Nikolaos (Yamaçköy) Formation are pink–reddish-coloured pelagic carbonates, locally with chert of diagenetic replacement origin. The pelagic carbonates are interbedded with several well-cemented limestone gravity-flow deposits, ranging from graded calcarenite (i.e. calciturbidites) in beds up several tens of centimetres thick to calc-breccias (i.e. mass-flow deposits) up to several metres thick (Fig. 12a). The clasts in these redeposited carbonate rocks are characteristic of the Triassic–Cretaceous Trypa (Tripa) Group, specifically the St Hilarion (Hilaryon) Formation and the Sykhari (Kaynakköy) Formation (Fig. 4).

The pinkish-coloured Ayios Nikolaos (Yamaçköy) Formation passes upwards into muddy hemipelagic carbonates with interbeds of normally graded, redeposited limestones (calciturbidites and carbonate debris-flow deposits). These typically thicken and coarsen upwards to form beds up to 2 m thick (Fig. 9, log 4). The clasts are again mainly dark-grey neritic limestone and dolomite, typical of the Trypa (Tripa) Group. A very similar transition is well exposed along the ridge crest road south of Yamaçköy (Ayios Nikolaos) (Baroz, 1979; Fig. 3).

A much thicker exposure of the Kalaograia–Ardana (Bahçeli–Ardahan) Formation is exposed further east in cuttings along the road from Ardahan (Ardana) to Kantara (Fig. 9, log 6) and also along the Geçitkale–Mersinlik (Lefkoniko–Flamoudi) road section in the Eastern Kyrenia Range (Fig. 12b). The base of the formation is not exposed in these sections. However, an upwards transition from the Ayios Nikolaos (Yamaçköy) Formation is seen along-strike to the west, specifically to the NW of Yamaçköy (Ayios Nikolaos). In the Ardahan (Ardana) to Kantara road section (Fig. 9, log 6), the lower part of the succession is dominated by sandstone turbidites with subordinate pale-grey hemipelagic marls and lenticular debris-flow conglomerates. Similar debris-flows are well exposed along the

Ericsonia robusta (Bramlette & Sullivan), sample no. K-12-18; slice of the Melounda (Mallıdağ) Formation above the Kalaograia–Ardana (Bahçeli–Ardahan) Formation; forest road 1 km NE of Maildağ (Melounda); (9) *Helicosphaera euphratis* Haq, sample no. K-12-2; Geçitkale–Mersinlik (Lefkoniko–Flamoudi) new road section; (10) *Helicosphaera salebrosa* Perch-Nielsen, sample no. K-12-7: higher in the same section; (11) *Reticulofenestra dictyoda* (Deflandre), sample no. K-12-10; near base of succession; forest road 1 km NE of Mallıdağ (Melounda); (12) *Reticulofenestra hillae* Bukry & Percival, sample no. K-12-21; near base of the formation; section or crest road north of Yamaçköy (Ayios Nikolaos); (13) *Reticulofenestra umbilica* (Levin), sample no. K-12-10; near base of succession; forest road 1 km NE of Mallıdağ (Melounda); (14) *Sphenolithus spiniger* Bukry, sample no. K-12-22; near base of the formation; section on crest road north of Yamaçköy (Ayios Nikolaos); (15) *Sphenolithus conspicuus* Martini, sample no. K-12-10; forest road 1 km NE of Maildağ (Melounda); (16) *Sphenolithus editus* Perch-Nielsen, sample no. K-12-10; location as above; (17) *Sphenolithus moriformis* (Brönnimann & Stradner), sample no. K-12-22; section on crest road north of Yamaçköy (Ayios Nikolaos); (18) *Sphenolithus obtusus* Bukry, sample no. K-12-2; near base of exposure in Geçitkale-Mersinlik (Lefkoniko–Flamoudi) new road section; (19) *Sphenolithus primus* Perch-Nielsen, sample no. K-12-16; forest road 1 km NE of Mallıdağ (Melounda). See Supplementary Publication Table S3 (available at http://journals.cambridge.org/geo) for the complete listing of taxa identified and the inferred ages.

https://doi.org/10.1017/S0016756813000563 Published online by Cambridge University Press

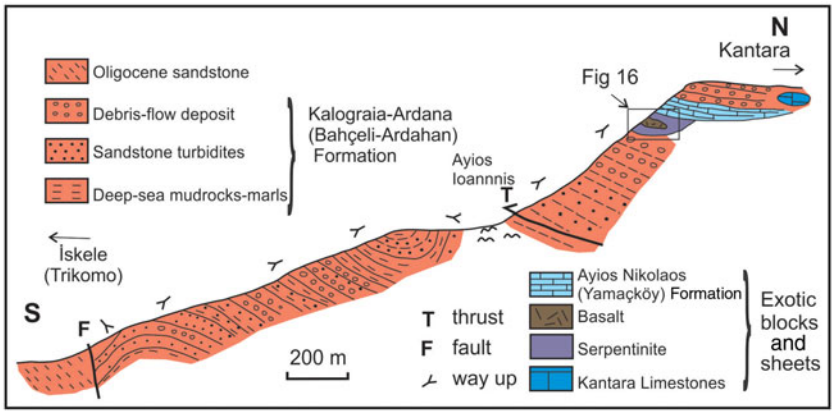

Figure 11. (Colour online) Sketch cross-section of the extensive exposure of the Kalaograia–Ardana (Bahçeli–Ardahan) Formation in the Eastern Range, as exposed along the new road from Ardahan (Ardara) to Kantara (see log 6 in Fig. 9).

Geçitkale–Mersinlik (Lefkoniko–Flamoudi) road section (Fig. 12c). The overall succession is affected by folding and a structural break (Fig. 9, log 6). There is also evidence of slumping and soft-sediment deformation (Fig. 13a).

The upper part of the succession is a thickening- and coarsening-upwards succession, dominated by mass-flow deposits with exotic blocks. The exotic blocks are mainly shallow-water limestone (equivalent to the Kantara Limestones), pelagic carbonate and basalt (equivalent to the Lapithos (Lapta) Group) plus sheared serpentinite, pillow basalt, radiolarian chert and rare pelagic limestone (Fig. 13b). Similar debris-flow-type conglomerates and breccia are well exposed, interspersed with large exotic blocks of neritic limestone (Kantara Limestones) near the crest of the range, ranging from the west (e.g. near Phonia) (Figs 9 (log 5), 12d, f) to further east (e.g. near Sinan Tepe/Shiaoros) (Fig. 9, log 7) and beyond Kantara (Figs 2, 3).

4.b. Successions in the Central Range

A transition from pelagic carbonates interbedded with redeposited limestones into shales, sandstone turbidites and debris-flow deposits exists in the Central Kyrenia Range (e.g. NW of the Armenian monastery/Antifonitis kilisi) (Figs 2, 3). However, the succession is strongly deformed by shearing, folding and northwards thrusting (Fig. 6iv). The lower part of the succession is dominated by poorly stratified chalky debris-flow deposits. These contain clasts of pelagic carbonate and basalt that can be correlated with the underlying Palaeocene – Early Eocene Ayios Nikolaos (Yamaçköy) Formation. Intact fragments of the source Paleogene succession are preserved as detached blocks (i.e. 'rafts'), up to ten metres long by several metres thick, set within chalky debris flows. Occasional limestone clasts can be correlated with the carbonate debris flow and carbonate breccia deposits that are exposed within the underlying Paleogene succession.

Slightly higher levels of the succession are exposed along the access road just south of the Armenian monastery (Antifonitis kilise), where crudely bedded debris-flow deposits include angular clasts of marble that can be correlated with the Triassic–Cretaceous Trypa (Tripa) Group (Figs 3, 9, log 3). Elsewhere, along the Değirmenlik (Kythrea) to Girne (Kyrenia) road (near Beşparmak/Pentadactylos Mountain; Fig. 3), chalky debris are dominated by pelagic carbonate and basalt that can be correlated with the Paleogene Ayios Nikolaos (Yamaçköy) Formation. The debris flows are intercalated with elongate blocks of sheared serpentinite, pillow basalt (highly weathered) and red ribbon radiolarite/red shale (Fig. 6iii). The lava is very vesicular and contains intrapillow pink pelagic limestone.

4.c. Successions in the Western Range

The Western Range differs fundamentally from the Central Range because of the absence of the E–W-trending steeply inclined thrust sheets of Mesozoic carbonate rocks (Trypa/Tripa Group). The Kalaograia–Ardana (Bahçeli–Ardahan) Formation forms two approximately E–W-trending outcrops (to the west of Kayalar/Orga) (Fig. 3), both dominated by debris-flow deposits. The more northerly of these is exposed along the coast and just inland, where the formation includes a large (tens-of-metre-sized) mass of marble that has been mapped as belonging to the St Hilarion (Hilaryon) Formation (Baroz, 1979). Where locally exposed beneath Quaternary terrace deposits, debris-flow deposits are packed with angular clasts of marble that are lithologically similar to the St Hilarion (Hilaryon) Formation. The limestone is likely to represent a large detached block ('olistolith') within the Kalaograia–Ardana (Bahçeli–Ardahan) Formation.

Along the coast in a bay near Karaoğlanoğlu (Ayios Georgios) (Fig. 3), there is an informative outcrop made up of steeply dipping, strongly sheared chalky debris-flow deposits (Figs 3, 9, log 1). These contain a 'raft' of chalky marl and basalt, lithologies typical of the Ayios Nikolaos (Yamaçköy) Formation (Fig. 6i).

https://doi.org/10.1017/S0016756813000563 Published online by Cambridge University Press

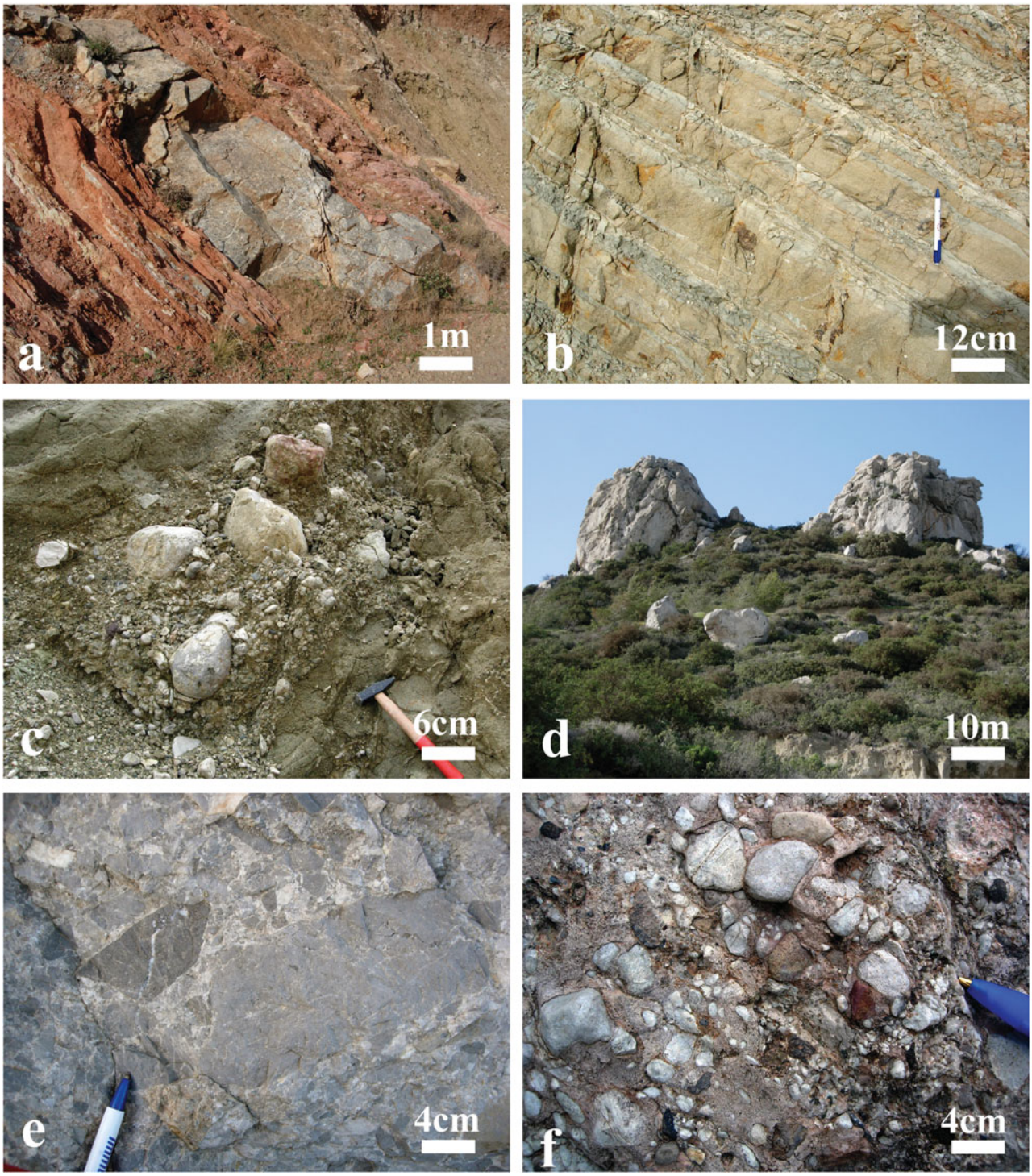

Figure 12. (Colour online) Field photographs. (a) Upper levels of the Ayios Nikolaos (Yamaçköy) Formation showing typical reddish-coloured background hemipelagic carbonates interbedded with a limestone debris flow, 1 km NE of Mallıdağ (Melounda), Eastern Range. (b) Well-bedded sandstones (high-density turbidites or mass-flow deposits) with mudstone intercalations (Geçitkale–Mersinlik/Lefkoniko–Flamoudi section; see Fig. 9, log 6). (c) Lenticular debris-flow deposit, including rounded clasts of neritic limestones, higher in the same section as (b). (d) Exotic blocks of Permian shallow-water limestone (Kantara Limestones) within a matrix of debris-flow deposits, crest of the Eastern Range near Phonia (see Fig. 9, log 5). (e) Limestone breccia related to the Kantara Limestones, interpreted as a contemporaneous slope deposit (not as part of the Eocene matrix of the sedimentary melange) near Kantara castle. (f) Debris-flow deposit dominated by well-rounded clasts of limestone (Kantara Limestones), interpreted as matrix of the sedimentary melange, near Phonia (see Fig. 9, log 5).

The debris flows are dominated by angular clasts of marble that can be correlated with the Mesozoic Trypa (Tripa) Group. There are also rare clasts of folded calc-schist, mica-schist, diabase and gabbro.

In summary, the lower levels of the Kalaograia–Ardana (Bahçeli–Ardahan) Formation in the Eastern Range are dominated by sandstone turbidites, together with conglomeratic debris-flow deposits.

https://doi.org/10.1017/S0016756813000563 Published online by Cambridge University Press

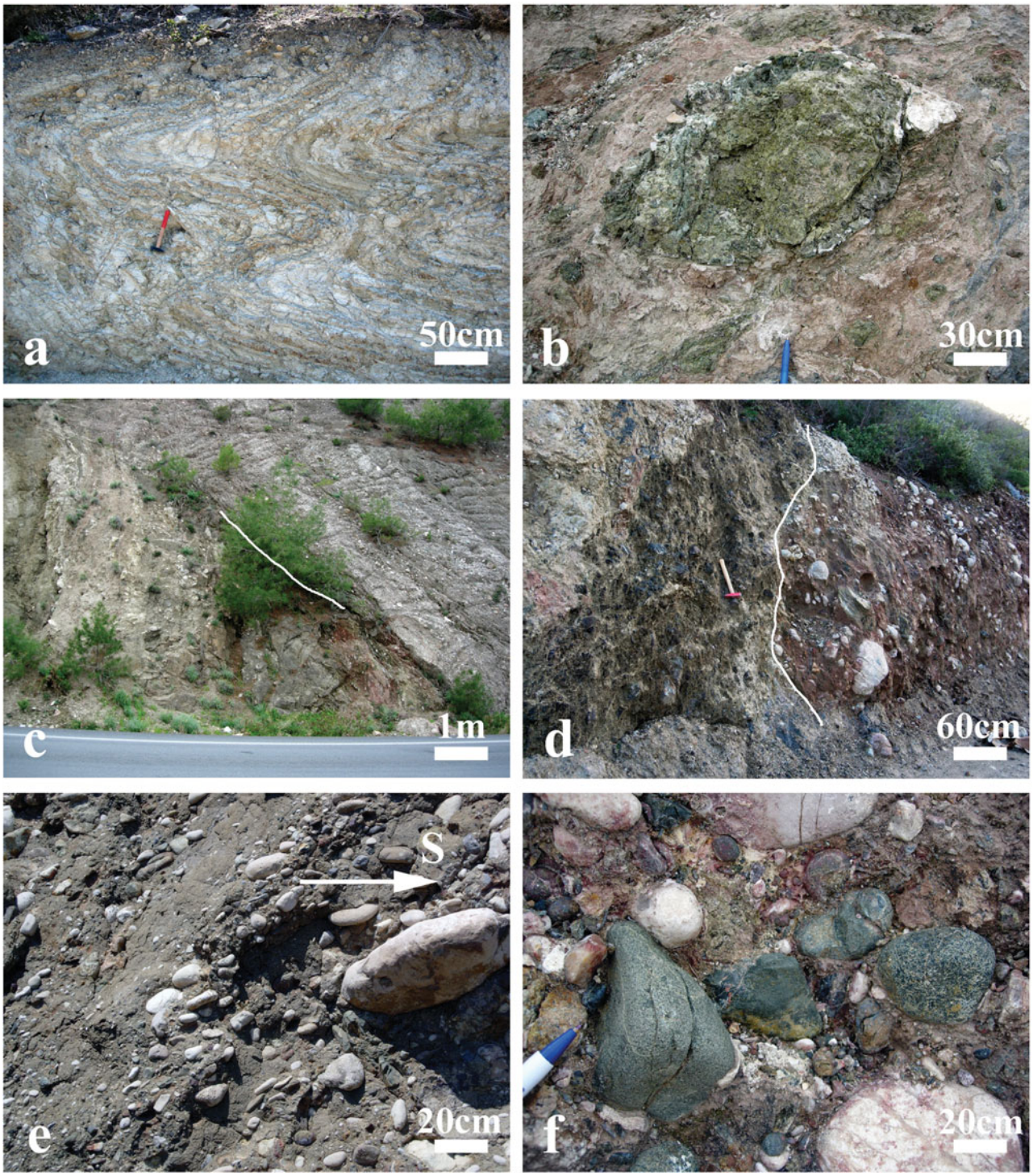

Figure 13. (Colour online) Field photographs. (a–d) Middle Eocene Kalaograia–Ardana (Bahçeli–Ardahan) Formation; (e, f) Late Eocene – Oligocene Bellapais (Beylerbey) Formation from the Central and Eastern ranges. (a) Soft-sediment slump deformation in the higher levels of the Geçitkale–Mersinlik (Lefkoniko–Flamoudi) road section, Eastern Range. (b) Detached block of serpentinized harzburgite in a matrix of sheared mudstones and debris-flow deposits; higher levels of the Ardahan (Ardana) to Kantara road section (see Fig. 9, log 6). (c) Unconformity (highlighted by white line) between Eocene bedded debris-flow deposits of the Kalaograia–Ardana (Bahçeli–Ardahan) Formation (subvertical) and the Upper Eocene – Oligocene basal conglomerates of the Bellapais (Beylerbey) Formation, road section 1 km WSW of Beşparmak (Pentadactylos). (d) Steep unconformity (marked as white line) between Eocene bedded debris-flow deposits of the Kalaograia–Ardana (Bahçeli–Ardahan) Formation and the Upper Eocene basal conglomerates of the Bellapais (Beylerbey) Formation (both subvertical), 0.4 km S of Beylerbey (Bellapais). (e) Basal conglomerate of the Beylerbey (Bellapais) Formation, showing well-developed clast imbrication picked out by elongate rounded limestone clasts, 1 km WSW of the site of Değirmenlik (Kythrea) spring; arrow shows inferred direction of palaeoflow. (f) Abundant well-rounded clasts of diabase and basalt in the basal conglomerate of the Bellapais (Beylerbey) Formation, 0.4 km S of Beylerbey (Bellapais).

https://doi.org/10.1017/S0016756813000563 Published online by Cambridge University Press

Similar gravity-controlled deposits are exposed in the lower levels of the succession in the Central Range (e.g. near Kythrea/Değirmenlik; Fig. 3). Higher levels of the formation in the Central Range are characterized by debris-flow deposits and sedimentary melange with ophiolite-related exotic blocks. In addition, the higher levels of the sequence in the Eastern Range are characterized by debris-flow deposits with exotic blocks of unmetamorphosed Middle Permian – Late Cretaceous limestones (Kantara Limestones). There are also some clasts of recrystallized carbonate rocks derived from the Mesozoic Trypa (Tripa) Group, which forms the core of the Central Range.

5. Lithofacies

The Kalaograia–Ardana (Bahçeli–Ardahan) Formation encompasses the main lithofacies as described in the following sections.

5.a. Pelagic chalks

Where developed, the background sediments are white–pale-grey soft, finely laminated chalks rich in clay, planktonic foraminifera and nannofossils. Washed samples were additionally found to contain abundant radiolaria and rare small benthic foraminifera. Relative to the other lithofacies, the pelagic chalks are most abundant in the lower and middle parts of the successions in the Eastern Kyrenia Range. Individual chalky interbeds are typically <30 cm thick but occasionally reach several metres in thickness in the form of repeated amalgamated units (e.g. Fig. 9, logs 4 and 6). In contrast, pelagic carbonates are rare or absent in the successions exposed at higher levels of the Eastern Range and throughout the Central and Western ranges.

5.b. Mudstones

Mudstones occur as thin partings within the pelagic chalks from the uppermost levels of individual gravity-flow deposits (<15 cm) (Fig. 12b) and also occur as discrete interbeds (mostly <50 cm thick). Mudstones mainly occur lower in the successions in the Eastern and Central ranges. A spot sample of mudstone from a short exposed sequence in the Central Range (from a road-cutting beneath Buffavento castle; Fig. 3) was analysed by X-ray diffraction (see G. McCay, unpublished PhD thesis, University of Edinburgh, 2010 for details of methods) and found to consist of calcite (52 %), palygorsite (16 %), quartz and chlorite (both *c.* 10 %), together with expandable clay, dolomite, albite, microcline, biotite and talc (each <5 %) plus minor muscovite, illite and kaolinite (each <5 %).

5.c. Sandstones

Sandstones mainly occur as normally graded interbeds, ranging up to several metres thick (Fig. 12b). Graded sandstones commonly contain rounded clasts up to tens of centimetres in diameter. Graded sandstones are best developed in the lower levels of the succession in the Eastern and Central ranges, where they are typically interbedded with mudstones and pelagic chalks. Most beds lack the internal sedimentary structures (e.g. parallel and cross-lamination) that characterize classical turbidity current deposits (Bouma, 1962).

A study of 20 representative thin-sections under the optical microscope revealed a wide range of constituents, as shown in Figure 14a–l.

1. Grains of ophiolite-related rocks in the form of abundant serpentinite, red radiolarian chert/shale (variably recrystallized) and minor basalt/diabase/microgabbro. Basalt is variably altered and ranges from aphyric to plagioclase-phyric (Fig. 14g, h, k, l).

2. Bioclastic grains, with variable amounts of reworked benthic foraminifera (often fragmented), shell fragments, echinoderm plates, calcareous algae and carbonate intraclasts (both pelagic and neritic derived) (Fig. 14a–d). The benthic foraminifera include *Orbitoclypeus ramaraoi ramaraoi*, *Nummulites* sp., *Discocyclina* sp., *Alveolina* sp. and *Sphaerogypsina* sp. (N. İnan, pers. comm. 2012).

3. Terrigenous grains, i.e. quartz, muscovite, biotite, ferromagnesian grains (clinopyroxene, amphibole), siltstone and also rare grains of metamorphic rocks (quartzite, folded mica schist, black phyllite and calcmylonite). Many of the quartz grains are unstrained, typical of quartz in plutonic rocks (e.g. granite) (Fig. 14e, i, j).

4. Well-lithified limestone (mainly micritic and biomicritic). Silicified limestone is also locally present in the form of grey microcrystalline chert.

5. Crystalline limestone (marble) and rare dolomite.

Other less-common grains include plagioclase, microcline, glauconite and chloritic lumps. Unrecrystallized limestone grains are common throughout the successions in the Eastern Range, while marble and dolomite are widespread in the Central and Western ranges. In some outcrops the upper part of the succession is dominated by serpentinite, basalt or radiolarian chert. Where a matrix is present this is generally micritic and is variably recrystallized to microspar-sized carbonate.

Five thin-sections representing typical sandstones from different parts of the range were point counted (400 points; 3 mm spacing). The data are plotted on three widely used ternary diagrams in Figure 15 (Dickinson & Suszec, 1979; Dickinson, 1985). The compositional fields of sandstones from the unconformably overlying Late Eocene – Miocene Kythrea (Değirmenlik) Group are shown for comparison (McCay & Robertson, 2012), as this highlights the rather unusual and specific composition of the Kalaograia–Ardana (Bahçeli–Ardahan) Formation.

The Q–F–L diagram (Fig. 15a) shows that the samples are overwhelmingly dominated by lithics, as are the sandstones from the overlying Kythrea

https://doi.org/10.1017/S0016756813000563 Published online by Cambridge University Press

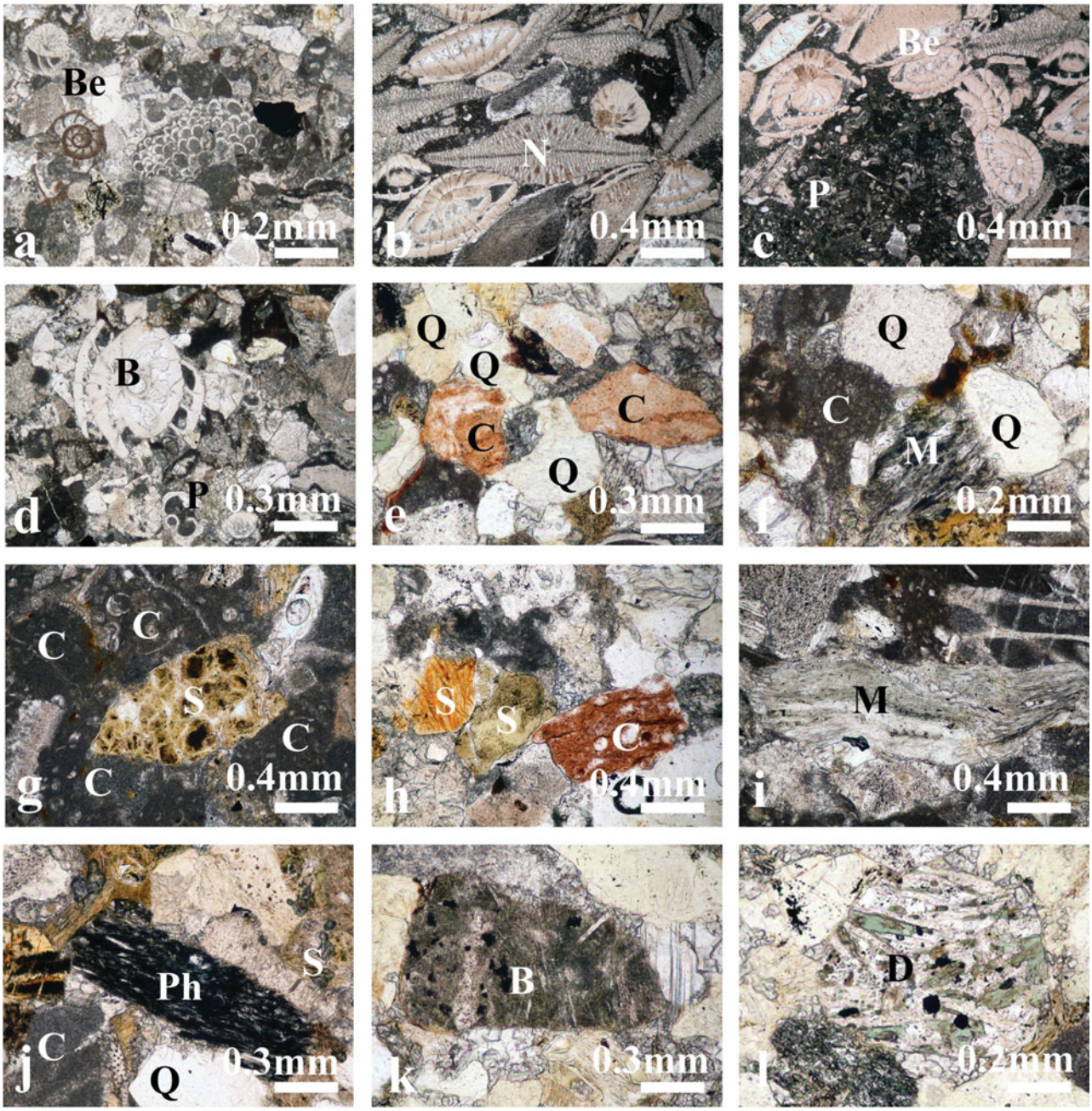

Figure 14. (Colour online) Photomicrographs of thin-sections viewed in plane-polarized light: (a–d) uppermost part of the Ayios Nikolaos (Yamaçköy) Formation; (e–l) Kalaograia–Ardana (Bahçeli–Ardahan) Formation. (a, b) Redeposited carbonate rich in benthic foraminifera, near Lapta (Lapithos), Central Range (see Fig. 6, section ii). (c) As (a, b) but showing the sparse matrix of biomicrite rich in planktonic foraminifera but free of terrigenous detritus. (d) Redeposited bioclastic carbonate rich in fragmented large foraminifera; near Beylerbey (Bellapais). (e) Terrigenous dominated sandstone, especially rich in angular fragments of quartz and radiolarian chert, near the Armenian Monastery (Antifonitis kilise), Central Range. (f) Typical mixed provenance sandstone including grains of quartz, calcareous bioclasts, serpentinite and schist, Geçitkale–Mersinlik (Lefkoniko–Flamoudi) road section. (g) Angular grains of serpentinite plus biomicrite and foliated micaschist; Geçitkale-Mersinlik (Lefkoniko-Flamoudi) road section. (h) Grains of serpentinite and radiolarian chert, plus mainly carbonate and quartz grains, near Mavri Skala, Eastern Range. (i) Foliated micaschist grain, Geçitkale–Mersinlik (Lefkoniko–Flamoudi) road section. (j) Black phyllite grain plus micritic carbonate, serpentinite and quartz, near Mavri Skala, Eastern Range. (k) Altered basalt grain, Geçitkale–Mersinlik (Lefkoniko–Flamoudi) road section. (l) Diabase grain with plagioclase microphenocrysts in a chloritized mesostasis near Kayalar (Orga), Eastern Range. B – basalt; Be – benthic foram; C – chert (variably recrystallized, both primary radiolarian chert and silica replaced carbonate); D – dolerite; M – metamorphic rock fragment; N – nummulitid; P –pelagic carbonate lithoclast; Ph – phyllite (metamorphic rock clast); Q – quartz; S – serpentinite (ophiolite-derived rock clast).

(Değirmenlik) Group. On the Qm–F–Lt diagram (Fig. 15b) the sandstones are very lithic rich, again similar to the Kythrea (Değirmenlik) Group. The sandstones are dominated by igneous lithics and sedimentary lithics on the Lm–Lv–Ls diagram (Fig. 15c), broadly similar to the overlying Kythrea (Değirmenlik). It should be noted that serpentinite, gabbro and microgabbo of plutonic (i.e. non-hyperbyssal origin)

https://doi.org/10.1017/S0016756813000563 Published online by Cambridge University Press

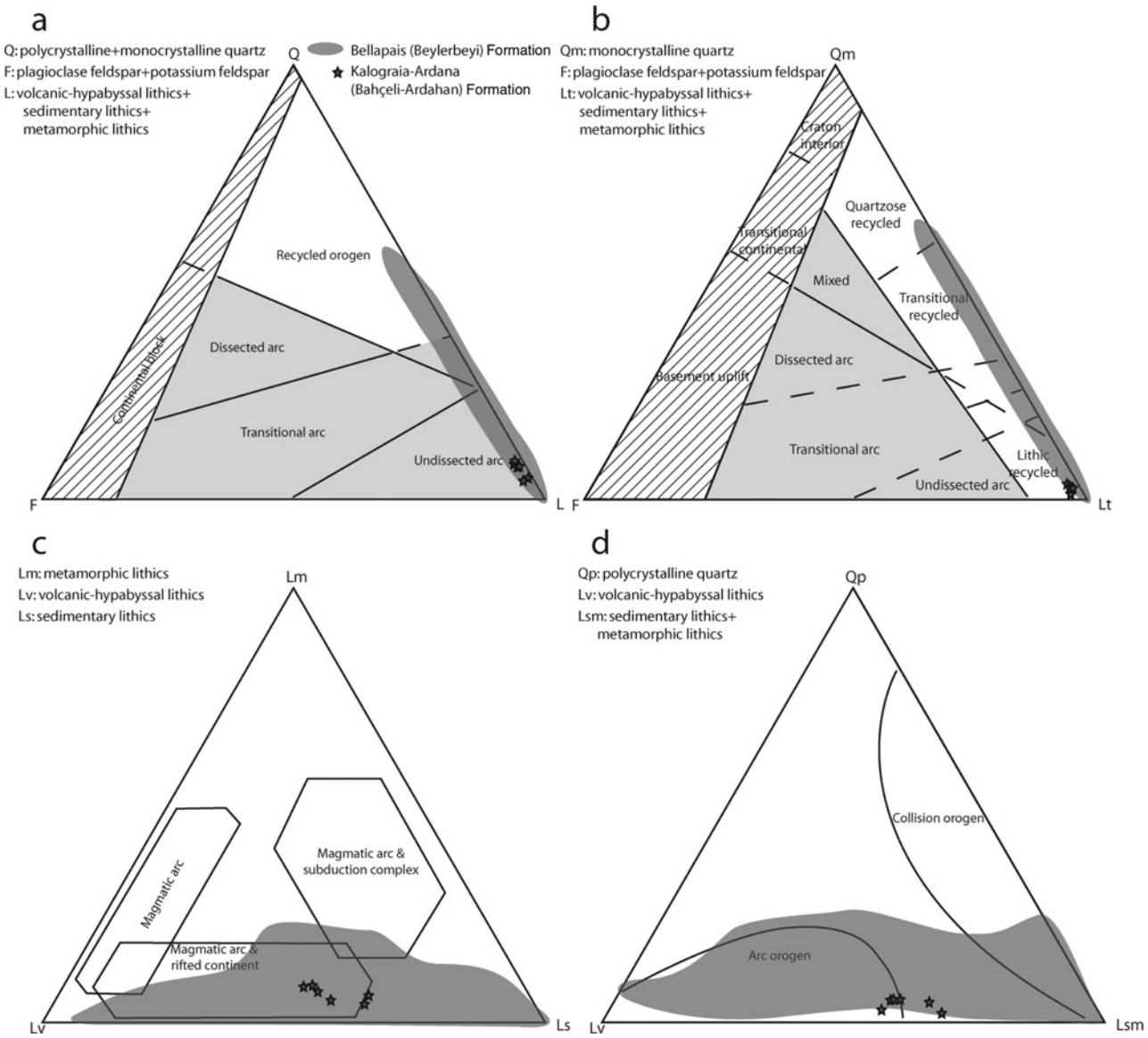

Figure 15. Point-count data (400 points per sample) for six representative sandstones from the different parts of the Kyrenia Range and comparisons with the composition of the unconformably overlying Late Eocene – Late Miocene Değirmenlik (Kythrea) Group (from G. McCay, unpubl. PhD thesis, University of Edinburgh, 2010; McCay & Robertson, 2012*a*). (a) Q-F-L plot (after Dickinson, 1985); (b) Qm-F-Lt diagram (after Suczec & Ingersoll, 1979); (c) Lm-Lv-Ls diagram (after Suczec & Ingersoll, 1979); (d) Qp-Lv-Lsm diagram (after Graham, Inresoll & Dickinson, 1976). See text for discussion.

are included within the igneous category. A plot of polycrystalline quartz versus volcanic-hyperbyssal lithics (again including plutonic rock grains) versus the combined sedimentary and metamorphic lithics (Qp–Lv–Lsm diagram; Fig. 15d) shows that the samples mainly lie within the much larger field of the overlying Kythrea (Değirmenlik) Group. The plots are greatly influenced by the abundance of serpentinite and carbonate clasts. When carbonate grains are excluded, a typical sample of sandstone from the Eastern Range contains 68 % ultramafic igneous grains (serpentinite), 15 % basic igneous grains (basalt, diabase, microgabbro), 12 % metamorphic grains (mainly schist) and 5 % sedimentary grains (shale and radiolarian chert). No significant compositional variation in the point-counted sandstones was observed according to location or stratigraphic position throughout the range.

5.d. Debris-flow deposits

Debris-flow deposits, which are commonly poorly consolidated, range in thickness from tens of centimetres to *c.* 10 m as individual depositional units (Fig. 12c). Debris-flow deposits occur throughout the succession in different areas from near the base upwards; however, they are most abundant higher in the succession in all areas (Fig. 12f). In the Eastern Range, the debris-flow deposits in the structurally lower successions are commonly interstratified with finer-grained deposits. The higher part of the succession in the Eastern Range and counterparts in the Central and Western ranges are almost entirely made up of mass-flow deposits and exotic blocks.

In the Eastern Range where the exposure is best (e.g. Fig. 9, logs 5–7), some of the individual debris-flow

https://doi.org/10.1017/S0016756813000563 Published online by Cambridge University Press

deposits map out as being lenticular on scales of metres to tens of metres. The more stratified debris-flow deposits in the lower levels are matrix supported and normally graded. In many cases, the matrix-supported conglomerates take the form of amalgamated units that pass upwards into graded sandstone. However, some of the debris-flow deposits are reverse graded, ungraded or show complex internal variation in clast size. South-directed clast imbrication was rarely observed in the Eastern Range. The mass-flow deposits in the upper levels of the succession, as best exposed in the Eastern Range, are generally thicker (up to *c.* 10 m thick as single depositional units) and vary from matrix supported to nearly clast supported (Fig. 9, log 6).

The composition of the debris-flow deposits varies considerably throughout the range. The clast composition was estimated in several sections. In the stratigraphically lower levels of the succession in the Eastern Range (Ardahan/Ardana to Kantara road section; Fig. 9, log 6) the clasts are estimated as 60% buff-coloured limestone (unrecrystallized) referable to the Kantara Limestones (i.e. exotic limestones), 20% marble and dolomite typical of the Trypa (Tripa) Group, 5% altered basaltic lava, 5% chalk typical of the Lapithos (Lapta) Group, 5% red radiolarian chert and 5% mudstone. Sandstone and shale intraclasts are locally present, together with rare metamorphic and ophiolite-related lithologies (e.g. schist, diabase/microgabbro). Some of the interstatified debris flows, especially those in the Central and Western ranges, are rich in pelagic carbonate and basalt typical of the Lapithos (Lapta) Group. Occasional clasts of well-lithified calcarenite, micro-conglomerate and sandstone suggest a polycyclic origin within the Middle Eocene basin.

The clast composition higher in the succession (Fig. 9, log 6) is variable, especially in the immediate vicinity of some blocks of limestone (Kantara Limestones) and dismembered thrust sheets of serpentinite. For example, one such debris-flow deposit made up of angular to subangular clasts (<30 cm in size) contains 70% carbonate rocks (referable to the Kantara Limestones), 10% marble and dolomite (typical of the Trypa/Tripa Group), 15% ophiolite-related lithologies (gabbro, diabase, serpentinite, basalt, red chert) and 5% metamorphic rocks (calcschist, quartzite, micaschist). In addition, there are scattered clasts of well-cemented micaceous sandstone and grey pelagic limestone. In contrast, several interbedded debris-flow units are much richer in microgabbro/diabase, red chert or serpentinized harzburgite (up to 90% by volume).

The degree of rounding and sorting varies greatly between different depositional units. For example, individual debris-flow units within a single succession can alternately be packed with clasts of radiolarian chert (rounded, slightly recrystallized), basalt/diabase (<2 m in size) or gabbro (rounded boulders <1 m in size). Close to the Kantara Limestone blocks limestone clasts of similar composition are highly angular, typical of subaqueous scree deposits.

5.e. Detached blocks

Detached blocks (defined as >1 m in size) are either of intraformational or exotic origin with respect to the rocks exposed in the Kyrenia Range. The lower and middle parts of the succession in the Central and Western ranges are characterized by elongate blocks of poorly lithified pelagic carbonate and basaltic volcanic rocks, similar to the Palaeocene – Early Eocene Ayios Nikolaos (Yamaçköy) Formation. At the lower end of the size spectrum the displaced units comprise attenuated beds (i.e. phacoids) several metres thick by <5 m long, set in a chalky matrix (e.g. near the Armenian monastery/Antifonitis kilise; Fig. 9, log 5). At the upper end of the size spectrum there are large displaced stratal packages, up to tens of metres long and many metres thick, set in poorly consolidated reworked chalk. These lithologies are well exposed along the road from the Armenian monastery (Antifonitis kilise) to Esentepe (Ayios Ambrosios), and also along the forest road westwards. The succession in the Western Range also contains abundant material typical of the Ayios Nikolaos (Yamaçköy) Formation (Fig. 9, log 1).

The upper parts of the successions throughout the range are characterized by exotic blocks that have no exposed source within the Kyrenia Range. These fall into two main lithological associations. The first is the Middle Permian – Late Cretaceous Kantara Limestones, while the second is represented by ophiolite-related lithologies. Clasts of basalt occur, especially in the higher stratigraphical levels associated with clasts of diabase, gabbro, serpentinite and red radiolarian chert.

The erosionally resistant Kantara Limestones characterize the crest of the Eastern Range, notably near Olimpos, Phonia, Sinan Tepe (Shiaoros) and Kantara (Figs 2, 3, 12d). The blocks are up to several hundred metres in size. Closely associated blocks appear to have been derived from the break-up of a once relatively continuous stratal unit (e.g. Sinan Tepe/Shiaoros; Fig. 9, log 7). Generally smaller limestone blocks (<10 m in size) are scattered within sandy mass-flow deposits (e.g. Phonia area; Fig. 9, log 5). In the type area (road to Kantara; Fig. 3) several limestone blocks lie on a carpet of serpentinite-derived mass-flow units, while others are enveloped in mass-flow deposits. In addition, blocks of serpentinite and other rocks are entrained in mass-flow units (e.g. higher levels of the Ardahan/Ardana to Kantara road section; Fig. 13b).

The Kantara Limestones are mainly micritic, ranging from shelly to pelletal, although sparitic carbonates are also locally present. Along the road to Kantara the limestones include weakly stratified sedimentary breccia that is made up of poorly sorted, angular clasts of micritic limestone (<30 cm in size), set in a pale granular matrix (Fig. 12e). The breccia includes occasional clasts of angular, medium-grained quartz-muscovite-rich sandstone.

The structurally and stratigraphically highest levels of the succession in the Eastern and Central ranges

https://doi.org/10.1017/S0016756813000563 Published online by Cambridge University Press

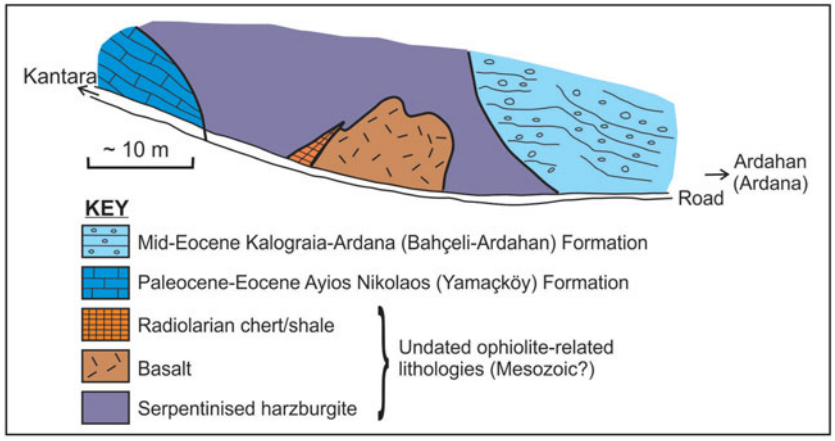

Figure 16. (Colour online) Field evidence of ophiolite-related lithologies in the upper part of the Kalaograia–Ardana (Bahçeli–Ardahan) Formation. The field relations are indicative of a pre-existing accretionary melange that included serpentinized harzburgite, pillow basalt and radiolarite. The older melange was emplaced as slide blocks within the debris-flow deposits of the Kalaograia–Ardana (Bahçeli–Ardahan) Formation in the upper part of the succession exposed along the Ardahan (Ardana) to Kantara road section, just S of the ridge crest (Fig. 9, log 6).

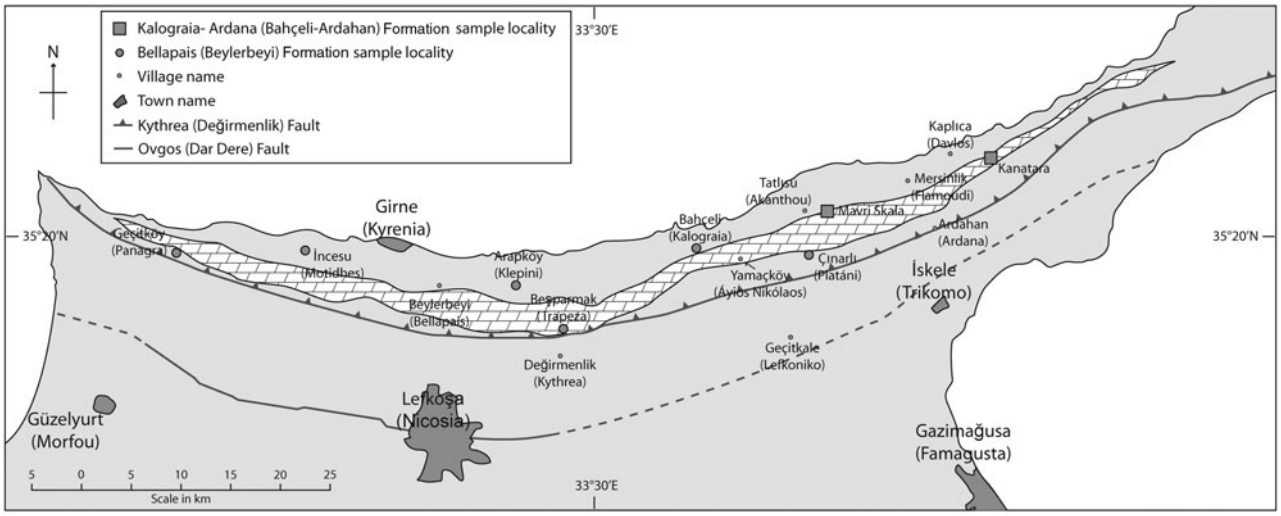

Figure 17. Locations of samples for which chemical analyses of basaltic rocks are reported here from the Middle Eocene Kalaograia–Ardana (Bahçeli–Ardahan) Formation (large filled squares) and the unconformably overlying Upper Eocene – Oligocene basal conglomerate of the Bellapais (Beylerbey) Formation (large filled circles); See Table 1.

include occasional elongate blocks and discontinuous sheets of serpentinized harzburgite (<20 m thick by several hundred metres long), for example, in the Kantara area (Fig. 9, log 6) and Beşparmak (Pentadactylos) areas (Fig. 6iii). The serpentinite is sheared and contains blocky inclusions (<1 m in size) of serpentinized harzburgite. Small sheets/blocks of radiolarian chert/shale, pillow lava and pillow breccia (highly altered) and gabbro are also locally present. The ophiolite-related rocks are in mutual contact with each other and define a block-against-block fabric (Fig. 16). This contrasts with the 'Kantara Limestone' blocks that occur individually within debris-flow deposits.

The field evidence suggests that the ophiolite-related blocks represent fragments of a pre-existing tectonic melange (i.e. recycled melange) that originally included serpentinite, basalt/microgabbo and radiolarian shale/chert.

5.f. Geochemistry of basaltic clasts

To determine the possible tectonic setting of origin of the basaltic rock, various samples of basalt, diabase and microgabbro were collected from the Mavri Skala, Kantara road and Sinan Tepe (Shiaoros) areas (Fig. 17). However, the mafic rocks are mostly strongly altered and only five samples proved to be compositionally suitable for tectonic discrimination (see Table 1).

The samples were analysed for major and trace elements by X-ray fluorescence (XRF) using the technique described by Fitton *et al.* (1998) and modified by Fitton & Godard (2004). When plotted on a diagram used to characterize altered basaltic rocks using elements that are immobile during weathering and low-grade alteration (Fig. 18b), the rocks plot in the basaltic field. Three of the samples are tholeiitic while two are of transitional composition (Fig. 18a).

https://doi.org/10.1017/S0016756813000563 Published online by Cambridge University Press

Table 1. Chemical data for basaltic clasts from conglomerates from the upper part of the Kalaograia–Ardana (Bahçeli–Ardahan) Formation. K samples: 24, 26: Mavri Skala; 34, 25: Ardahan–Kantara road section (see Fig. 16); 46: east of 34 and 25 on the road to Kantara. gam samples: gam-B2 and gam-B3 from Kalaograia (Bahçeli) village; gam-I3 and gam-I5 from Motidhes (İncesu) village; gam-C4, gam-C6 and gam-C7 collected from Platáni (Çınarlı) village; gam-K2R and gam-K10 from Kythrea (Değirmenlik) village; gam-P8 and gam-P9 from Panagra (Geçitköy) village. See Figure 17 for sample locations.

Sample name	K/10/24	K/10/26	K/10/34	K/10/35	K/10/46	gam-B2	gam-B3	gam-I3	gam-I5	gam-C4	gam-C6	gam-C7	gam-K2R	gam-K10	gam-P8	gam-P9
SiO_2	51.52	51.68	58.76	61.53	49.30	50.44	58.89	51.84	51.25	49.76	50.73	50.63	52.08	54.32	53.78	47.43
TiO_2	0.99	0.64	0.55	0.74	0.20	0.23	0.44	0.21	0.36	1.34	1.05	1.05	0.25	0.42	0.34	0.13
Al_2O_3	14.84	15.61	7.78	9.20	12.45	13.68	14.79	13.03	14.55	15.81	14.90	16.21	12.93	14.79	15.51	14.99
Fe_2O_3	10.84	10.78	3.04	4.28	8.12	8.22	8.58	6.45	9.21	9.93	10.32	9.95	8.50	9.68	9.46	8.34
MgO	8.03	7.96	1.39	1.87	11.04	10.47	4.74	12.03	8.82	6.73	6.83	6.40	9.86	6.31	7.03	12.33
CaO	8.20	9.06	13.43	9.67	12.31	8.22	4.42	12.82	8.98	11.53	8.59	10.82	9.36	9.08	8.78	12.72
Na_2O	2.91	2.36	1.31	1.32	1.62	3.59	2.64	0.46	1.68	2.07	3.95	3.14	3.18	0.58	2.44	0.65
K_2O	0.51	0.63	1.23	1.44	0.10	0.28	1.66	0.33	0.94	0.53	0.26	0.25	0.14	0.22	0.47	0.08
P_2O_5	0.09	0.04	0.09	0.10	0.02	0.02	0.05	0.01	0.02	0.12	0.08	0.09	0.02	0.03	0.02	0.01
MnO	0.15	0.16	0.10	0.10	0.15	0.15	0.16	0.08	0.14	0.17	0.16	0.18	0.14	0.14	0.14	0.13
LOI	2.43	1.15	12.35	9.91	4.69	4.29	3.17	2.32	3.53	1.82	2.63	1.28	3.56	3.95	1.89	3.36
Sum	100.51	100.07	100.02	100.16	100.00	99.59	99.54	99.58	99.48	99.81	99.50	99.99	100.01	99.51	99.87	100.17
Ni	84.70	108.80	65.50	98.20	116.60	184.30	139.90	259.80	184.50	48.80	48.80	58.60	132.00	83.50	84.30	205.50
Sc	42.90	48.90	11.00	12.60	58.60	41.90	36.10	53.30	50.90	51.10	44.80	43.10	55.90	44.20	50.40	60.70
Ba	215.00	310.00	212.20	253.30	7.70	150.40	64.30	176.50	382.10	194.60	41.20	41.80	292.80	1009.30	156.00	201.60
Nb	2.00	1.10	9.30	12.10	0.50	0.10	1.00	0.20	0.60	1.40	0.80	1.10	0.30	0.60	0.50	0.10
Rb	6.90	4.70	48.10	55.20	1.10	2.40	15.90	1.00	4.50	2.30	1.40	2.20	2.40	2.20	2.80	1.00
Sr	102.70	115.10	230.10	189.60	161.10	93.20	103.40	187.00	438.70	180.10	139.10	138.00	159.30	498.30	188.30	156.90
Th	0.80	0.40	5.50	6.70	0.30	−0.60	−0.30	−0.40	−0.70	0.10	−0.20	−0.10	−0.40	−0.30	−0.20	−0.20
U	0.20	0.50	1.50	1.90	−0.30	0.00	0.30	0.00	0.10	0.00	0.00	−0.20	−0.10	0.00	−0.20	0.00
V	308.40	328.20	76.00	94.40	221.60	231.20	257.40	281.40	283.20	345.00	352.70	291.80	282.20	325.60	292.30	237.10
Zr	57.30	24.00	87.80	129.00	8.40	3.40	31.30	4.20	8.60	85.10	55.40	61.20	5.80	10.10	8.40	3.20
Y	24.70	15.80	28.20	23.80	9.50	7.50	13.20	7.10	12.40	33.00	24.80	26.40	8.80	12.70	11.50	4.00
La	−0.80	−1.90	29.40	32.20	−1.90	−0.70	1.30	−0.60	−0.60	1.30	−0.40	−0.40	0.20	−0.40	−1.60	−1.70
Ce	6.10	1.90	57.80	69.90	0.40	−0.10	6.30	−0.10	0.30	11.70	10.70	9.60	−0.60	−2.80	0.50	0.80
Nd	4.10	0.90	28.50	31.70	−0.40	−0.20	1.10	0.40	−1.80	8.30	5.40	6.10	−0.80	−5.20	0.50	−2.90
Cs	–	–	–	–	–	0.80	0.20	<0.1	0.30	<0.1	0.40	0.10	0.70	0.10	0.10	<0.1
Hf	–	–	–	–	–	0.30	1.20	0.30	0.40	2.60	1.70	2.20	0.40	0.50	0.70	0.10
Ta	–	–	–	–	–	1.00	0.90	0.40	0.20	0.80	0.80	0.80	0.70	0.60	0.70	0.40
La	–	–	–	–	–	0.50	1.60	0.20	0.40	3.20	2.30	2.60	0.70	0.50	0.50	0.20
Ce	–	–	–	–	–	0.60	4.10	0.40	0.70	10.20	7.00	7.80	0.90	1.00	0.90	0.30
Pr	–	–	–	–	–	0.10	0.62	0.07	0.13	1.72	1.21	1.31	0.13	0.16	0.15	0.06
Nd	–	–	–	–	–	<0.3	3.40	0.60	1.10	9.70	6.50	8.10	0.50	1.00	1.00	0.60
Sm	–	–	–	–	–	0.34	1.29	0.29	0.50	3.05	2.29	2.42	0.35	0.56	0.50	0.15
Eu	–	–	–	–	–	0.15	0.35	0.15	0.19	1.17	0.90	0.91	0.16	0.23	0.21	0.10
Gd	–	–	–	–	–	0.73	1.66	0.60	1.08	4.41	3.19	3.35	0.78	1.15	0.96	0.44
Tb	–	–	–	–	–	0.17	0.33	0.15	0.24	0.85	0.64	0.65	0.18	0.26	0.24	0.10
Dy	–	–	–	–	–	1.06	2.09	1.10	1.77	5.26	3.84	4.00	1.23	1.99	1.76	0.63
Ho	–	–	–	–	–	0.26	0.47	0.25	0.43	1.15	0.83	0.86	0.30	0.45	0.37	0.18
Er	–	–	–	–	–	0.90	1.38	0.82	1.37	3.33	2.52	2.66	1.01	1.50	1.19	0.52
Tm	–	–	–	–	–	0.15	0.23	0.14	0.23	0.52	0.40	0.42	0.17	0.24	0.22	0.09
Yb	–	–	–	–	–	0.86	1.24	0.92	1.46	3.11	2.30	2.51	1.09	1.57	1.28	0.53
Lu	–	–	–	–	–	0.16	0.22	0.15	0.25	0.49	0.38	0.40	0.18	0.26	0.23	0.08

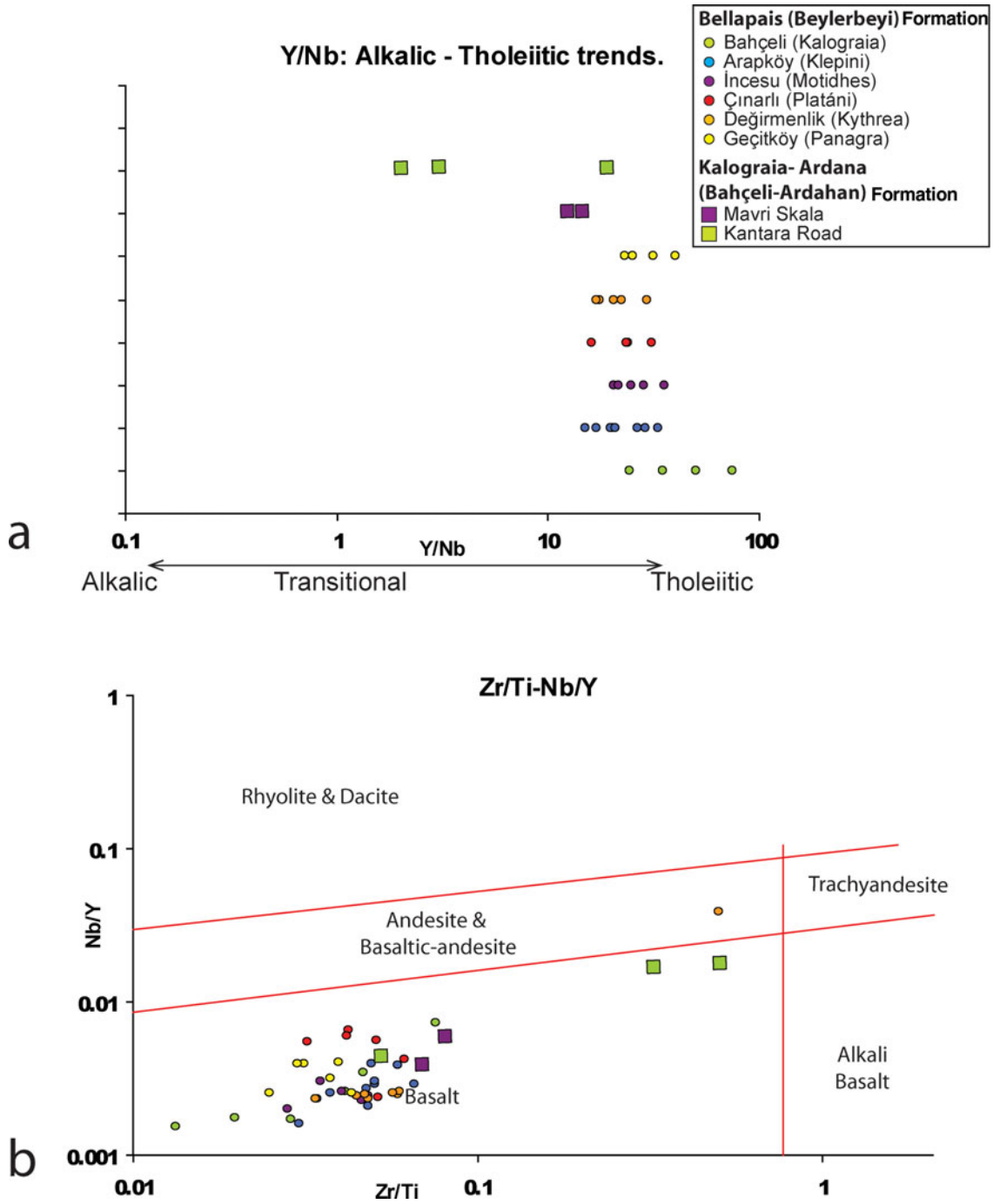

Figure 18. (Colour online) Rock nomenclature and rock characterization diagrams for basaltic clasts analysed from the Middle Eocene Kalaograia–Ardana (Bahçeli–Ardahan) Formation and the unconformably overlying Upper Eocene – Oligocene basal conglomerate of the Bellapais (Beylerbey) Formation. (a) Rock composition diagram showing that all of the clasts considered except two are tholeiitic (diagram from Pearce & Cann, 1973), (b) Rock classification showing that all but one of the rocks plotted are basaltic (diagram from Pearce, 1996). See Figure 17 for sample locations.

On normalized mid-ocean ridge basalt (N-MORB-) 'spider' plots that can be used to indicate the similarities to or differences from typical MORB (Fig. 19a), three samples plot close to MORB for most of the high-field-strength elements (HFSE). Two samples show strong magmatic depletion and exhibit U-shaped profiles, comparable with boninites (i.e. high-magnesian andesites). The large-ion-lithophile elements (LILE) are relatively enriched, which may reflect weathering. On bivariate diagrams that are used to infer tectonic setting (Fig. 20a–c), the samples are scattered through several different fields. However, two samples plot exclusively in the IAT (island arc tholeiite) or the VAB (volcanic arc basalt) fields (Fig. 20a, c). On the Ti/100 versus Zr versus Yx3 ternary diagram (Fig. 21a) the samples plot within or near the CAB (calc-alkaline basalt), IAT+MORB and IAT fields. On the TiO_2 versus MnO×10 versus P_2O_5×10 diagram (Fig. 21b), all of the samples plot within or close to the IAT field (with one on a boundary line) and the boninite field.

https://doi.org/10.1017/S0016756813000563 Published online by Cambridge University Press

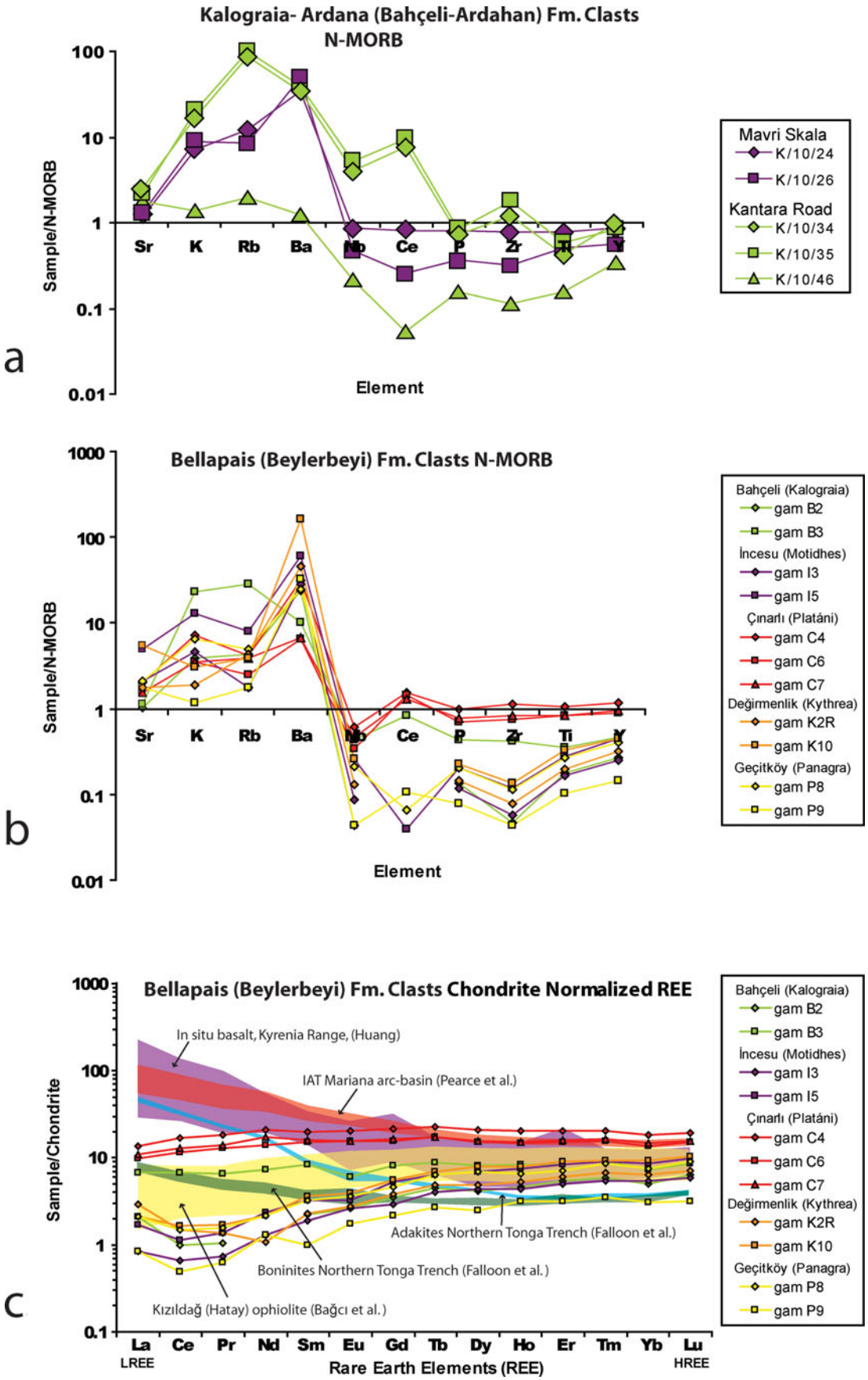

Figure 19. (Colour online) Normalized 'spider' diagrams. (a) N-MORB plot of clasts from the Middle Eocene Kalaograia–Ardana (Bahçeli–Ardahan) Formation. (b) N-MORB plot of clasts from the Upper Eocene – Ologocene basal conglomerate of the Bellapais (Beylerbey) Formation. (c) Chondrite-normalized plots of clasts from the Middle Eocene Kalaograia–Ardana (Bahçeli–Ardahan) Formation. Normalizing values from Sun & McDonough (1989). Comparative fields (shaded and labelled) from Kızlıdağ ophiolite (Pearce *et al.* 2005; K. Huang, unpubl, Masters thesis, University of Hong Kong, 2007; Bağçı *et al.* 2008; Faloon *et al.* 2008). See Figure 17 for sample locations.

https://doi.org/10.1017/S0016756813000563 Published online by Cambridge University Press

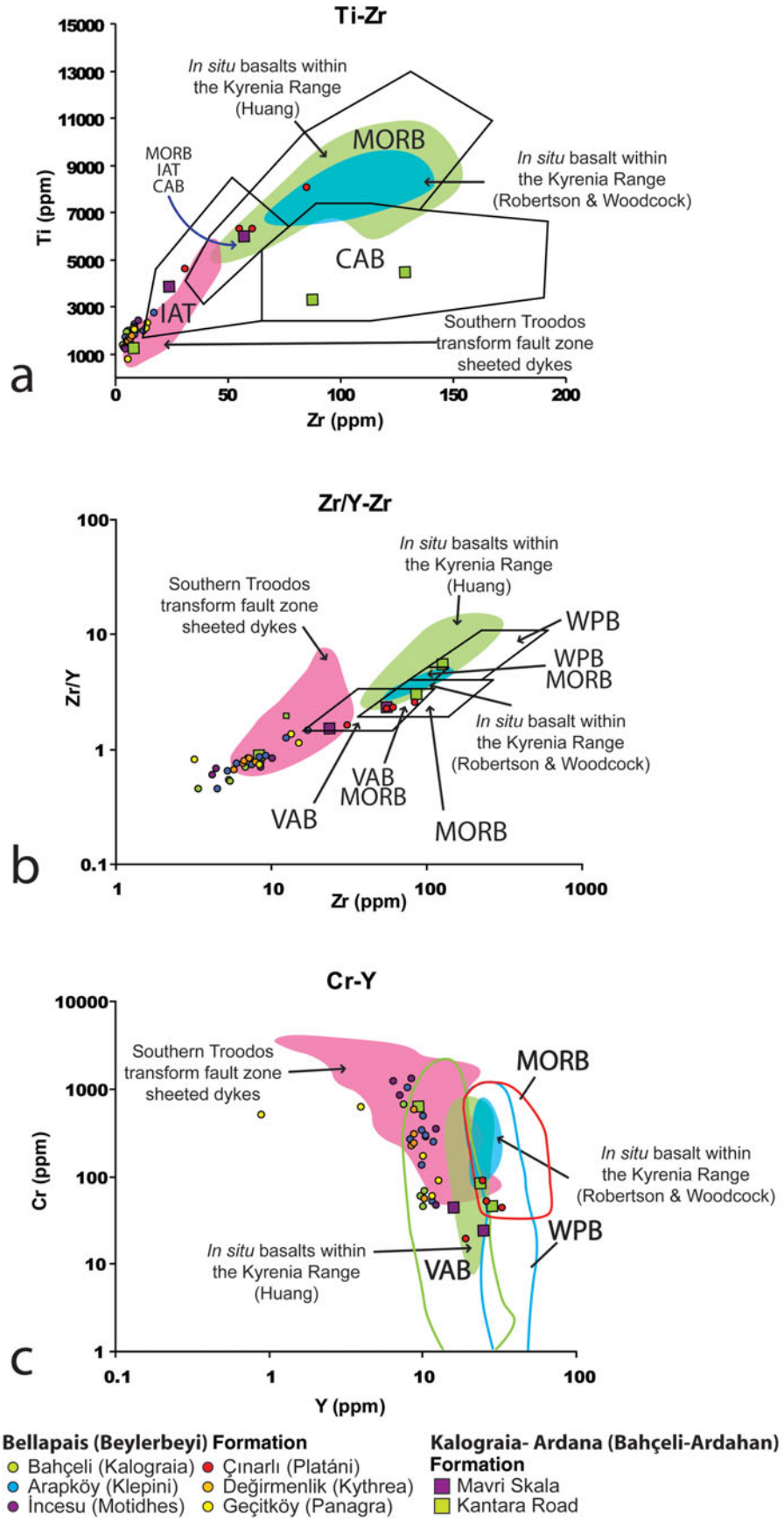

Figure 20. (Colour online) Bivariate tectonic discrimination diagrams for basaltic clasts from the upper part of the Middle Eocene Kalaograia–Ardana (Bahçeli–Ardahan) Formation and the unconformably overlying conglomerates (Late Eocene – Oligocene) of the Beylerbey (Bellapais) Formation: (a) Ti versus Zr (diagram from Pearce & Cann, 1973); (b) Zr/Y versus Zr (diagram from Pearce & Norry, 1979); and (c) Cr versus Y (diagram from Pearce, 1982). Comparative fields: Kyrenia Range (Robertson & Woodcock, 1986; K. Huang, unpubl, Masters thesis, University of Hong Kong, 2007) and South Troodos Transform Fault Zone (Gass *et al.* 1994). See Figure 17 for sample locations.

https://doi.org/10.1017/S0016756813000563 Published online by Cambridge University Press

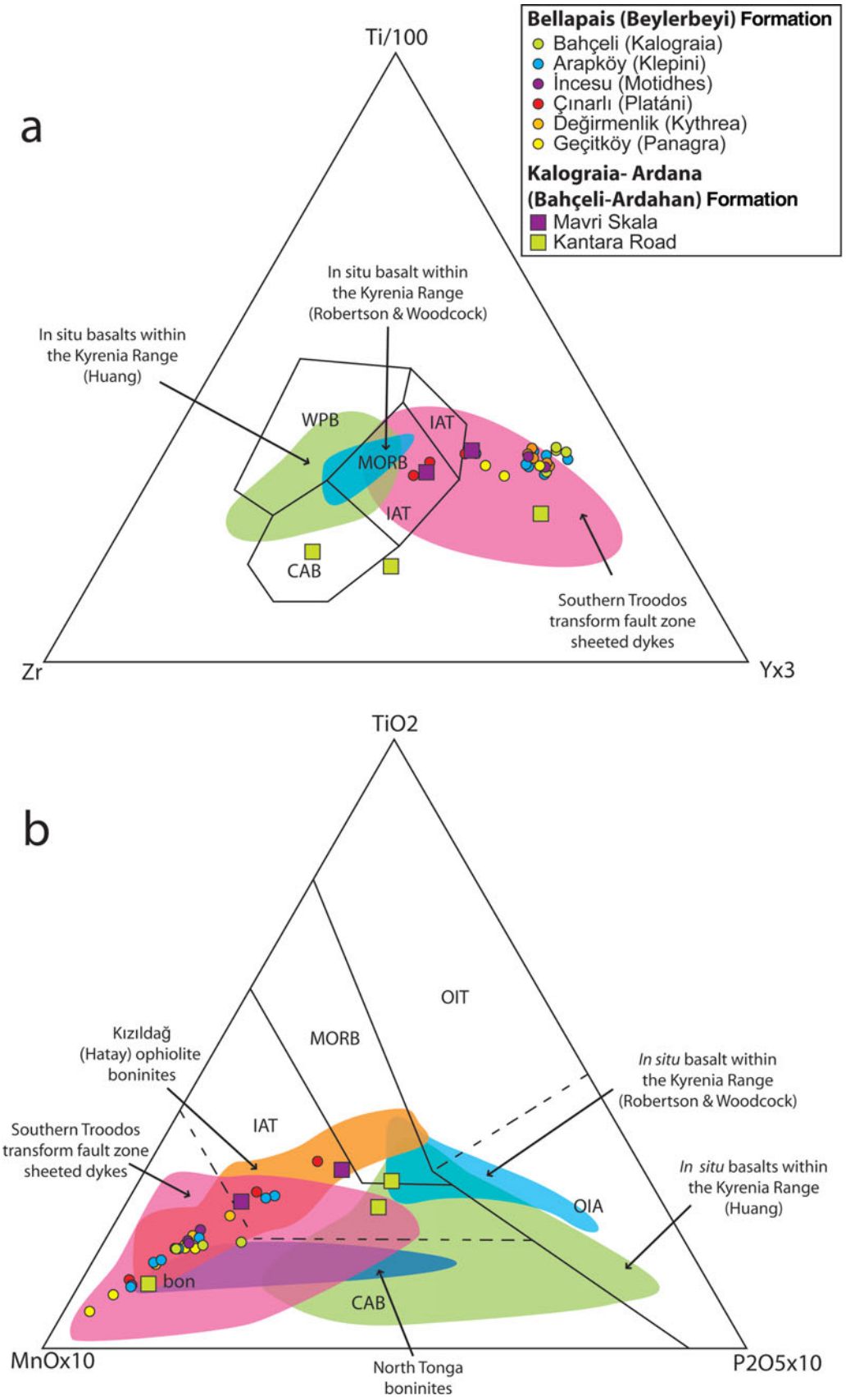

Figure 21. (Colour online) Ternary tectonic discrimination diagrams for basaltic clasts from the upper part of the Middle Eocene Kalaograia–Ardana (Bahçeli–Ardahan) Formation and the unconformably overlying conglomerates (Late Eocene) of the Bellapais (Beylerbey) Formation: (a) Ti versus Zr versus Yx3 (diagram from Pearce & Cann, 1973) and (b) TiO_2 versus MnO×10 versus $P_2O_5 \times 10$ (diagram from Mullen, 1983). See Figure 20 for key to fields and data sources.

https://doi.org/10.1017/S0016756813000563 Published online by Cambridge University Press

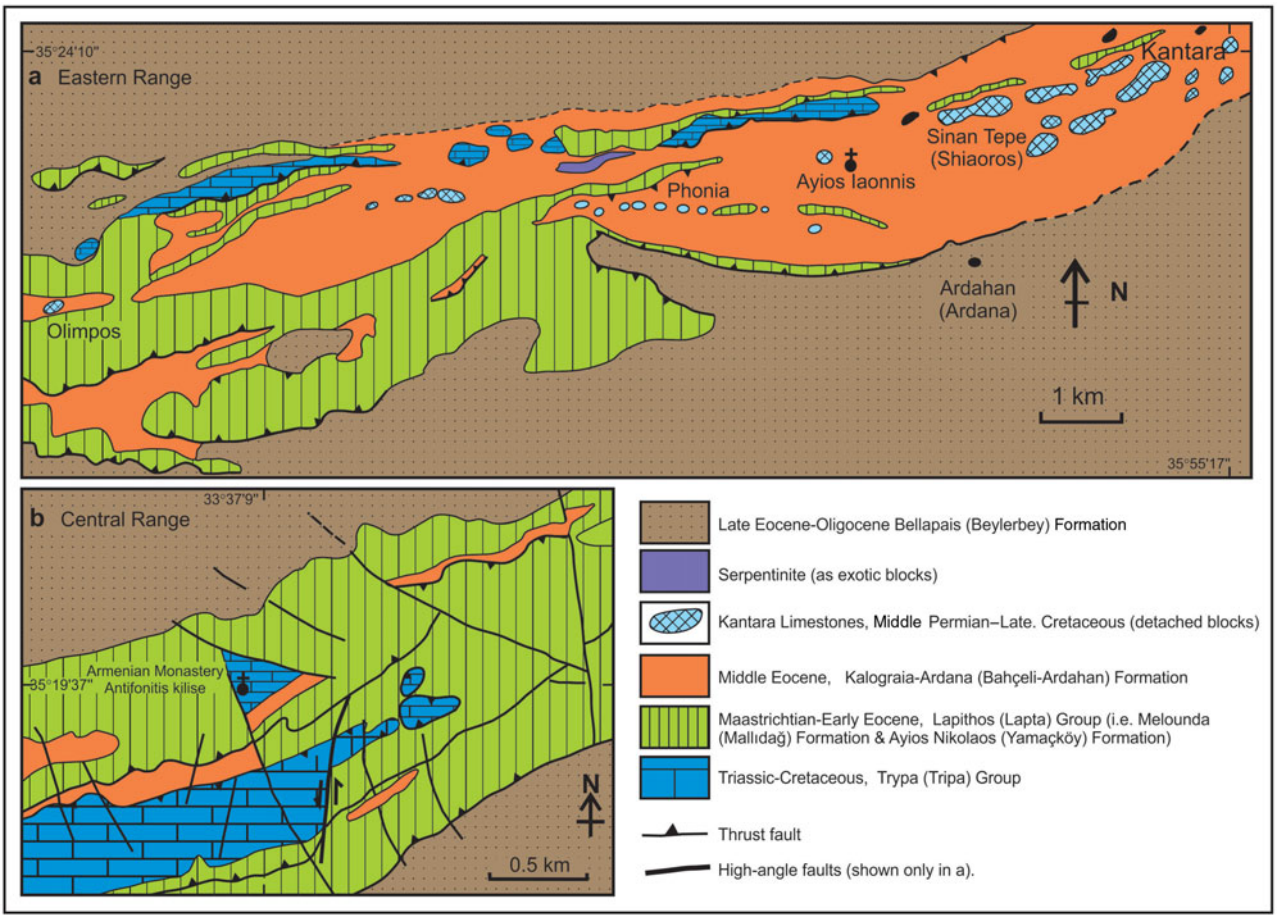

Figure 22. (Colour online) Key structural relationships showing: (a) the dissection of the Eastern Range into several large thrust sheets and (b) the contact area between the Central Range and the Eastern Range (both modified from Baroz, 1979).

On several of the tectonic discrimination diagrams, a few samples plot within the compositional field of the Maastrichtian – Early Eocene basalts of the Lapithos (Lapta) Group. The basalts of the Kyrenia Range are mainly of enriched within-plate type (Pearce, 1975; Robertson & Woodcock, 1986). However, some of the basalts exhibit a negative Nb anomaly, suggestive of a subduction influence (K. Huang, unpubl. Masters thesis, University of Hong Kong 2007). Such basalts cannot be distinguished from ophiolite-related basalts using the available geochemical data. However, some the basalts are inferred to have been derived from the Lapithos (Lapta) Group based on their co-occurrence with pelagic chalk derived from the Lapithos (Lapta) Group.

On each of the tectonic discrimination diagrams, at least one of the samples lies well outside the compositional range of the Lapithos (Lapta) Group. These samples, which include boninite, co-occur with clasts of ophiolite-related rocks (e.g. serpentinite, gabbro, radiolarian chert), suggesting an ophiolite-related origin.

6. Structural evidence

The entire stratigraphy beneath the Late Eocene – Oligocene Bellapais (Beylerbey) Formation was deformed into a pile of southwards-verging thrust sheets. The timing of thrusting is constrained as during or after the Middle Eocene deposition of the Kalaograia–Ardana (Bahçeli–Ardahan) Formation but prior to the accumulation of the unconformably overlying Late Eocene basal conglomerates of the Bellapais (Beylerbey) Formation.

The Eastern Range is dissected into two major thrust sheets, both of which are folded (Fig. 22a). In the Central Range, the Kalaograia–Ardana (Bahçeli–Ardahan) Formation is locally exposed in a lower thrust sheet. This is overthrust by a major thrust sheet of Mesozoic rocks that forms the core of the Central Kyrenia Range and includes extensive exposures of the Kalaograia–Ardana (Bahçeli–Ardahan) Formation. In the Western Range the formation is present in the lowest and highest levels of the thrust stack.

Throughout the Kyrenia Range the Maastrichtian – Early Eocene succession shows evidence of a penetrative pressure solution cleavage, which is best preserved in the well-lithified competent limestones compared to chalks and lavas. Widespread soft-sediment folding, mainly in the marls, chalks and sandstones, formed while the sediments were still poorly consolidated (Fig. 13a).

Throughout the range as a whole, the thrust geometry (e.g. fold and thrust vergence) is generally southwards-facing (Baroz, 1979; Robertson & Woodcock, 1986). In

https://doi.org/10.1017/S0016756813000563 Published online by Cambridge University Press

contrast, along the northern flank of the Central Range in some areas (e.g. near Bahçeli/Kalaograia; Figs 2, 6d) pelagic carbonates of the Lapithos (Lapta) Group exhibit outcrop-scale asymmetrical folding, C/S (where C is equivalent to the shear plane and S to the foliation) fabrics and small-scale duplexing, which indicate northwards displacement. The overlying Late Eocene – Late Miocene sedimentary rocks including the basal conglomerates lack this style of deformation.

The Kalaograia–Ardana (Bahçeli–Ardahan) Formation is commonly affected by high-angle faulting that is orientated subparallel to the range (e.g. in the type succession near Bahçeli/Kalaograia; Figs 2, 5). This deformation probably relates to left-lateral strike-slip transpression of at least partly Late Miocene – earliest Pliocene age (McCay & Robertson, 2013). In addition, the range is transected by numerous cross-cutting faults, the majority of which do not cut the overlying Late Eocene – Recent sediments (McCay & Robertson, 2013).

Regional mapping (Ducloz, 1972; Baroz, 1979) indicates that exposures of the Kalaograia–Ardana (Bahçeli–Ardahan) Formation in the Eastern Range trace westwards into the lower structural levels of the Central Range (Fig. 22b). The area where the Central Range passes into the Eastern Range is offset by an array of generally NNE–SSW-trending, mostly left-lateral, faults suggesting that the Central Range has been offset southwards with respect to the Eastern Range. This in turn suggests that facies typical of the Eastern Range may be present beneath the exposed front of the Central Range. Turbiditic and debris-flow deposits, comparable with the succession in the Eastern Range, are indeed locally exposed along the southern margin of the Central Range beneath younger deposits (e.g. below Bufavento castle; Fig. 3).

7. Geochemistry and provenance of clasts in overlying conglomerates

The sedimentology and composition of the basal conglomerates of the Bellapais (Beylerbey) Formation are important; their sedimentology sheds light on the regional palaeoenvironments during the Late Eocene – Oligocene, while their composition (lithological and geochemical) provides important information on the regional provenance of the sediments.

The basal conglomerates are interpreted as non-marine alluvial fan deposits (McCay & Robertson, 2012). These pass upwards into shallow-marine deltaic deposits and then into finer-grained deeper-marine gravity-flow deposits (McCay & Robertson 2012).

The clasts in the basal conglomerates are generally well rounded and well sorted. The conglomerates are mostly clast supported and were transported generally southwards, based on palaeocurrent evidence (e.g. clast imbrication) that was mainly collected from the southern flank of the range (McCay & Robertson, 2012; Fig. 13e). The conglomerates along the northern flank of the range are relatively disorganized (Fig. 13f), but where clast imbrication is present this is again generally southwards (McCay & Robertson, 2012).

The clasts making up the basal conglomerates are mainly sedimentary rocks, especially recrystallized carbonate, dolomite and pelagic carbonate (see G. A. McCay, unpubl. PhD thesis, University of Edinburgh, 2010 for quantitative clast count data). Igneous clasts are common, mainly dolerite and microgabbro (Fig. 13f). There are also occasional metamorphic rocks (e.g. marble, quartzite, schist), calcite vein material and intraclasts (e.g. shale). Relatively unaltered basalt is rare due to preferential weathering compared to diabase and microgabbro but was collected for chemical analysis where present. The sedimentary rocks can be correlated with the Triassic–Cretaceous Trypa (Tripa) Group and the Maastrichtian–Paleogene Lapithos (Lapta) Group. The conglomerates are relatively enriched in erosionally resistant rocks, especially radiolarian chert, quartzite and diabase. The conglomerates are thinner in the Eastern Range (<5 m) and mainly reflect the composition of the subjacent rocks, that is, the Maastrichtian–Paleogene Lapithos (Lapta) Group and the Middle Eocene Kalaograia–Ardana (Bahçeli–Ardahan) Formation. Clasts of lithologies similar to the Kantara Limestones are relatively abundant in the Eastern Range.

Forty-two clasts of basaltic composition (basalt, dolerite and microgabbro) were analysed by XRF (using the methods specified in Section 5.f.) from a total of six localities on both the northern and southern flanks of the range (see Fig. 17). Of these, 11 representative samples were analysed for Rare Earth Elements (REE) by inductively coupled plasma mass spectrometry (ICP-MS) at the Acme Analytical Laboratories Ltd., British Columbia, Canada (see Table 1).

The analysed clasts contain phenocrysts of plagioclase and clinopyroxene, together with microphenocrysts of plagioclase and pyroxene (altered) in a very fine-grained to glassy mesostasis. The phenocrysts show a glomero-porphyritic texture in some cases (G. McCay, unpubl. PhD thesis, University of Edinburgh, 2010).

Based on the abundances of relatively immobile elements, all but one of the samples are both basaltic and tholeiitic (Fig. 18a, b). On N-MORB spider plots (Fig. 19b) some of the basalts have a near-MORB composition of HFSEs but are relatively depleted in Nb. Other samples are more depleted in HFSEs with or without a relative negative Nb depletion. The U-shaped trends of the immobile elements in a number of the samples are characteristic of boninites. In addition, all of the samples are relatively enriched in LILEs which is probably due to alteration. On a chrondrite-normalized plot (Fig. 19c) some of the samples exhibit relatively primitive compositions, while others are relatively depleted. Some of the chrondrite-normalized patterns are similar to island arc tholeiites and boninites from several modern settings, including the northern Tonga trench and the Mariana arc-basin system.

https://doi.org/10.1017/S0016756813000563 Published online by Cambridge University Press

The samples were also plotted on a range of tectonic discriminations diagrams. On the Ti versus Zr diagram (Fig. 20a) some samples plot in the IAT (island arc tholeiite) field, while others extend into the MORB+IAT+CAB field. The majority of the samples plot outside the IAT field however, due to strong depletion in the relevant elements. The strong depletion is also apparent on the Zr/Y versus Zr diagram (Fig. 20b) in which only a small number of samples plot in the recognized MORB, WPB and IAT fields. On the Cr-Y versus Y diagram (Fig. 20c) the majority of the samples plot in the VAB field, with several in the MORB+WPB fields.

Further discrimination is achieved on the Ti/100 versus Zr versus Yx3 diagram (Fig. 21a), in which most of the samples plot outside the recognized fields due to strong depletion in Zr, with some in the MORB+VAB fields. Finally, on the TiO_2 versus $MnO\times10$ versus $P_2O_5\times10$ diagram (Mullen, 1983; Fig. 21b) the samples mainly plot in the boninite field, with some in the IAT field.

The most obvious source, the underlying basalts of the Maastrichtian–Palaeocene Lapithos (Lapta) Group, was not a major contributor to the analysed clasts in the basal conglomerates because few plot in the compositional field of these rocks. However, some less-depleted samples do lie within the range of compositions of the Lapithos (Lapta) Group basalts, reflecting the fact that some of these volcanic rocks exhibit a subduction influence (Huang, Malps & Xenophontos, 2007; K. Huang, unpubl. Masters thesis, University of Hong Kong, 2007). On the other hand, many of the samples are compositionally similar to the diabase dykes reported from the South Troodos Transform Fault Zone, which is generally accepted to have formed in a supra-subduction zone setting (Gass, 1990; Robinson & Malpas, 1990; MacLeod & Murton 1993; Gass *et al.* 1994). They are also compositionally similar to the sheeted dykes of the Eastern Albanian ophiolite (Phillips-Lander & Dilek, 2009) and some other ophiolites formed in supra-subduction zone settings.

8. Regional-scale structure

To place the Middle Eocene Kalaograia–Ardana (Bahçeli–Ardahan) Formation and the overlying basal conglomerates of the Bellapais (Beylerbey) Formation in the context of the Kyrenia Range as a whole, eight structural profiles were prepared based on reconnaissance traverses. The structural profiles (Fig. 23) highlight several key features as follows.

1. The stack of thrust sheets comprising the Kyrenia Range was finally emplaced southwards over Late Miocene gravity-flow deposits of the Kythrea (Değirmenlik) Group (Henson, Browne & McGinty, 1949; Robertson & Woodcock, 1986; Harrison *et al.* 2004; McCay & Robertson 2013; Fig. 23a–h). The basal thrust along the southern front of the range can be equated with the Kythrea Fault, as mapped by Baroz (1979) (Fig. 2; McCay & Robertson, 2013).

2. Late Eocene – Miocene sediments of the Kythrea (Değirmenlik) Group are incorporated into the structurally lower levels of the thrust stack, especially in the western part of the Central Range (Fig. 23a). The thrust stack therefore cuts downwards in the direction of overall tectonic transport during the Late Miocene – earliest Pliocene late-stage phase of thrusting.

3. Local stratigraphical way-up reversals indicate the presence of large-scale south-verging recumbent folds (nappes) in several areas (e.g. Eastern Range: Fig. 23g, h; Western Range: see Robertson, Taslı & İnan, 2012*b*). These are of potentially of Eocene and/or Late Miocene – earliest Pliocene age.

4. The stratigraphy is dissected by approximately E–W-trending high-angle faults, especially in the Eastern Range (Fig. 23f, g); these faults are interpreted as left-lateral strike-slip faults, again potentially of Eocene and/or Late Miocene – earliest Pliocene age.

5. North-verging backthrusting is widely developed along the northern flank of the range, related to both the Middle Eocene and the Late Miocene – Early Pliocene phases of thrusting (Fig. 23a, g).

6. In addition, the thrust stack is cut by numerous approximately N–S-trending faults of different offset (e.g. separating the Eastern and Western ranges) that do not appear in the N–S traverses.

9. Discussion and interpretation

The lithologies making up the Middle Eocene Kalaograia–Ardana (Bahçeli–Ardahan) Formation and the overlying Beylerbey (Bellapais) Formation are interpreted below in the light of the Permian–Recent geological development of the Kyrenia Range.

9.a. Late Palaeozoic – Cretaceous

The oldest-known rocks in the Kyrenia Range are represented by the Permo-Carbonifeorus limestone exotics (Kantara Limestones). These carbonates accumulated on a shallow, subsiding carbonate shelf that was populated by large foraminifera (fusulinids). The foraminiferal assemblage (e.g. *Hemigordius* sp.) is typical of a marginal Gondwana-related setting (Jin & Yang, 2004). Tectonic instability is suggested by the occurrence of the poorly stratified talus breccias in the Eastern Range. The presence of clasts of quartz-muscovite-rich sandstone further suggests that these carbonates accumulated on a continental basement rather than in an oceanic setting as seamounts. The additional presence of Mesozoic limestone exotics (Baroz, 1979) suggests that the carbonate platform persisted from Late Palaeozoic to Late Mesozoic time.

Early-stage northwards subduction is inferred to have lead to burial and greenschist facies metamorphism of the Mesozoic Trypa (Tripa) Group during Late Cretaceous time (Robertson, Taslı and İnan,

https://doi.org/10.1017/S0016756813000563 Published online by Cambridge University Press

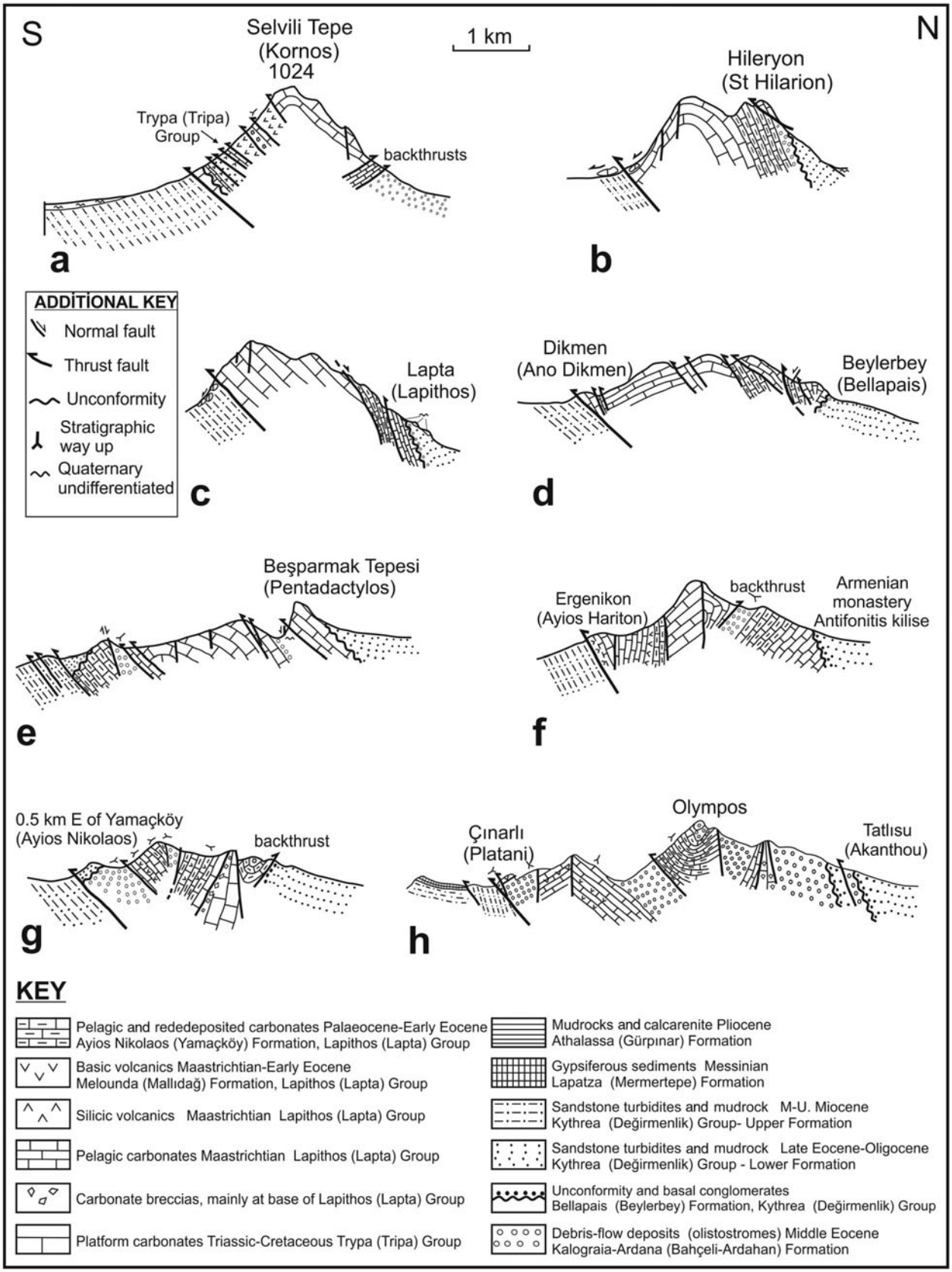

Figure 23. Structural profiles of the Kyrenia Range illustrating the relative roles of the Late Eocene versus Late Miocene thrusting. See Figures 2 and 3 for locations. Note the setting of the Middle Eocene Kalaograia–Ardana (Bahçeli–Ardahan) Formation and the unconformably overlying Late Eocene – Oligocene Bellapais (Beylerbey) Formation. The range as a whole is thrust southwards over Middle Miocene turbidites and locally evaporitic sediments of the Kythrea (Değirmenlik) Group. The basal thrust fault of the range is laterally continuous although locally obscured by Quaternary deposits (e.g. landslips). Individual profiles show the following distinctive features. (a) Imbrication of Neogene (Oligocene – Upper Miocene) terrigenous sediments (Kythrea/Değirmenlik Group) within the thrust stack; local stratigraphic inversion indicates the presence of large-scale S-facing recumbent folds; back thrusting (Late Miocene) characterizes the north margin of the range in this area. (b) High-angle faulting and large-scale landslipping

https://doi.org/10.1017/S0016756813000563 Published online by Cambridge University Press

2012*b*; Fig. 4). This was followed by exhumation during Maastrichtian time and the formation of subaqueous carbonate breccias. These coarse clastic sediments pass upwards into pelagic carbonates and then into terrigenous turbidites and mudrocks (Kiparisso Vouno/Alevkaya Tepe Member). The terrigenous sediments were derived from an adjacent continental margin setting onto which ophiolite-related rocks had been emplaced (Robertson, Taslı and İnan, 2012*b*; Fig. 4).

The northwards subduction also gave rise to Late Cretaceous arc volcanism in the Kyrenia Range (Baroz, 1979, 1980; Huang, Malpas & Xenophontos, 2007; K. Huang, unpubl. Masters thesis, University of Hong Kong, 2007; Robertson, Taslı and İnan, 2012*b*). Such volcanism is also reflected in the presence of arc-derived volcaniclastic sediments (Kannaviou Formation) in SW Cyprus (Robertson, 1977*c*; Gilbert & Robertson, 2013).

During the Maastrichtian – Early Eocene the meta-platform rocks of the Kyrenia Range, by then exhumed, were blanketed by pelagic carbonates of the Lapithos (Lapta) Group in a deep-sea carbonate-depositing setting. Locally interbedded carbonate-rock breccias were derived from the underlying meta-carbonate platform by gravity-flow processes, probably related to mass wasting of subaqueous fault scarps. Outpouring of basalts of mainly alkaline composition took place in an extensional or transtensional setting (Pearce, 1975; Robertson & Woodcock, 1986; Huang, Malpas & Xenophontos, 2007; K. Huang, unpubl. Masters thesis, University of Hong Kong, 2010). The subduction signature in some of the basalts may reflect chemical inheritance from the preceding Late Cretaceous subduction (Robertson, Taslı and İnan, 2012*b*). The Late Cretaceous (Campanian–Maastrichtian) – Early Eocene volcanism took place during the anticlockwise palaeorotation of the Troodos microplate (Campanian – Early Eocene; Morris *et al.* 2006; Inwood *et al.* 2009).

9.b. Middle Eocene sedimentary processes

The base of the Kalaograia–Ardana (Bahçeli–Ardahan) Formation is marked by an influx of fine-grained argillaceous sediments over Early Eocene deep-water pelagic carbonates (Ayios Nikolaos/Yamaçköy Formation). The floor of the pre-existing pelagic-depositing basin was destabilized by subaqueous faulting, as indicated by the appearance of coarse, proximal mass-flow deposits. The background sedimentation continued to be of deep-water origin, as shown by the intercalations of pelagic carbonates rich in calcareous nannofossils, planktonic foraminifera and radiolarians. The mudrocks are interpreted as hemipelagic sediments, that is, mixed fine-grained terrigenous and pelagic sediment.

The abundance of palygorskite in the mudstones suggests that weathering in the source area may have taken place in an environment that was subject to high salinity. Evaporitic deposits are widespread during the Eocene on the Turkish mainland (e.g. in the Ulukışla and Sivas basins; Clark & Robertson, 2005).

The graded sandstones (generally without well-developed Bouma-type sequences) are generally interpreted as high-density turbidity current deposits (e.g. Mutti & Ricci Lucci, 1975, 1978; Pickering, Hiscott & Hien, 1989). In addition, there are many examples of amalgamated depositional units which show considerable variability. For example, graded or ungraded sandstones alternate with intervals rich in intraformational clasts of mudstone or chalk. These may be composite co-genetic flows that characterize unstable slopes where flow concentration increases with the distance of travel (i.e. flow run-out) (Haughton *et al.* 2009). Flow partitioning can then give rise to repeated alternations of depositional units akin to turbidites and debris-flow deposits (debrites). The intercalations of mass-flow units and pelagic carbonates can be related to the progradation of subaqueous channels that were influenced by switches in the locus of sediment supply. In addition, the well-rounded nature of many of the clasts in the conglomerates is indicative of reworking in a shallow-marine or fluvial setting, followed by final deposition within gravity flows.

The petrographic evidence shows that up to 50 % or more of the silt- to sand-sized grains in the Kalaograia–Ardana (Bahçeli–Ardahan) Formation are carbonate lithoclasts. Micritic grains, locally with planktonic foraminifera, are likely to have been derived from the subjacent Maastrichtian – Early Eocene Lapithos (Lapta) Group, while recrystallized limestone (marble) and dolomite were derived from the Triassic–Cretaceous Trypa (Tripa) Group. Common grains of unrecrystallized (or weakly recrystallized) carbonate were derived from platform carbonates, as represented

(Early–Middle Pleistocene) along the southern range front; southwards-directed thrusting. (c) South-directed thrusting; high-angle faulting and also large-scale landslipping along the southern range front; top-to-north normal faulting may relate to pre-Neogene exhumation. (d) Large-scale southwards imbrication of the Mesozoic carbonate platform; folding (Late Eocene) and lateral displacement along high-angle strike-slip or transpressional faults; top-to-north normal faulting along the northern range margin (possibly related to pre-Neogene exhumation). The unconformity between the Middle Eocene Kalaograia–Ardana (Bahçeli–Ardahan) Formation and the Upper Eocene – Upper Miocene Bellapais (Beylerbey) Formation is locally overturned. (e) Southwards imbrication of Mesozoic and Paleogene lithologies relates to Eocene thrusting. Evidence of strike-slip displacement and steep (neotectonic) normal faulting (e.g. SSW face of Beşparmak (Pentadactylos). (f) Range interior cut by steep faults that probably originated as Eocene thrusts that were steepened and reactivated by strike-slip (or transpression). (g) Late Eocene thrusting associated with large-scale S-verging folding; the unconformity between the Mesozoic meta-carbonate (Trypa/Tripa Group) and the Maastrichtian Melounda (Mallıdağ) Formation was reactivated by high-angle faulting (Late Miocene or possibly younger). Late Miocene backthrusting affected the northern margin of the range. (h) Eocene and Late Miocene southwards thrusting and high-angle faulting.

https://doi.org/10.1017/S0016756813000563 Published online by Cambridge University Press

by the Middle?–Late Permian – Late Cretaceous exotic limestone blocks in the melange.

In addition, clasts of limestone that are rich in large foraminifera (e.g. *Nummulites* sp.) were observed in several areas e.g. south of Alsancak (Karavas) and near Beylerbey (Bellapais) ('Milous Breccias' of Baroz, 1979; see also online Supplementary Material available at http://journals.cambridge.org/geo). These nummulitid limestones were derived from a carbonate shelf of Middle Eocene age that is not preserved in the Kyrenia Range. As a result, the shelf carbonates were redeposited onto the pre-existing Early Eocene pelagic chalks of the Ayios Nikolaos (Yamaçköy) Formation. The pelagic carbonates of the Ayios Nikolaos (Yamaçköy) Formation are interpreted to have passed northwards (continentwards) into a carbonate slope and shelf. During an early stage in the construction of the Kalaograia–Ardana (Bahçeli–Ardahan) Formation, the carbonate shelf/slope was disrupted and disintegrated creating the gravity flows rich in large foraminifera.

The Kalaograia–Ardana (Bahçeli–Ardahan) Formation includes abundant non-calcareous material, predominantly serpentinite, together with subordinate basalt, diabase and micro-gabbro, for which ophiolitic rocks are the obvious source. In addition, scattered to locally abundant grains of red shale, radiolarian-rich shale and radiolarite (variably recrystallized) are interpreted as being derived from deep-marine pelagic sedimentary rocks, probably of Mesozoic age. Sparse but persistent metamorphic rock grains (mainly phyllite, micaschist) are likely to have been reworked from continentally derived lithologies. Possible sources include low-grade phyllite and mica-schist intercalations within the deformed and metamorphosed Mesozoic Trypa (Tripa) Group in the Kyrenia Range and also various metamorphic rocks on the Turkish mainland.

The thrusting that affected the Kalaograia–Ardana (Bahçeli–Ardahan) Formation (Fig. 23) is likely to have affected areas further north first and then migrated southwards to the area of the Kyrenia Range. The thrusting in the hinterland is inferred to have triggered erosion of Paleogene marginal carbonate sediments, the inferred Late Cretaceous accretionary melange and the northwards extension of the Late Palaeozoic – Mesozoic carbonate platform. This resulted in southwards progradation of various gravity flows and exotic blocks (equivalent to Kantara Limestones) derived from the different observed lithologies.

After removing the effects of deformation of different ages (Eocene and Late Miocene – Early Pliocene), the Kalaograia–Ardana (Bahçeli–Ardahan) Formation is restored as relatively proximal (in the north) to more distal (in the south). The similarity in the composition of the sandstones throughout the range suggests that similar rocks were exposed in a broad area to the north. A single tectonically controlled sedimentary basin formed in the area of the present Kyrenia Range. More distal equivalents were presumably deposited further south but are not exposed or were removed (e.g. by later subduction).

The southerly part of the basin is inferred to have extended from the Eastern Range (and the Karpas Peninsula) through to the Western Range. This area was dominated by sandy and conglomeratic mass-flow deposits that are interbedded with mudrocks and pelagic carbonates. In contrast, the more proximal (northerly) part of the basin experienced extreme tectonic instability, marked by the emplacement of debris-flow deposits and detached blocks ('olistoliths') of ophiolite-related rocks and the Kantara Limestones.

The differences in facies along the range can be explained by local differences in the source areas, which are interpreted as different parts of a pre-existing E–W-trending thrust belt (Late Cretaceous?). In the area of the Eastern Range, the leading edge of the advancing thrust front included Permian–Cretaceous platform carbonates (Kantara Limestones) plus ophiolite-related melange. In contrast, in the area of the Central Range the front of the advancing thrust pile was dominated by ophiolitic-related melange.

Following the Middle–Late Eocene folding and thrusting, a short period of subaerial weathering and erosion is represented by thin palaeo-colluvial deposits (McCay & Robertson, 2012). Alluvial fans, including abundant rounded ophiolite-related clasts (diabase, microgabbo, radiolarian chert) then transgressed the land surface, marking the base of the Late Eocene – Oligocene Bellapais (Beylerbey) Formation (Fig. 24). The source area of the basal conglomerates was mainly to the north, including pre-existing accretionary melange and ophiolitic rocks (e.g. boninites).

10. Regional setting

Any interpretation needs to take account of the geology of the adjacent areas, especially equivalents of the Kalaograia–Ardana (Bahçeli–Ardahan) Formation exposed in southern Turkey.

The Kyrenia Range extends NE-wards beneath Cilicia Basin to re-emerge on the mainland as the Misis Range (Fig. 1). The Misis Range is dominated by blocks of Mesozoic platform carbonate set in a siliciclastic matrix of gravity-flow deposits (Kelling *et al.* 1987; Gökçen *et al.* 1988; Robertson *et al.* 2004). The Misis Range is covered by, or faulted against, Quaternary sediments to the north, while it is thrust southwards over Early Miocene deep-water clastic sedimentary rocks to the south. The main difference between the Eastern Kyrenia Range (plus the Karpas Peninsula) and the Misis Range is that in the latter area the clastic matrix between exotic blocks of limestone is reported to range from the Eocene to the Early Miocene (Gökçen *et al.* 1988; see also Robertson *et al.* 2004), whereas only Middle–Late Eocene matrix sediments occur in the Kyrenia Range. In the eastern part of the Misis Mountains the melange is underlain by thrust sheets of basic volcanic rocks and volcaniclastic sediments that

https://doi.org/10.1017/S0016756813000563 Published online by Cambridge University Press

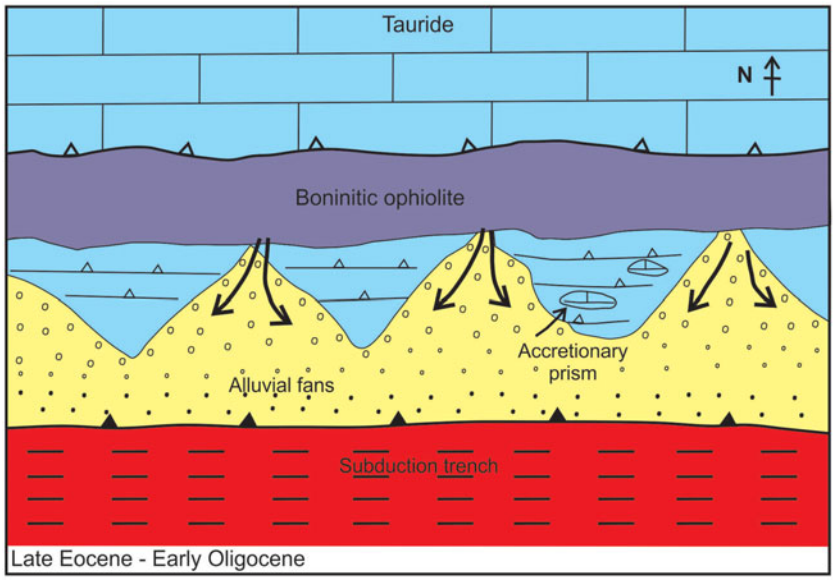

Figure 24. (Colour online) Inferred tectonic setting of the alluvial fan facies comprising the basal conglomerates of the Bellapais (Beylerbey) Formation. Ophiolitic rocks rich in boninitic extrusive rocks were then located to the north of the Kyrenia Range (now beneath the deep-marine Cilicia Basin) and fed coarse alluvial material southwards over the pre-existing Middle Eocene thrust belt that dominates the Kyrenia Range.

are interbedded with Late Cretaceous pelagic carbonates and radiolarites (Robertson *et al.* 2004).

The Misis Range turns NE-wards and continues as the Andırın Range (Fig. 1), which is also dominated by melange (Misis-Andırın Complex of Robertson *et al.* 2004). Rather than being a narrow lineament similar to the Kyrenia and Misis ranges (<5 km), the Andırın Range is up to tens of kilometres across and includes thrust sheets of Mesozoic platform carbonates (Andırın Limestone), pelagic sedimentary rocks and dismembered ophiolitic rocks (e.g. serpentinized harzburgite, pillow basalt and red radiolarian chert), all associated with mass-flow-type deposits (Robertson *et al.* 2004). Beneath this are deep-water carbonates and volcanic rocks that can be compared with the Lapithos (Lapta) Group in the Kyrenia Range. The melange and related units are unconformably covered by Miocene carbonate or siliciclastic sedimentary rocks and were thrust SE-wards over Early Miocene deep-water gravity deposits to the SE (Robertson *et al.* 2004).

The Andırın Range curves eastwards to form the front of the Tauride allochthon in the Engizek Range (Perinçek & Kozlu, 1984; MTA, 2002; Fig. 1). In this area, a comparable sedimentary melange is dominated by blocks of Mesozoic carbonate-platform-derived rocks set in a matrix of gravity-flow deposits. The melange is transgressed by Early–Middle Miocene mixed carbonate-siliciclastic sediments and is thrust southwards over Miocene gravity-flow deposits (Robertson *et al.* 2004; Hüsing *et al.* 2009).

Taken as a whole, the regional evidence indicates that the Kyrenia Range represents one segment of a larger belt of thrust sheets and related melange and so must be interpreted in this context.

To the north of the Kyrenia Range, beyond the Cilicia Basin, coastal southern Turkey is dominated by a relatively autochthonous Palaeozoic–Paleogene continental sequence within what is known as the Geyik Dağ (Fig. 1). This is covered by a series of thrust sheets and ophiolitic rocks that were emplaced in two phases during Late Cretaceous and Early–Middle Eocene time (Özgül, 1997; Mackintosh & Robertson, 2013). The exposed allochthonous platform carbonates were overthrust southwards by accretionary melange (Mersin melange) and ophiolitic rocks (Mersin ophiolite) during latest Cretaceous time (Parlak & Robertson, 2004; Parlak, 2006). The melange includes serpentinite, within-plate-type volcanic rocks (interpreted as rift-related units or emplaced oceanic seamounts), Triassic–Jurassic radiolarites, limestone blocks and dismembered thrust sheets of Permian–Cretaceous age. The overriding ophiolite exhibits a complete upper mantle and crustal sequence of geochemically supra-subduction zone type (Parlak *et al.* 2004). The melange is locally covered by transgressive Palaeocene shallow-marine carbonates, passing upwards into more extensive Eocene–Oligocene and Miocene sediments which blanket much of the area (see Parlak & Robertson, 2004). There is no evidence that the ophiolite and melange were tectonically transported relative to the platform basement and its cover after latest Cretaceous time.

Further east in SE Turkey there is widespread evidence of subduction-related magmatism cutting the Tauride continental rocks. Granitic rocks intruded the Malatya–Keban platform, part of the Tauride continent, during the Late Cretaceous (Yazgan & Chessex, 1991; Parlak 2006; Rızaoğlu *et al.* 2006, 2009). There

https://doi.org/10.1017/S0016756813000563 Published online by Cambridge University Press

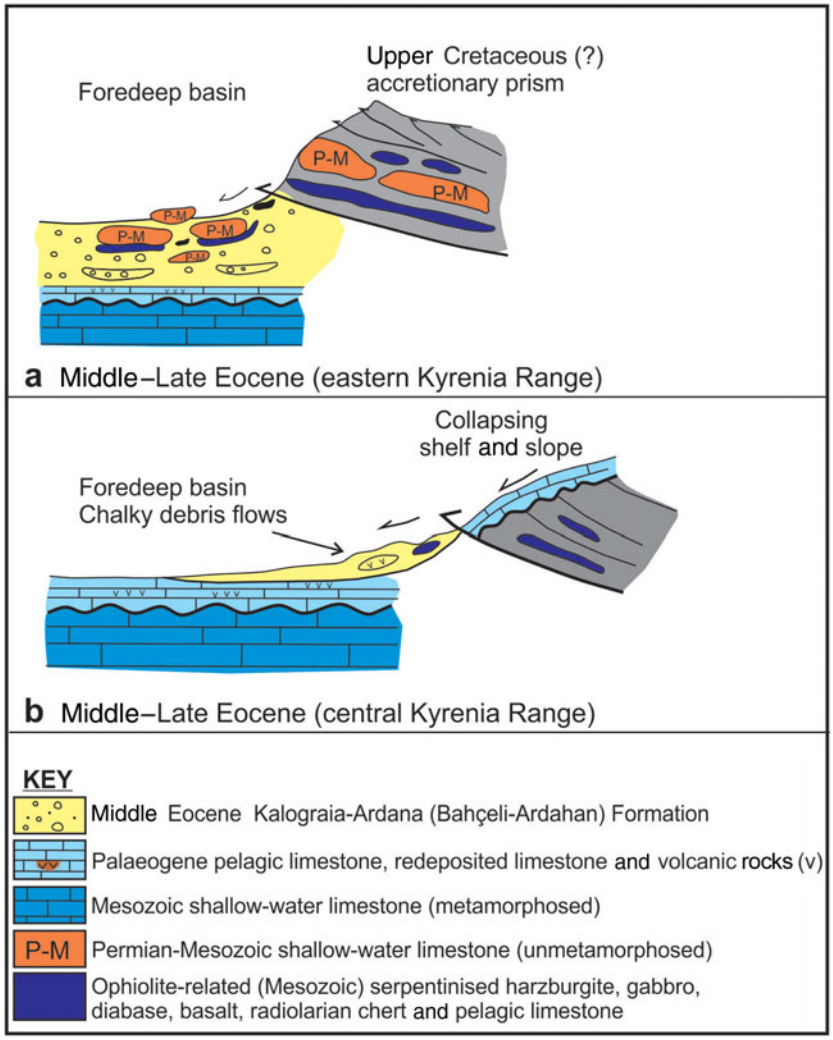

Figure 25. (Colour online) Sedimentary-tectonic interpretation of the Middle Eocene Kalaograia–Ardana (Bahçeli–Ardahan) Formation as the fill of a foredeep that was created as a flexural response to southwards thrusting. (a) Eastern Kyrenia Range (the largest outcrop). The overriding thrust sheets include unmetamorphosed Middle Permian – Cretaceous shallow-water carbonates (Kantara Limestones) and a variety of ophiolite-related rocks, emplaced in response to re-thrusting and mass-wasting. The material that was emplaced is likely to have originated from a pre-existing accretionary complex (i.e. as recycled melange). (b) Central Kyrenia Range. Large volumes of Paleogene chalk and volcanic rocks were redeposited, coupled with the emplacement of ophiolite-derived blocks. Exotic blocks of unrecrystallized limestone (Kantara Limestones) are absent from this area. Only the features that can be logically inferred from the field exposures are shown (see Fig. 26 for a plate tectonic model).

is also evidence of arc-type granitic magmatism dated as 53–45 Ma (Early–Middle Eocene) in the Doğanşehir area (Karaoğlan *et al.* 2013).

To the NW of the Kyrenia Range, coastal southern Turkey is dominated by the metamorphic rocks of the Alanya Massif (Fig. 1) which comprise three main thrust sheets. The middle thrust sheet includes a blueschist melange of inferred Late Cretaceous age that, critically is interpreted as an oceanic remnant (Okay & Özgül, 1984; Çetinkaplan *et al.* 2009). The metamorphic rocks there were exhumed during Late Cretaceous time. The thrust sheets making up the Alanya Massif as a whole were emplaced northwards over unmetamorphosed continental margin and oceanic (ophiolitic) rocks of the Mesozoic Antalya Complex (equivalent to the Antalya Nappes). The Alanya Complex in this area is inferred to have formed along the southern margin of the Tauride carbonate platform (Özgül, 1984; Robertson *et al.* 1991; Robertson, 1993). The allochthonous rocks of the Alanya Massif, plus the Antalya Complex, were finally emplaced northwards over the relatively autochthonous Tauride platform (Geyik Dağ) during Early–Middle Eocene time. There was also late-stage southwards overthrusting of a Tauride thrust sheet in the SE (MTA 2002).

The Alanya Massif has been restored as a small Mesozoic ocean basin termed the Alanya Ocean, with the Tauride continent plus the Antalya Complex to the north and a smaller continental fragment to the south (Görür *et al*. 1998; Robertson 1998; Robertson, Taslı & İnan, 2012*b*; Robertson, Parlak & Ustaömer, 2013). The southern margin of this inferred oceanic

https://doi.org/10.1017/S0016756813000563 Published online by Cambridge University Press

basin could be contiguous with the Mesozoic carbonate platform of the Kyrenia Range (Robertson, Parlak & Ustaömer, 2012*a*, 2013).

The İzmir–Ankara–Erzincan ocean was located to the north of the Tauride microcontinent (Geyik Dağ) and its former continental margin, now represented by the Tauride thrust sheets; this finally sutured in Early–Middle Eocene time (Şengör & Yılmaz, 1981; Robertson & Dixon, 1984; Görür *et al.* 1984, 1998). The closure fuelled the final southwards emplacement of the Tauride thrust sheets and also the related northwards backthrusting (e.g. south margin of the Alanya massif). After closure of the İzmir–Ankara–Erzincan Ocean, the convergence of Africa and Eurasia is inferred to have jumped to the Southern Neotethys Ocean, the only Mesozoic oceanic basin remaining between Africa and Eurasia. As a result the hinterland of the Kyrenia Range to the north was reactivated and thrust southwards, resulting in uplift, southwards thrusting erosion and mass-wasting to form the Kalaograia–Ardana (Bahçeli–Ardahan) Formation (Fig. 25).

11. Role in Neotethyan tectonic development

The sedimentary melange of the Middle Eocene Kalaograia–Ardana (Bahçeli–Ardahan) Formation records a key part of the development of the northerly active continental margin of the Southern Neotethys. The Neotethys rifted during Late Permian –Triassic time, existed during the Mesozoic and largely closed during the Cretaceous, leaving remnants in the east (SE Turkey) until the Early Miocene and in the west (SW of Cyprus) until present day (Robertson, Parlak & Ustaömer, 2013). The sedimentary melange is interpreted as having formed in a flexurally controlled foredeep that was underlain by a continental-related carbonate platform (Trypa/Tripa Group) rather than oceanic crust. This suggests that the sedimentary melange is not a conventional accretionary prism related to subduction. This platform was located along the southern margin of an active continental margin that was underlain by a northwards-dipping subduction zone. In addition, the melange includes exotic blocks that were probably derived from a subduction complex of probable Late Cretaceous age to the north. The boninite ophiolitic volcanic rocks of the Late Eocene – Oligocene Bellapais (Beylerbey) Formation were also derived from the north. Several driving mechanisms can be considered, as follows.

1. *Subduction zone roll-forward.* This could have caused compression and imbrication of the continental margin. Subduction zone roll-forward is likely if young, hot buoyant oceanic crust (<50 Ma) was subducted. However, the subducting crust would be expected to be old because spreading began during the Triassic (e.g. Robertson *et al.* 1991). It has recently been suggested from evidence in SE Turkey (Doğanşehir area) that a spreading axis subducted in order to create Early Eocene granulite facies metamorphic rocks (cooling ages of 52–50 Ma) that occur as blocks associated with a metamorphosed ophiolite (Berit metaopholite) (Karaoğlan *et al.* 2013). However, there is no independent evidence of the age of the oceanic crust being subducted during the Eocene.

2. *Steady-state northwards subduction.* Eocene subduction-related magmatism is documented in SE Turkey (Yılmaz, 1993; Robertson *et al.* 2006; Karaoğlan *et al.* 2013). However, steady-stage subduction processes alone cannot have generated the Kalaograia–Ardana (Bahçeli–Ardahan) Formation and also imbricated the associated continental margin.

3. *Acceleration or reactivation of northwards subduction.* This could have caused a pulse of compression, leading to destabilization and southwards thrusting of the active continental margin. A Palaeocene–Eocene 'flare-up' of subduction has indeed been inferred for the along-strike continuation of the Southern Neotethyan margin in Iran (Verdel *et al.* 2007, 2011).

4. *Collision of a topographic edifice (continental fragment or oceanic seamount) with a trench*. This could have deformed the continental margin but lacks supporting evidence (e.g. accretion of seamount material).

5. *Southwards-directed compression related to collision elsewhere in Neotethys.* The Middle Eocene timing of the genesis and emplacement of the Kalaograia–Ardana (Bahçeli–Ardahan) Formation approximately corresponds to the suturing of the İzmir–Ankara–Erzincan ocean ('N Neotethys') to the north. This ocean straddled what is today Anatolia from the Aegean region to Iran (Şengör & Yılmaz, 1981; Robertson & Dixon, 1984) and finally closed during Early–Middle Eocene time (i.e. pre-Bartonian) (Şengör & Yılmaz, 1981; Görür *et al.* 1984; Andrew & Robertson, 2002; Mackintosh & Robertson, 2013). The closure and collision affected much of central and western Turkey and drove the final southwards emplacement of the Tauride oceanic- and continental-margin-derived thrust sheets onto the Tauride continent. Several tectonic lineaments were active during Early–Middle Eocene time to the north of the Kyrenia Range, mainly involving southwards thrusting (Fig. 1).

The Kyrenia Range is likely to have been tectonically juxtaposed with the Alanya Massif at least by Paleogene time. The present-day Cilicia Basin is inferred to have formed from the Oligocene onwards (Robertson & Woodcock, 1986) and therefore did not separate Cyprus from southern Turkey during the Eocene. The southwards-directed compression that affected the Taurides and the Alanya Massif area could therefore also have affected the Kyrenia Range. In this interpretation, a southwards-moving wave of compression triggered flexural subsidence of continental crust to the south, extending at least as far as the Kyrenia Range. The overriding thrust sheets, which were predominantly made up of ophiolite-related lithologies and Middle?–Late Permian – Late Cretaceous limestones then underwent mass-wasting to form the

https://doi.org/10.1017/S0016756813000563 Published online by Cambridge University Press

debris-flow deposits and exotic blocks/sheets. Southwards-directed compression culminated in the imbrication of the Kyrenia continental margin, including the Middle Eocene foredeep.

After southwards thrusting ended, northwards subduction continued to be active and the oceanic slab rolled back southwards. The continental margin collapsed allowing clastic material to prograde southwards to form the Late Eocene – Oligocene non-marine to shallow-marine basal conglomerates of the Bellapais (Beylerbey) Formation (Baroz, 1979; Robertson & Woodcock, 1986; McCay & Robertson, 2012; Fig. 24). During this time the Troodos ophiolite to the south continued to be overlain by deep-water pelagic sediments, unaffected by thrusting or collisional tectonics (e.g. Robertson, 1977*b*).

A key remaining question is the source of the subduction-related boninite-type clasts, particularly in the Bellapais (Beylerbey) Formation. Comparable ophiolite-related melange formed during the Late Cretaceous, for example elsewhere along the southern margin of the Tauride continent (e.g. Antalya Complex: Woodcock & Robertson, 1982; Robertson, 1998; Misis-Andırın Complex: Robertson *et al.* 2004). Several possible source areas for the boninitic clasts can be considered, as follows.

1. The boninitic clasts originated from an ophiolitic thrust sheet that was emplaced at a high-structural level during the Middle Eocene southwards thrusting. The boninitic rocks were then subaerially eroded, shedding boninitic clasts into the Late Eocene – Oligocene basal conglomerates (Bellapais/Beylerbey Formation). However, the rarity of basaltic clasts in the palaeo-colluvium at the base of the Bellapais (Beylerbey) Formation in several areas (McCay & Robertson, 2012) suggests that the Kyrenia Range itself was not an important source

2. The boninite-type clasts originated to the south, associated with the Troodos ophiolite. For example, similar boninitic lavas are exposed along the South Troodos Transform Fault Zone in the south of the island and its extension into SW Cyprus (McLeod & Murton, 1993; Gilbert & Robertson, 2013). The palaeocurrents in the overlying conglomerates are southwards directed (McCay & Robertson, 2012), however, suggesting that the main source of the ophiolitic rocks was to the north.

3. A southerly derivation could also be envisaged if ophiolitic rocks were translated inboard (to the north) of the Kyrenia Range by strike-slip. Boninites are also, for example, associated with the Hatay ophiolite, S Turkey (Bağçi, Parlak & Höck, 2008) and the Baer–Bassit ophiolite, N Syria (Al-Riyami & Robertson, 2002) to the east. However, these ophiolites correlate with the Troodos ophiolite that was positioned to the south of the Kyrenia Range in palaeotectonic reconstructions (Robertson, Taslı & İnan, 2012*b*) and there is no independent evidence of strike-slip translation of ophiolitic rocks during the required Middle–Late Eocene time.

4. The boninitic clasts in the basal conglomerates were eroded from large outcrops of ophiolite-related rocks to the north of the Kyrenia Range (now beneath the Cilicia Basin) during Late Eocene – Oligocene time.

Option 4 fits the available evidence best. Assuming such a northerly origin, there are two possible ocean basins from which the ophiolitic rocks could have been derived. The first is a correlation with the Mersin ophiolite (Fig. 1; see above), which is inferred to have been emplaced from a Mesozoic ocean basin to the north of the Tauride carbonate platform (i.e. Inner Tauride ocean; Parlak & Robertson, 2004; Parlak *et al*. 2012). Boninitic lavas have not been reported from the Mersin ophiolite but could be concealed by cover sediments. The Mersin melange beneath the ophiolite (Parlak & Robertson, 2004) includes large detached blocks of Permian limestone, serpentinite and pelagic sedimentary rocks (e.g. radiolarites), lithologies that, broadly speaking, are present as blocks in the Kalaograia–Ardana (Bahçeli–Ardahan) Formation. However, against such a northerly origin, from the Palaeocene onwards the Mersin ophiolite and melange were covered by sediments and show no evidence of thrust displacement after their initial, latest Cretaceous emplacement.

The second alternative is that the boninitic clasts were derived from an ocean basin (Alanya Ocean) that existed between the Mesozoic platform of the Kyrenia Range and the Tauride continent to the north (Okay & Özgül, 1984; Robertson, 1998; Robertson, Parlak & Ustaömer, 2013; see above). In this interpretation, ophiolitic rocks including the boninites formed above a northwards-dipping subduction zone within the Alanya ocean basin and were thrust beneath the Tauride carbonate platform, probably during latest Cretaceous time. The overriding plate made up of Permian – Late Cretaceous platform carbonates became the source of the unmetamorphosed Kantara Limestone blocks. The Alanya Ocean may have closed during the Late Cretaceous but, more probably, only finally closed during Early–Middle Eocene time, perhaps driven by the regional-scale suturing of the İzmir–Ankara–Erzincan Ocean to the north. The second alternative is more consistent with the available geological evidence.

12. Conclusions: sedimentary-tectonic model

The Kyrenia Range crust (Kyrenia microcontinent) is likely to have been separated from the Tauride continent to the north by a small Mesozoic ocean basin (Alanya Ocean; see Fig. 26a, b) that sutured prior to Late Eocene time.

Ophiolitic rocks including boninitic extrusive rocks formed within the Alanya Ocean above a northwards-dipping subduction zone (Fig. 26b), together with accretionary melange (Fig. 26c). The overriding plate of the Alanya Ocean was made up of Permian–Cretaceous neritic carbonate platform rocks of the Tauride continent became the source of the large exotic blocks (Kantara Limestones) in the Kyrenia Range (Fig. 26d). During the Late Cretaceous the Troodos ophiolite subducted northwards beneath the Kyrenia microcontinent generating Late Cretaceous arc

https://doi.org/10.1017/S0016756813000563 Published online by Cambridge University Press

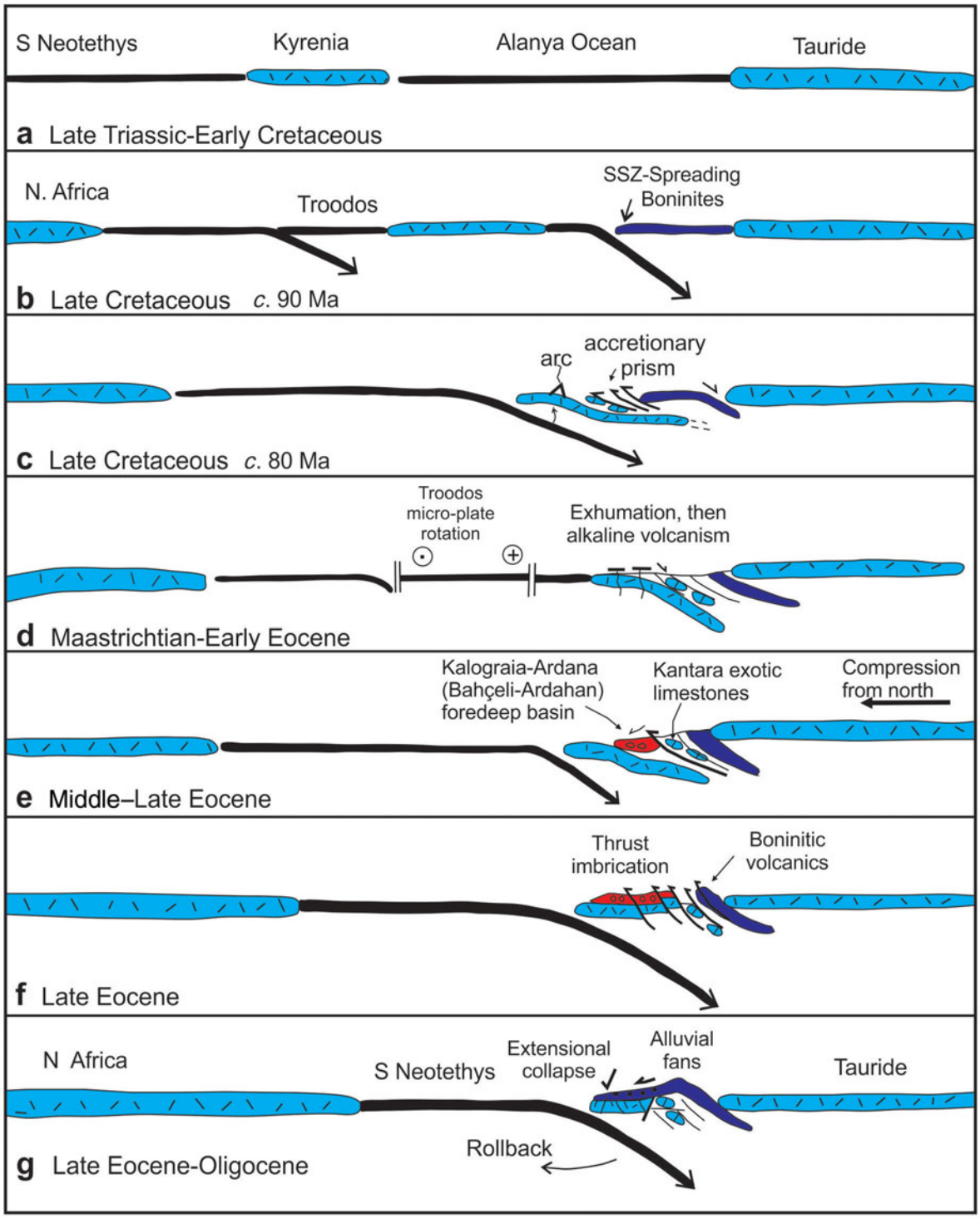

Figure 26. (Colour online) Plate tectonic model for the development of the Kyrenia Range in light of evidence from the Middle Eocene Kalaograia–Ardana (Bahçeli–Ardahan) Formation. (a) The Kyrenia Range originated as a rifted platform (microcontinent) between North Africa to the south and the Tauride microcontinent to the north. (b) Both the oceans to the north (Alanya) and the south (Troodos) underwent subduction and supra-subduction zone (SSZ) spreading. (c) During northwards subduction accretionary melange formed in the north. Arc magmatism was active to the south of the Kyrenia carbonate platform which was buried in a trench to the north, metamorphosed to greenschist facies and exhumed. Supra-subduction zone (SSZ) oceanic crust to the north was thrust beneath the Tauride platform together with accretionary melange. (d) The Kyrenia platform exhumed and was covered by carbonate breccias, pelagic carbonates, terrigenous gravity flows and alkaline basaltic rocks in a deep-marine setting. The Troodos micro-plate rotated 90° anticlockwise during Campanian – Early Eocene time (see Clube, Creer & Robertson, 1985; Clube & Robertson, 1986; Morris *et al.* 2006; Hodgson *et al.* 2010). (e) Following final closure of the major İzmir–Ankara–Erzincan Ocean (central Anatolia) during Early–Middle Eocene time, the locus of Africa–Eurasian convergence migrated to the northern, active margin of the Southern Neotethys. The pre-existing suture zone between the Kyrenia and the Tauride continental units was reactivated; the resulting downflexure of the footwall and mass-wasting of the overriding hanging wall of the thrust zone formed the Middle Eocene Kalaograia–Ardana (Bahçeli–Ardahan) Formation. (g) With continuing southwards compression, subduction accelerated (or was reactivated) and the overriding plate margin underwent extensional collapse allowing ophiolite-derived boninite-rich conglomerates to prograde southwards to form the Upper Eocene – Oligocene basal conglomerates of the Bellapais (Beylerbey) Formation.

https://doi.org/10.1017/S0016756813000563 Published online by Cambridge University Press

volcanism, followed by its 90° anticlockwise rotation (Fig. 26c, d).

During the Early–Middle Eocene, the İzmir–Ankara–Erzincan Ocean sutured driving southwards compression and final closure or suturing tightening of the Alanya Ocean (Fig. 26e). The Kyrenia microcontinental crust to the south underwent flexural collapse to form a regional-scale foreland basin, of which the southern part is represented by the Middle Eocene Kalaograia–Ardana (Bahçeli–Ardahan) Formation (Fig. 26e). During the convergence, previously accreted ophiolitic rocks and associated ophiolite-related melange were reactivated and re-thrust southwards (Fig. 26e).

Erosion created large volumes of ophiolite-derived clastic material (sand to exotic block sized; mainly serpentinitic) that was shed into a subaqueous foredeep to form a thick pile of sandstone turbidites and debris-flow deposits, plus exotic blocks (Fig. 26e). Middle Permian – Late Cretaceous exotic limestone blocks (Kantara Limestones) slid into the basin from the overriding former northern continental margin of the Alanya Ocean.

With continuing southwards compression (Middle–Late Eocene) the foredeep basin and its substratum were imbricated to form a south-vergent thrust belt (Fig. 26f). This was modified by backthrusting and possible late-stage extensional collapse.

During Late Eocene – Oligocene, subduction of the Southern Neotethys beneath the, by then, assembled Kyrenia–Alanya–Tauride continent resumed. The subducting oceanic slab rolled back, resulting in extensional collapse of the Kyrenia active continental margin and southwards progradation of alluvial to shallow-marine deltaic conglomerates (Fig. 26g). With further subduction zone rollback, the continental borderland to the north extended and collapsed to form a deep-marine basin (Cilicia Basin) in which terrigenous gravity flows accumulated during Oligocene – Late Miocene time.

During the ensuing latest Miocene – earliest Pliocene phase of southwards thrusting, the deformed Middle Eocene foredeep was overridden and largely concealed beneath the frontal thrust of the Kyrenia Range. Final uplift and exposure of the Kyrenia Range was delayed until Late Pliocene – Quaternary time.

Acknowledgements. We thank Dr Mehmet Necdet for encouragement with this work. Dr Nick Odling kindly assisted with the XRF analysis. We are also very grateful to Dr Hayati Koç for assistance with preparing diagrams. We thank Aynur Gürbüz (Mersin University of Advanced Technology, Education and Aplication Centre) for taking the SEM photographs of planktonic foraminifera. Dr Nurdan İnan (Mersin University, Mersin) kindly determined the benthic foraminifera. Concerning the fieldwork, the first author acknowledges the support of the University of Edinburgh while the second author was supported financially by a NERC training award. The third and fourth authors thank their home institutions for financial support related to the laboratory-based biostratigraphical studies. The manuscript benefitted from reviews by Professor A. Lord and an anonymous referee. In addition, Dr T.C. Kinnaird provided some helpful comments on the manuscript.

References

AL-RIYAMI, K. & ROBERTSON, A. H. F. 2002. Mesozoic sedimentary and magmatic evolution of the Arabian continental margin, northern Syria: evidence from the Baer-Bassit Melange. *Geological Magazine* **139**, 395–420.

AMERICAN GEOLOGICAL INSTITUTE, 1961. *Dictionary of Geological Terms*. New York: Dolphin Books.

ANDREW, T. & ROBERTSON, A. H. F. 2002. The Beyşehir-Hoyran-Hadim Nappes: genesis and emplacement of Mesozoic marginal and oceanic units of the northern Neotethys in southern Turkey. *Journal of the Geological Society of London* **159**, 529–43.

BAĞÇI, U., PARLAK, O. & HÖCK, V. 2008. Geochemistry and tectonic environment of divese magma generations forming the crustal units of the Kızıldağ (Hatay) Ophiolite, Southern Turkey. *Turkish Journal of Earth Sciences* **17**, 43–71.

BAROZ, F. 1979. *Etude Géologique dans le Pentadaktylos et la Mesaoria (Chypre Septentrionale)*. Docteur D'Etat Thesis. Université de Nancy, France, **1** & **2**. Published thesis.

BAROZ, F. 1980. Volcanism and continent-island arc collision in the Pentadaktylos range, Cyprus. In *Proceedings of International Symposium on Ophiolites* (ed. A. Panayiotou), pp. 73–5. Nicosia, Cyprus: Geological Survey Department.

BOUMA, A. H. 1962. *Sedimentology of some Flysch Deposits: a Graphic Approach to Facies Interpretation*. Amsterdam: Elsevier.

ÇETİNKAPLAN, M., CANDAN, O., OKAY, A. I., OBERHANSLI, R., KORALAY, O. E. & KOZLU, H. 2009. Tectonostratigraphy and polimetamorphic evolution of the Alanya Massif. 62nd *Geological Kurultai of Turkey*, 13–17 April 2009, MTA, Ankara, Türkiye. Abstract Book, 26–7.

CHANG, C.-P., ANGELIER, J. & HUANG, C. Y. 2000. Origin and evolution of a mélange: the active plate boundary and suture zone of the Longitudinal Valley, Taiwan. *Tectonophysics* **325**, 43–62.

CLARK, M. & ROBERTSON, A. H. F. 2005. Uppermost Cretaceous-Lower Tertiary Ulukışla Basin, south-central Turkey: sedimentary evolution of part of a unified basin complex within an evolving Neotethyan suture zone. *Sedimentary Geology* **173**, 15–51.

CLEINTAUR, M. R., KNOX, G. J. & EALEY, P. J. 1977. The geology of Cyprus and its place in the East-Mediterranean framework. *Geologie en Mijnbouw* **56**, 66–82.

CLOOS, M. & SHREVE, R. L. 1988. Subduction-channel model of prism accretion, melange formation, sediment subduction, and subduction erosion at convergent plate margins: 1. Background and description. *Pure and Applied Geophysics* **128**, 455–500.

CLUBE, T. M. M., CREER, K. M. & ROBERTSON, A. H. F. 1985. The palaeorotation of the Troodos microplate. *Nature* **317**, 522–5.

CLUBE, T. M. M. & ROBERTSON, A. H. F. 1986. The palaeorotation of the Troodos microplate, Cyprus, in the Late Mesozoic-Early Cenozoic plate tectonic framework of the Eastern Mediterranean. *Surveys in Geophysics* **8**, 375–437.

COWAN, D. S. & B. M. Page, 1975. Recycled Franciscan material in Franciscan melange west of Paso Robles,

California, *Geological Society of America Bulletin* **86**, 1089–95.

DICKINSON, W. R. 1985. Interpreting provenance relations from detrital modes of sandstones. In *Provenance of Arenites* (eds G.G. Zuffa), pp. 333–61. Dordrecht, Netherlands: Reidel.

DICKINSON, W. R. & SUCZEK, C. A. 1979. Plate tectonics and sandstone compositions. *American Association of Petroleum Geologists Bulletin* **63**, 2164–82.

DUCLOZ, C. 1972. The Geology of the Bellapais-Kyrthrea Area of the Central Kyrenia Range. *Cyprus Geological Survey Bulletin* **6**, 75p.

EVANS, D., HARRISON, Z., SHANNON, P. M., LABERG, J. S., NIELSEN, T., AYERS, S., HOLMES, R., HOULT, R. J., LINDBERG, B. & HAFLIDASON, H. 2005. Palaeoslides and other mass failures of Pliocene to Pleistocene age along the Atlantic continental margin of NW Europe. *Marine and Petroleum Geology* **22**, 1131–48.

FALLOON, T. J., DANYUSHEVSKY, L. V., CRAWFORD, A. J., MEFFRE, S., WOODHEAD, J. D. & BLOOMER, S. H. 2008. Boninites and adakites from the nortern termination of the Tonga Trench: Implications for adakite petrogenesis. *Journal of Petrolgy* **49**, 497–715.

FITTON, J. G. & GODARD, M. 2004. Origin and evolution of magmas on the Ontong Java Plateau. In *Origin and Evolution of the Ontong Java Plateau* (eds J.G. Fitton, J.J. Mahoney, P.J. Wallace & A.D. Saunders). pp. 151–78. Geological Society of London, Special Publication no. 229.

FITTON, J. G., SAUNDERS, A. D., LARSEN, L. M., HARDARSON, B. S. & NORRY, M. S. 1998. Volcanic rocks of the southeast Greenland margin. *Proceedings of the Ocean Drilling Program*, Scientific Results **152**, 331–50.

GASS, I. G. 1990. Ophiolites and ocean lithosphere. In *Ophiolites Oceanic Crustal Analogues. Proceedings of the Symposium,'Troodos 1987'*. (eds J. Malpas, E.M. Moores, A. Panayiotou & C. Xenophontos), pp. 1–10. Nicosia, Cyprus: Geological Survey Department.

GASS, I. G., MACLEOD, C. J., MURTON, B. J., PANAYIOTOU, A., SIMONIAN, K. O. & XENOPHONTOS, C. 1994. The geology of the South Troodos Transform Fault Zone. Geological Survey Department, Cyprus, Memoir **9**, 218 p.

GEOLOGICAL MAP OF CYPRUS, 1979. Scale 1:250,000. Nicosia, Cyprus: Geological Survey Department.

GILBERT, M. & ROBERTSON, A. H. F. 2013. Upper Cretaceous volcaniclastic sedimentation in W Cyprus: evidence for a Southern Neotethyan volcanic arc. In *Geological Development of the Anatolian continent and the Eastern Mediterranean region* (eds A.H.F. Robertson, O. Parlak & Ü. Ünlügenç), pp. 273–98. Geological Society of London, Special Publication no. 372.

GÖKÇEN, S. L., KELLING, G., GÖKÇEN, N. & FLOYD, P. A. 1988. Sedimentology of a Late Cenozoic collisional sequence: the Misis Complex, Adana, southern Turkey. *Sedimentary Geology* **59**, 205–35.

GÖRÜR, N., OKAY, A. I., ŞENGÖR, A. M. C., TÜYSÜZ, O., SAKINÇ, M., YIĞITBAŞ, E., AKKÖK, R., BARKA, A., OKTAY, F. Y., SARICA, N., YALTIRAK, C., YILMAZ, B., ERSOY, S., ELMAS, A., ÖRÇEN, S., ERCAN, T., ŞAROĞLU, F., AKYÜREK, B. 1998. *Triassic to Miocene Palaeogeographic Atlas of Turkey*. Ankara: MTA Enstitüsü (General Directorate of Mineral Research and Exploration).

GÖRÜR, N., OKTAY, F. Y., SEYMEN, I. & ŞENGÖR, A. M. C. 1984. Paleo-tectonic evolution of the Tuzgölü basin complex, Central Turkey: sedimentary record of a Neo-Tethyan closure. In *The Geological Evolution of the Eastern Mediterranean* (eds J. E. Dixon & A. H. F. Robertson), pp. 467–82. Geological Society of London, Special Publication no. 17.

GRADSTEIN, F. M., OGG, J. G. & SMITH, A. G. 2004. *A Geological Time Scale*. Cambridge: Cambridge University Press.

GRAHAM, S. A., INRESOLL, R. V. & DICKINSON, W. R. 1976. Common provenance for lithic grains in Carboniferous sandstones from Ouachita Mountains and Black Warrior Basin. *Journal of Sedimentary Petrology* **24**, 620–32.

HAKYEMEZ, A. & ÖZKAN-ALTINER, S. 2007. Beşparmak Dağları'ndaki (Kuzey Kıbrıs) Üst Maastrihtiyen-Eosen İstifinin Planktonik Foraminifer Biyostratigrafisi (Planktonic foraminiferal biostratigraphy of the Upper Maastrichtian – Eocene sequence in the Beşparmak Range, Northern Cyprus). *60th Geological Congress of Turkey*, Ankara, Abstract, p. 416–19.

HAKYEMEZ, Y., TURHAN, N., SÖNMEZ, İ. & SÜMENGEN, M. 2002. *Kuzey Kıbrıs Türk Cumhuriyeti'nin Jeolojisi* (Geology of the Northern Cyprus Turkish Republic). Ankara: Mineral Research and Exploration Institute of Turkey, 44 pp.

HARRISON, R. W., NEWELL, W. L., BATIHANLI, H., PANAYIDES, I., MCGEEHIN, J. P., MAHAN, S. A., OZHUR, A., TSIOLAKIS, E. & NECDET, M. 2004. Tectonic framework and Late Cenozoic tectonic history of the northern part of Cyprus: implications for earthquake hazards and regional tectonics. *Journal of Asian Earth Sciences* **23**, 191–210.

HAUGHTON, P., DAVIS, C., MCAFFREY, W. & BAKER, S. 2009. Hybrid sediment gravity flow deposits-Classification, origin and significance. *Marine and Petroleum Geology* **26**, 1900–18.

HENSON, F. R. S., BROWNE, R. V. & MCGINTY, J. 1949. A synopsis of the stratigraphy and geological history of Cyprus. *Quarterly Journal of the Geological Society of London* **CV**, 2–37.

HODGSON, E., MORRIS, A., ANDERSON, M. & ROBERTSON, A. H. F. 2010. First palaeomagnetic results from the Kyrenia Range terrane of northern Cyprus. Vienna: European Union of Geosciences, Published Abstract.

HUANG, K., MALPS, J. & XENOPHONTOS, C. 2007. Geological studies of igneous rocks and their relationships along the Kyrenia Range. In *Abstracts of the 6th International Congress of Eastern Mediterranaen Geology* April 2–5 2007 (eds K. Moumani, K. Shawabkeh, A. Al-Malabeh & M. Abdelghafoor), p. 53, Amman, Jordan.

HUHNERBACH, V. & MASSON, D. G. 2004. Landslides in the North Atlantic and its adjacent seas: an analysis of their morphology, setting and behaviour. *Marine Geology* **213**, 343–62.

HÜSING, S. K., ZACHARIASSE, W.-J., VAN HINSBERGEN, D. J. J., KRIJGSMAN, W., İNCEÖZ, M., HARZHAUSER, M., MANDIC, O., KROH, A. 2009. Oligocene-Miocene basin evolution in SE Anatolia, Turkey: constraints on the closure of the central Tethys gateway. In *Collision and Collapse at the Africa–Arabia–Eurasia Subduction Zone* (eds D. J. J. Van Hinsbergen, M. A. Edwards & R. Govers), pp. 107–32. Geological Society of London, Special Publication no. 311.

INWOOD, J., MORRIS, A., ANDERSON, M. W. & ROBERTSON, A. H. F. 2009. Neotethyan intraoceanic microplate rotation and variations in spreading axis orientation: palaeomagnetic evidence from the Hatay ophiolite (southern Turkey). *Earth and Planetary Science Letters* **280**, 105–17.

JIN, X. & YANG, X. 2004. Palaeogeographic implications of the Shanita-Hemigordius fauna (Permian foramininifer) in the reconstruction of Permian Tethys. *Episodes*, **24**(4), 273–8.

KARAOĞLAN, F., PARLAK, O., ROBERTSON, A., THONI, M., KLÖTZLI, U., KOLLER, F. & OKAY, A. İ. 2013. Evidence of Eocene HT/HP metamorphism of ophiolitic rocks and granitoid intrusion related to Neotethyan subduction processes (Doğanşehir area, SE Anatolia). In *Geological Development of the Anatolian Continent and the Eastern Mediterranean Region* (eds A. H. F. Robertson, O. Parlak & Ü. Ünlügenç). Geological Society of London, Special Publication no. 372.

KELLING, G., GÖKÇEN, S. L., FLOYD, P. A. & GÖKÇEN, N. 1987. Neogene tectonics and plate convergence in the eastern Mediterranean: new data from southern Turkey. *Geology* **15**, 249–72.

LIU, G. & EINSELE, G. 1996. Various types of olistostromes in a closing ocean basin, Tethyan Himalaya (Cretaceous, Tibet). *Sedimentary Geology* **104**, 203–26.

LORD, A. R., HARRISON, R. W., BOUDAGHER-FADEL, M., STONE, B. D. & VAROL, O. 2009. Miocene mass-transport sediments, Troodos Massif, Cyprus. *Proceedings of the Geologists Association* **120**, 133–8.

MACKINTOSH, P. W. & ROBERTSON, A. H. F. 2013. Structural development and restoration of the north-Gondwana margin in the central Taurides, Turkey. In *Geological Development of the Anatolian Continent and the Eastern Mediterranean Region* (eds A. H. F. Robertson, O. Parlak & Ü. Ünlügenç), pp. 299–322. Geological Society of London, Special Publication no. 372.

MACLEOD, C. & MURTON, B. J. 1993. Structure and tectonic evolution of the Southern Troodos Transform Fault Zone, Cyprus. In *Magmatic Processes and Plate Tectonics*. (eds H. M. Prichard, T. Alabaster, N. B. W. Harris & C. R. Neary), pp. 141–76. Geological Society of London, Special Publication no. 76.

MARTINI, E. 1971. Standard Tertiary and Quaternary Calcareous nannoplankton zonation. In *Proceedings of the Second Plankton Conference*, Rome, 1970 (ed. A. Farinacci), pp. 739–85. Rome: Edizioni Tecnoscienza, vol. **2**.

McCAY, G. A. & ROBERTSON, A. H. F. 2012. Sedimentology and provenance of Upper Eocene-Upper Miocene clastic sediments of the Girne (Kyrenia) Range, northern Cyprus: depositional processes along the northerly, active margin of the Southern Neotethys. *Sedimentary Geology* **265–6**, 30–55.

McCAY, G. A. & ROBERTSON, A. H. F. 2013. Upper Miocene-Pleistocene deformation of the Girne (Kyrenia) Range and Dar dere (Ovgos) lineaments, N Cyprus: role in collision and tectonic escape in the easternmost Mediterranean region. In *Geological Development of the Anatolian Continent and the Eastern Mediterranean Region* (eds A. H. F. Robertson, O. Parlak & Ü. Ünlügenç), pp. 421–5. Geological Society of London, Special Publication no. 372.

McCAY, G. A., ROBERTSON, A. H. F., KROON, D., RAFFFI, I., ELLAM, R. M. & NECDET, M. 2013. Implications of new $^{87}Sr/^{86}Sr$ isotopic, nannoplankton and foraminiferal dating for Neogene sedimentation in the northern part of Cyprus. *Geological Magazine* **150**, 333–59.

MORRIS, A., ANDERSON, M. W., INWOOD, J. & ROBERTSON, A. H. F. 2006. Palaeomagnetic insights into the evolution of Neotethyan oceanic crust in the eastern Mediterranean. In *Tectonic Development of the Eastern Mediterranean Region* (eds A.H.F. Robertson & D. Mountrakis), pp. 351–72. Geological Society of London, Special Publication no. 260.

MTA, 2002. *Geological Map of Turkey* 1:500,000. Ankara: Maden Tektik ve Arama Genel Müdürlüğü (General Directorate of Mineral Research and Exploration).

MULDER, T. & COCHONAT, P. 1996. Classification of offshore mass movements *Journal of Sedimentary Research* **66**, 43–57.

MULLEN, E. D. 1983. $MnO/TiO_2/P_2O_5$: a minor element discrimination for basaltic rocks of oceanic environment and its implications for petrogenesis. *Earth and Planetary Science Letters* **62**, 53–62.

MUTTI, E. & RICCI LUCCHI, F. 1975. Turbidite facies and facies associations. Examples of turbidite facies and facies association from selected formations of the Northern Apennines. Field Trip Guidebook, pp. 21–36, 9th Congress of the International Association of Sedimentologists, Nice.

MUTTI, E. & RICCI LUCCHI, F. 1978. Turbidites of the northern Apennines: introduction to facies analysis. *International Geology Review* **20**, 125–66.

OKAY, A. İ. & ÖZGÜL, N. 1984. HP/LT metamorphism and the structure of the Alanya Massif, Southern Turkey: an allochthonous composite tectonic sheet. In *Geological Evolution of the Eastern Mediterranean* (eds J.E. Dixon & A.H.F. Robertson), pp. 415–29. Geological Society of London, Special Publication no. 17.

ÖZGÜL, N. 1984. Geology of the Alanya tectonic window and its western part. *TJK Ketin Sempozyumu* (Turkish Gelogical Society Ketin Symposium), 97–120 (in Turkish).

ÖZGÜL, N. 1997. Stratigraphy of the tectonic-stratigeraphic units in the region Bozkır-Hadim-Taşkent (northern central Taurides). *Maden Tetkik ve Arama Dergisi* **119**, 113–74 (in Turkish).

PARLAK, O. 2006. Geodynamic significance of granitoid magmatism in southeast Anatolia: geochemical and geochronological evidence from the Göksun–Afşin (Kahramanmaraş, Turkey) region. *International Journal of Earth Sciences* **95**, 609–27.

PARLAK, O., HÖCK, V., KOZLU, H. & DELALOYE, M. 2004. Oceanic crust generation in an island arc tectonic setting, SE Anatolian Orogenic belt (Turkey). *Geological Magazine* **141**, 583–603.

PARLAK, O., KARAOĞLAN, F., RIZAOĞLU, T., KLÖTZLI, U., KOLLER, F. & BILLOR, Z. 2012 U–Pb and 40Ar–39Ar geochronology of the ophiolites and granitoids from the Tauride belt: Implications for the evolution of the Inner Tauride suture. *Journal of Geodynamics*, http://dx.doi.org/10.1016/j.jog.2012.06.012.

PARLAK, O. & ROBERTSON, A. H. F. 2004. The ophiolite-related Mersin Melange, southern Turkey: its role in the tectonic-sedimentary setting of Tethys in the Eastern Mediterranean. *Geological Magazine* **141**, 257–86.

PEARCE, J. A. 1975. Basalt geochemistry used to investigate past tectonic environments in Cyprus. *Tectonophysics* **25**, 41–67.

PEARCE, J. A. 1982. Trace element characteristics of lavas from destructive plate boundaries. In *Orogenic Andesites and Related Rocks* (ed. R.S. Thorpe), pp. 525–48. Chichester: J. Wiley & Sons.

PEARCE, J. A. 1996. A users guide to basalt discrimination diagrams. In *Trace Element Geochemistry of Volcanic Rocks: Applications for Massive Sulphide Exploration*. (ed D.A. Wyman), pp. 79–113. Geological Association of Canada, Geochemistry Short Course Notes no. 12.

PEARCE, J. A. & CANN, J. R. 1973. Tectonic setting of basaltic volcanic rocks determined using trace element analysis. *Earth and Planetary Science Letters* **19**, 290–300.

PEARCE, J. A. & NORRY, M. J. 1979. Petrogenetic implications of Ti, Zr, Y, and Nb variations in volcanic rocks. *Contributions to Mineralogy and Petrology* **69**, 33–47.

PEARCE, J. A., STERN, R. J., BLOOMER, S. H. & FRYER, P. 2005. Geochemical mapping of the Mariana arc-basin system: implications for the nature and distribution of subduction components. *Geochemistry Geophysics Geosystems* **6**, Q07006, doi:10.1029/2004GC000895.

PEARSON, P. N., OLSSON, R. K., HUBER, B. T., HEMLEBEN, C., BERGGREN, W. A. (eds) 2006. *Atlas of Eocene Planktonic Foraminifera*. Cushman Foundation, Special Publication no. 41.

PERCH-NIELSEN, K. 1985. Cenozoic calcareous nannofossils. In *Plankton Stratigraphy* (eds H. M. Bolli, J. B. Saunders & K. Perch-Nielsen), pp. 427–554. Cambridge: Cambridge University Press.

PERINÇEK, D. & KOZLU, H. 1984. Stratigraphical and structural relations of the units in the Afşin-Elbistan-Doğanşehir region (Eastern Taurus). In *Geology of the Taurus Belt* (eds O. Tekeli & M. C. Göncüoğlu), pp. 181–98. Proceedings of International Symposium, MTA, Ankara.

PHILLIPS-LANDER, C. M. & DILEK, Y. 2009. Structural architecture of the sheeted dike complex and extensional tectonics of the Jurassic Mirdita ophiolite, Albania. *Lithos* **108**, 192–206.

PICKERING, K. T., HISCOTT, R. N. & HIEN, F. J. 1989. *Deep Marine Environments: Clastic Sedimentation and Tectonics*. London: Unwin Hyman.

RAYMOND, L. A. (ed.) 1984. *Melanges: Their Nature, Origin and Significance*. Geological Society of America, Special Paper **198**.

REICHEL, M. 1945*a*. Sur un Miliolide nouveau du Permien de l'ile de Chypre. *Verhandlungen der Naturforschenden Gesellschaft im Basel* **56**, 521–30.

REICHEL, M. 1945*b*. Sur quelques foraminiferes nouveaux du Permien Mediterranean. *Eclogae Geologicae Helvetiae* **38**, 524–60.

RIZAOĞLU,, T., PARLAK, O., HÖCK, V. & İŞLER, F. 2006. Nature and significance of Late Cretaceous ophiolitic rocks and its relation to the Baskil granitoid in Elazığ region, SE Turkey. In *Tectonic Development of the Eastern Mediterranean Region* (eds A.H.F Robertson & D. Mountrakis), pp. 327–50. Geological Society of London, Special Publication no. 260.

RIZAOĞLU, T., PARLAK, O., HÖCK, V., KOLLER, F., HAMES, W. E. & BILLOR, Z. 2009. Andean-type active margin formation in the eastern Taurides: Geochemical and geochronogical evidence from the Baskil granitoid (Elazığ, SE Turkey). *Tectonophysics* **473**, 188–207.

ROBERTSON, A. H. F. 1977*a*. The Moni Melange, Cyprus: an olistostrome formed at a destructive plate margin. *Journal of the Geological Society London* **133**, 447–66.

ROBERTSON, A. H. F. 1977*b*. Tertiary uplift history of the Troodos massif, Cyprus. *Geological Society of America Bulletin* **88**, 1763–72.

ROBERTSON, A. H. F. 1977*c*. The Kannaviou Formation, Cyprus: volcaniclastic sedimentation of a probable Late Cretaceous volcanic arc. *Journal of Geological Society of London* **134**, 269–92.

ROBERTSON, A. H. F. 1993. Mesozoic-Tertiary sedimentary and tectonic evolution of Neotethyan carbonate platorms, margins and small ocean basins in the Antalya complex, S.W. Turkey. In *Tectonic Controls and Signatures in Sedimentary Successions* (eds L. Frostick & R. Steel), pp. 415–65. International Association of Sedimentologists, Special Publication no. 20.

ROBERTSON, A. H. F. 1998. Mesozoic–Cenozoic tectonic evolution of the easternmost Mediterranean area: integration of marine and land evidence. In *Proceedings of the Ocean Drilling Program, Scientific Results* (eds A. H. F. Robertson, K.-C. Emeis & A. Camerlenghi eds), pp. 723–82.

ROBERTSON, A. H. F., CLIFT, P. D., DEGNAN, P. J. & JONES, G. 1991. Palaeogeographical and palaeotectonic evolution of the Eastern Mediterranean Neotethys. *Palaeoceanography, Palaeoclimatology, Palaeoecology* **87**, 289–343.

ROBERTSON, A. H. F. & DIXON, J. E. 1984. Introduction: Aspects of the Geological Evolution of the Eastern Mediterranean. In *The Geological Evolution of the Eastern Mediterranean* (eds J. E. Dixon & A. H. F. Robertson), pp. 1–74. Geological Society of London, Special Publication no. 17.

ROBERTSON, A. H. F. & OCEAN DRILLING PROGRAM LEG 160 SCIENTIFIC PARTY. 1996. Mud volcanism on the Mediterranean Ridge: Initial results of Ocean Drilling Program Leg 160. *Geology* **24**, 239–42.

ROBERTSON, A. H. F., PARLAK, O. & USTAÖMER, T. 2009. Melange genesis and ophiolite emplacement related to subduction of the northern margin of the Tauride-Anatolide continent, central and western. In *Geodynamics of Collision and Collapse at the Africa–Arabia–Eurasia Subduction Zone* (eds D. J. J. van Hinsbergen, M. A. Edwards & G. Gowers), pp. 9–66. Geological Society of London, Special Publication no. 311.

ROBERTSON, A. H. F., PARLAK, O. & USTAÖMER, T. 2012*a*. Overview of the Palaeozoic- Neogene evolution of Neotethys in the Eastern Mediterranean region (S Turkey, Cyprus, Syria. *Petroleum Geoscience* **18**, 381–404.

ROBERTSON, A. H. F., PARLAK, O. & USTAÖMER, T. 2013. Late Palalaeozoic-Early Cenozoic tectonic development of Southern Turkey and the easternmost Mediterranean region: evidence from the inter-relations of continental and oceanic units. In *Geological Development of Anatolia and the Eastern Mediterranean Region* (eds A. H. F. Robertson, O. Parlak & Ü. Ünlügenç), pp. 9–48. Geological Society of London, Special Publication no. 372.

ROBERTSON, A. H. F., TASLI, K. & İNAN, N. 2012*b*. Evidence from the Kyrenia Range, Cyprus, of the northerly active margin of the Southern Neotethys during Late Cretaceous–Early Cenozoic time. *Geological Magazine* **149**, 264–90.

ROBERTSON, A. H. F., UNLÜGENÇ, Ü. C., İNAN, N. & TASLI, K. 2004. The Misis–Andırın Complex: a Mid-Tertiary melange related to late-stage subduction of the Southern Neotethys in S Turkey. *Journal of Asian Earth Sciences* **22**, 413–53.

ROBERTSON, A. H. F., USTAÖMER, T., PARLAK, O., UNLÜGENÇ, U. C., TASLI, K. & İNAN, N. 2006. The Berit transect of the Tauride thrust belt, S Turkey: Late Cretaceous-Early Cenozoic accretionary/collisional processes related to closure of the Southern Neotethys. *Journal of Asian Earth Sciences* **27**, 108–45.

ROBERTSON, A. H. F. & WOODCOCK, N. H. 1980. Tectonic setting of the Troodos massif in the east Mediterranean. In *Proceedings International Ophiolite Symposium* (ed. A. Panayiotou), pp. 36–49. Cyprus: Geological Survey Department.

ROBERTSON, A. H. F. & WOODCOCK, N. H. 1986. The role of the Kyrenia Range lineament, Cyprus, in the geological evolution of the Eastern Mediterranean area. In *Major Crustal Lineaments and their Influence on the Geological History of the Continental Lithosphere* (eds

H. G. Reading, J. Watterson & S. H. White), *Philosophical Transactions of the Royal Society of London, Series A*, **317**, 141–71.

ROBINSON, P. T. & MALPAS, J. 1990. The Troodos Ophiolite of Cyprus: new perspectives on its origin and emplacement. In *Ophiolites: Oceanic Crustal Analogues* (eds E.M. Moores, A. Panayiotou, & C. Xenophontos), pp. 13–36. Nicosia, Cyprus: Geological Survey Department.

ŞENGÖR, A. M. C. 2003. The repeated rediscovery of melanges and its implications for the possibility and the role of objective evidence in the scientific enterprise. In *Ophiolite Concept and the Evolution of Geological Thought* (eds Y. Dilek & S. Newcomb), pp. 85–445. Geological Society of America, Special Paper no. 373.

ŞENGÖR, A. M. C. & YILMAZ, Y. 1981. Tethyan evolution of Turkey: A plate tectonic approach. *Tectonophysics* **75**, 181–241.

SUCZEK, C. A. & INGERSOLL, R. V. 1979. Petrology and provenance of Neogene sand from Nicobar and Bengal fans, DSDP Sites 211 and 218. *Journal of Sedimentary Research* **49**, 1217–28.

SUN, S. S. & MCDONOUGH, W. F. 1989. Chemical and isotopic systematics of oceanic basalts: implications for mantle composition and processes. In *Magmatism in the Ocean Basins* (eds A. D. Saunders & M. J. Norry), pp. 313–47. Geological Society of London, Special Publication no. 42.

SWARBRICK, R. E. & NAYLOR, M. A. 1980. The Kathikas Melange south-west Cyprud; late Cretaceous submarine debris flows. *Sedimentology* **27**, 63–78.

TAIRA, A., TOKUYAMA, H. & SOH, W. 1989. Accretion tectonics and evolution of Japan. In *The Evolution of the Pacific Ocean Margins* (ed. Z. Ben-Avraham), pp. 100–23. Oxford: Oxford University Press.

VAROL, O. 1999. Paleogene. In *Calcareous Nannofossil Biostratigraphy* (ed P. R. Bown), British Micropaleontological Society, Publications Series, 314 pp.

VERDEL, C., WERNICKE, B. P., HASSANZADEH, P. R. & GUEST, B. 2011. A Paleogene extensional arc flare-up in Iran. *Tectonics* **30**, doi:10.1029/2010TC002809, 2011.

VERDEL, C., WERNICKE, B. P., RAMEZANI, J., HASSANZADEH, J., RENNE, P. R. & SPELL, T. L. 2007. Geology and thermochronology of Tertiary Cordilleran-style metamorphic core complexes in the Saghand region of central Iran. *Geological Society of America*, *Bulletin* **119**, 961–77.

WILLIAMS, P. R., PIGRAM, C. J. & DOW, D. B. 1984. Melange production and the importance of shale diapirism in accretionary terranes. *Nature* **309**, 145–6.

WOODCOCK, N. H. & ROBERTSON, A. H. F. 1982. Wrench and thrust tectonics along a Mesozoic-Cenozoic continental margin: Antalya Complex, SW Turkey. *Journal of the Geological Society London* **139**, 147–63.

YAZGAN, E. & CHESSEX, R. 1991. Geology and tectonic evolution of the Southeastern Taurides in the region of Malatya. *Bulletin of Turkish Association of Petroleum Geologists* **3**(1), 1–42.

YILMAZ, Y. 1993. New evidence and model on the evolution of the southeast Anatolian orogen. *Geological Society of America Bulletin* **105**, 251–71.